คอมโพสิทจากกราฟีนและเบนซอกซาซีนสำหรับประยุกต์ใช้เป็นแผ่นไบโพลาร์ในเซลล์เชื้อเพลิง

นางสาวรัตน์ชา เปล่งอุดมกิจ

วิทยานิพนธ์นี้เป็นส่วนหนึ่งของการศึกษาตามหลักสูตรปริญญาวิศวกรรมศาสตรมหาบัณฑิต
สาขาวิชาวิศวกรรมเคมี ภาควิชาวิศวกรรมเคมี
คณะวิศวกรรมศาสตร์ จุฬาลงกรณ์มหาวิทยาลัย
ปีการศึกษา 2556

GRAPHENE-BENZOXAZINE COMPOSITES FOR AN APPLICATION AS BIPOLAR PLATES IN FUEL CELLS

Miss Ratcha Plengudomkit

A Thesis Submitted in Partial Fulfillment of the Requirements
for the Degree of Master of Engineering Program in Chemical Engineering
Department of Chemical Engineering
Faculty of Engineering
Chulalongkorn University
Academic Year 2013

Thesis Title	GRAPHENE-BENZOXAZINE COMPOSITES FOR AN APPLICATION AS BIPOLAR PLATES IN FUEL CELLS
By	Miss Ratcha Plengudomkit
Field of Study	Chemical Engineering
Thesis Advisor	Associate Professor Sarawut Rimdusit, Ph.D.

Accepted by the Faculty of Engineering, Chulalongkorn University in Partial Fulfillment of the Requirements for the Master's Degree

.....Dean of the Faculty of Engineering

(Professor Bundhit Eua-arporn, Ph.D.)

THESIS COMMITTEE

.....Chairman

(Varun Taepaisitphongse, Ph.D.)

.....Thesis Advisor

(Associate Professor Sarawut Rimdusit, Ph.D.)

.....Examiner

(Associate Professor Siriporn Damrongsakkul, Ph.D.)

.....External Examiner

(Sunan Tiptipakorn, D.Eng.)

รัตน์ชา เปล่งอุดมกิจ : คอมโพสิทจากกราฟีนและเบนซอกซาซีนสำหรับประยุกต์ใช้เป็นแผ่นไบโพลาร์ในเซลล์เชื้อเพลิง. (GRAPHENE-BENZOXAZINE COMPOSITES FOR AN APPLICATION AS BIPOLAR PLATES IN FUEL CELLS) อ.ที่ปรึกษาวิทยานิพนธ์หลัก: รศ. ดร.ศราวุธ ริมดุสิต, 91 หน้า.

ในงานวิจัยนี้เป็นการการพัฒนาวัสดุที่เหมาะสมและมีประสิทธิภาพเพื่อนำไปประยุกต์ใช้เป็นแผ่นไบโพลาร์ ที่ใช้ในเซลล์เชื้อเพลิงชนิดเยื่อแลกเปลี่ยนโปรตอน โดยทั่วไปแผ่นไบโพลาร์ที่สามารถนำไปใช้งานได้อย่างมีประสิทธิภาพนั้น ต้องการวัสดุที่มีสมบัติทางความร้อนที่สูง สมบัติทางไฟฟ้าที่สูง และมีสมบัติทางกลที่ดี ดังนั้นในงานวิจัยนี้จึงมีวัตถุประสงค์เพื่อศึกษา สมบัติทางความร้อน สมบัติทางไฟฟ้าและสมบัติทางกลของพอลิเมอร์คอมพอสิท ระหว่างพอลิเบนซอกซาซีนซึ่งใช้เป็นเมทริกซ์และใช้สารเติมเป็นกราฟีนโดยทำการขึ้นรูปภายใต้สภาวะการผสมที่อุณหภูมิ 200 องศาเซลเซียส ความดันจากเครื่องอัดไฮดลอลิกที่ 15 เมกะปาสคาล เป็นเวลา 3 ชั่วโมง เพื่อให้ได้พอลิเมอร์คอมพอสิทที่มีการบ่มตัวอย่างสมบูรณ์ องค์ประกอบของกราฟีนที่เติมลงไปในคอมพอสิทอยู่ในช่วงระหว่าง 10 ถึง 60 เปอร์เซ็นต์ โดยน้ำหนัก โดยพบว่าค่าความหนาแน่นของกราฟีนคอมพอสิทจะอยู่ในช่วง 1.185-1.637 กรัมต่อลูกบาศก์เซนติเมตร ซึ่งเป็นไปตามกฎของการผสม จากการทดลองพบว่าปริมาณการเติมกราฟีนสูงสุดอยู่ที่ 60 เปอร์เซ็นต์โดยน้ำหนัก หรือ 44.8 เปอร์เซ็นโดยปริมาตร ทั้งนี้พบว่าค่ามอดูลัสการสะสมที่อุณหภูมิห้องของระบบพอลิเบนซอกซาซีนคอมพอสิทที่มีปริมาณการเติมกราฟีนสูงสุดข้างต้น มีค่าสูงถึง 25.1 จิกะปาสคาล ซึ่งมีค่าเพิ่มขึ้นจาก ค่ามอดูลัสของพอลิเบนซอกซาซีนบริสุทธิ์ ที่มีค่า 5.9 จิกะปาสคาล ถึง 322 เปอร์เซ็นต์ นอกจากนี้ยังพบว่าอุณหภูมิการเปลี่ยนสถานะคล้ายแก้ว (T_g) ของกราฟีนคอมพอสิทอยู่ในช่วงระหว่าง 174 ถึง 188 องศาเซลเซียส โดยมีค่าเพิ่มขึ้นตามปริมาณกราฟีนที่เพิ่มสูงขึ้นอย่างมีนัยสำคัญ ทั้งนี้เกิดจากความสามารถในการยึดเกาะที่ดีระหว่างอนุภาคกราฟีนและเบนซอกซาซีน นอกจากนี้พบว่าคอมพอสิทที่ได้ มีความสามารถในการนำความร้อนสูงถึง 8.0 วัตต์ต่อเมตรเคลวิล ที่ปริมาณการเติมกราฟีนสูงสุด นอกจากนั้นค่า มอดูลัสของการดัดโค้งและ ค่าความแข็งแรงต่อแรงดัดโค้งของระบบการเติมกราฟีนคอมพอสิท อยู่ที่ 18 จิกะปาสคาลและ 42 เมกกะปาสคาล ตามลำดับ ค่าการดูดซึมน้ำของระบบกราฟีนคอมพอสิทมีค่าประมาณ 0.06 เปอร์เซ็นต์ ที่เวลาผ่านไป 24 ชั่วโมง ซึ่งเป็นค่าที่ค่อนข้างต่ำ นอกจากนี้ยังพบว่าความสามารถในการนำไฟฟ้าของระบบคอมพอสิทที่เติมกราฟีน มีค่าสูงถึง 357 ซีเมนต์ต่อเซนติเมตร ดังนั้นจากข้อมูล สมบัติทางความร้อนที่ค่อนข้างสูง อีกทั้งสมบัติทางไฟฟ้า และสมบัติทางกล มีค่าเป็นไปตามความต้องการของกรมพลังงานของสหรัฐอเมริกา (DOE) จึงทำให้คอมพอสิทระหว่างพอลิเบนซอกซาซีนกับกราฟีนมีความเหมาะสมที่จะนำไปประยุกต์ใช้เป็นแผ่นไบโพลาร์ในเซลล์เชื้อเพลิงชนิดเยื่อแลกเปลี่ยนโปรตอน

ภาควิชา วิศวกรรมเคมี ลายมือชื่อนิสิต .....

สาขาวิชา วิศวกรรมเคมี ลายมือชื่อ อ.ที่ปรึกษาวิทยานิพนธ์หลัก .....

ปีการศึกษา 2556

5570347121 : MAJOR CHEMICAL ENGINEERING
KEYWORDS: POLYMER COMPOSITE / GRAPHENE / FUEL CELL / POLYBENZOXAZINE / BIPOLAR PLATE

RATCHA PLENGUDOMKIT: GRAPHENE-BENZOXAZINE COMPOSITES FOR AN APPLICATION AS BIPOLAR PLATES IN FUEL CELLS. ADVISOR: ASSOC. PROF. DR.SARAWUT RIMDUSIT, 91 pp.

Development of a suitable and efficient bipolar plate material for polymer electrolyte membrane fuel cell (PEMFC) is scientifically and technically important due to the critical demand on higher thermal properties, higher electrical conductivity and higher mechanical properties of this material. This research emphasizes on the development of highly filled graphene-polybenzoxazine composites and investigates thermal, electrical and mechanical properties of the obtained composites. The condition for the compression molding to produce highly filled graphene-polybenzoxazine composites was at temperature of 200°C and a hydraulic pressure of 15 MPa for 3 hours to convince a fully cured composites. The compositions of graphene loading was achieved to be in the range of 10 to 60%wt. The densities of the obtained composites were linearly increased with graphene content and the values were determined to be 1.185-1.637 g/cm^3 which followed the rule of mixture. The experimental results revealed that at the maximum graphene content of 60wt% (44.8vol%) filled in the polybenzoxazine, storage moduli at room temperature of the composites were considerably enhanced with the amount of the graphene i.e. from 5.9 GPa of the neat polybenzoxazine to about 25.1 GPa at 60wt% of graphene, which is about 322% improvement. The glass-transition temperatures (T_g) of the obtained composites were observed to be in the range of 174 to 188°C for graphene-filled composites. The T_g values substantially increased with increasing the filler contents implying substantial interfacial interaction between the filler and the matrix. At the maximum loading of graphene in the composites, thermal conductivity as high as 8.0 W/mK is achieved for a graphene-filled polybenzoxazine. Furthermore, at the maximum graphene content of 60wt%, the flexural modulus and flexural strength of the composites were found to be as high as 18 GPa and 42 MPa, respectively. Water absorption of graphene filled-composite was relatively low with the value of only about 0.06% at 24 hours immersion. Additionally, electrical conductivity were measured to be 357 S/cm at maximum loading of graphene-filled composite. Consequently, the high thermal conductivity and the data on electrical conductivity and mechanical properties of graphene-filled polybenzoxazine composites indicated the values that highly satisfied the United States Department of Energy (DOE) requirements. Therefore, these graphene-filled composites based on polybenzoxazine are highly attractive for bipolar plates in PEMFC applications.

Department: Chemical Engineering Student's Signature .....

Field of Study: Chemical Engineering Advisor's Signature .....

Academic Year: 2013

ACKNOWLEDGEMENTS

I would like to express my sincerest gratitude and deep appreciation to my advisor, Assoc. Prof. Dr.Sarawut Rimdusit, for his kindness, invaluable supervision, guidance, advice, and encouragement throughout the course of this study.

I also gratefully thank Dr. Varun Taepaisitphongse, Assoc. Prof. Dr. Siriporn Damrongsakkul, and Dr. Sunan Tiptipakorn for their invaluable comments as a thesis committee.

This research was supported by the Research, Development and Engineering (RD&E) Fund through National Nanotechnology Center (NANOTEC), National Science and Technology Development Agency (NSTDA), Thailand (Project P-12-00292).

In addition, I would like to thank the Ratchadaphiseksomphot Endowment Fund of Chulalongkorn University (RES560530007-AM), Bangkok, Thailand for financial support and Mektec Manufacturing Corporation (Thailand) Limited for the kind support in the use of laser flash apparatus for thermal conductivity measurement.

Moreover, I would like to extend my grateful thanks to all members of Polymer Engineering Laboratory, Department of Chemical Engineering, Faculty of Engineering, Chulalongkorn University, for their assistance, discussion, and friendly encouragement in solving problems and also to every person whose names cannot be all listed who deserves thanks for encouragement and support.

Finally, I would like to express my deepest regards to my family, particularly my parents, who have always been the source of my unconditional love, understanding, and generous encouragement during my studies.

CONTENTS

Page

THAI ABSTRACT v
ENGLISH ABSTRACT vi
ACKNOWLEDGEMENTS vi
CONTENTS vii
LIST OF TABLES x
LIST OF FIGURE xi
CHAPTER I 1
CHAPTER II 5
THEORY 5
2.1 Fuel Cell 5
2.2 Proton-exchange membrane fuel cell (PEMFC) 6
2.2.1 Operation of a PEMFC 6
2.2.2 PEMFC Components 8
2.4 Bipolar Plate Development 13
2.4.1. Non-Porous Graphite Bipolar Plates 13
2.4.2 Metallic Bipolar Plates 15
2.4.3 Composite Bipolar Plate 16
2.5 Graphene 19
2.6 Benzoxazine Resin 23
CHAPTER III 26
LITERATURE REVIEWS 26
CHAPTER IV 35
EXPERIMENTAL 35
4.1 Materials and Monomer Preparation 35
4.1.1 Benzoxazine Monomer Preparation 35
4.1.2 Graphene Characteristics 35
4.2 Specimen Preparation 36

Page

4.3 Characterization Methods 37
4.3.1 Differential Scanning Calorimetry (DSC) 37
4.3.2 Density Measurement 37
4.3.3 Dynamic Mechanical Analysis (DMA) 38
4.3.4 Thermogravimetric Analysis (TGA) 38
4.3.5 Specific Heat Capacity Measurement 39
4.3.6 Thermal Diffusion Measurement 39
4.3.7 Thermal Conductivity Measurement 39
4.3.8 Flexural Properties Measurement 40
4.3.9 Water Absorption 40
4.3.10 Electrical Conductivity Measurement 41
4.3.11 Scanning Electron Microscope (SEM) 41
CHAPTER V 42
RESULTS AND DISCUSSION 42
5.1 Curing Behavior of Benzoxazine Resin Filled with Graphene Curing Condition 42
5.2 Actual Density and Theoretical Density Measurement of Highly Filled Graphene-Polybenzoxazine Composites 43
5.3 Dynamic Mechanical Properties of Highly Filled Graphene-Polybenzoxazine Composites 44
5.4 Effect of Graphene Loading on Thermal Stability of Highly Filled Graphene-Polybenzoxazine Composites 46
5.5 Specific Heat Capacity of Highly Filled Graphene-Polybenzoxazine Composites at Various Graphene Contents 47
5.6 Effects of Graphene Contents on Thermal Diffusivity of Highly Filled Graphene-Polybenzoxazine Composites 48
5.7 Thermal Conductivity of Highly Filled Graphene-Polybenzoxazine Composites 50

Page

5.8 Effect of the Graphene Loading on Flexural Properties of Highly-Filled Graphene-Polybenzoxazine Composites 51
5.9 Water Absorption of Polybenzoxazine and Graphene-Filled Polybenzoxazine Composites at Various Graphene Contents 53
5.10 Electrical Conductivity of Highly Filled Graphene-Polybenzoxazine Composites 54
5.11 SEM Characterization of Highly Filled Graphene-Polybenzoxazine Composites 55
CHAPTER VI 81
CONCLUSIONS 81
REFERENCES 83
APPENDIX 88
VITA 91

LIST OF TABLES

Page

Table 2. 1 Types of fuel cells and their features 5

Table 2. 2 US DOE technical targets for composite bipolar plates 12

Table 2. 3 Properties of graphene. 20

Table 2. 4 Properties of aromatic amines 25

Table 2. 5 Properties of arylamine-based benzoxazine resin 25

Table 3. 1 Polymer composites systems with thermal conductivity value 31

Table 4. 1 Typical Properties of xGNP Graphene Nanoplatelets 36

Table 5. 1 Thermal characteristics of polybenzoxazine and graphene-filled polybenzoxazine composites 66

Table 5. 2 Specific heat capacity values of graphene-filled polybenzoxazine at different graphene contents 69

Table 5. 3 Thermal conductivity of highly filled-graphene polybenzoxazine composites at 25^{o}C 72

LIST OF FIGURE

Page

Figure 2. 1 Diagram of a PEM fuel cell 7

Figure 2. 2 Fuel cell stack 8

Figure 2. 3 MEA Schematic 9

Figure 2. 4 A simple flow field plate with a serpentine flow channel. 11

Figure 2. 5 Classification of materials for bipolar plates used in PEM fuel cells 13

Figure 2. 6 Graphite bipolar plate 14

Figure 2. 7 Metallic bipolar plate 15

Figure 2. 8 Composites bipolar plates 17

Figure 2. 9 Graphene powder 19

Figure 2. 10 Synthesis route of BA-a-type benzoxazine resin. 24

Figure 2. 11 Formation of polybenzoxazine resin network by thermal curing process 24

Figure 3. 1 The electrical conductivity versus filler content for PET/graphene nanocomposites and PET/graphite composites 26

Figure 3. 2 Damping behavior of neat epoxy and epoxy/graphene nanocomposites 27

Figure 3. 3 TGA and DTG thermograms for the unfilled solid (PC) and graphene reinforced solid polycarbonate (PCg) 28

Figure 3. 4 Flexural properties of PPS/GNP nanocomposites made by Solid state ball mill 29

Figure 3. 5 Thermal conductivity of EGNP/epoxy composites 30

Figure 3. 6 Thermal conductivity of boron nitride-filled polybenzoxazine as a function of filler contents 32

Figure 3. 7 Thermal conductivity at 25°C of graphite-filled polybenzoxazine as a function of filler contents 33

Figure 3. 8 Effect of the graphite content on electrical conductivity (in-plane) of graphite-filled polybenzoxazine composites..... 34

Figure 5. 1 DSC thermograms of benzoxazine molding compound at different graphene contents: (●) neat polybenzoxazine, (■) 10wt%, (◢) 20wt%, (◣) 30wt%, (♦) 40wt%, (▼) 50wt%, (▲) 60wt%..... 57

Figure 5. 2 DSC thermograms of the composite at 10wt% of graphene content with various curing times at 200°C: (●) uncured molding compound, (■) 1 hour, (◢) 2 hours, (♦) 3 hours. 58

Figure 5. 3 FTIR spectra of as-received graphene-grade H from XG Sciences, USA use in this research..... 59

Figure 5. 4 Theoretical and actual densities of graphene-filled polybenzoxazine composites at different contents of graphene: (●) theoretical density, (O) actual density. 60

Figure 5. 5 DMA thermograms of storage modulus of graphene-filled polybenzoxazine composites: (●) neat polybenzoxazine, (■) 10wt%, (◢) 20wt%, (◣) 30wt%, (♦) 40wt%, (▼) 50wt%, (▲) 60wt%. 61

Figure 5. 6 DMA thermograms of loss modulus of graphene-filled polybenzoxazine composites: (●) neat polybenzoxazine, (■) 10wt%, (◢) 20wt%, (◣) 30wt%, (♦) 40wt%, (▼) 50wt%, (▲) 60wt%. 62

Figure 5. 7 DMA thermograms of loss tangent of graphene-filled polybenzoxazine composites: (●) neat polybenzoxazine, (■) 10wt%, (◢) 20wt%, (◣) 30wt%, (♦) 40wt%, (▼) 50wt%, (▲) 60wt%. 63

Figure 5. 8 TGA thermograms of graphene-filled polybenzoxazine composites: (●) neat polybenzoxazine (■) 10wt%, (◢) 20wt%, (◣) 30wt%, (♦) 40wt%, (▼) 50wt%, (▲) 60wt%, (O) neat graphene..... 64

Figure 5. 9 Calculation and experimental char yield at 800^{o}C of graphene-filled polybenzoxazine composites at difference graphene contents: (O) theoretical char yield, (●) experimental char yield..... 65

Figure 5. 10 Specific heat capacity of graphene-filled polybenzoxazine composites: (●) neat polybenzoxazine (■) 10wt%, (◢) 20wt%, (◣) 30wt%, (♦) 40wt%, (▼) 50wt%, (▲) 60wt%, (O) neat graphene..... 67

Figure 5. 11 Specific heat capacity extrapolated at 25^{o}C of graphene-filled polybenzoxazine as a function of graphene contents..... 68

Figure 5. 12 Thermal diffusivity at 25^{o}C of graphene-filled polybenzoxazine as a function of graphene contents..... 70

Figure 5. 13 Thermal diffusivity of graphene-filled polybenzoxazine composites: (●) neat polybenzoxazine (■) 10wt%, (◢) 20wt%, (◣) 30wt%, (♦) 40wt%, (▼) 50wt%, (▲) 60wt%..... 71

Figure 5. 14 Thermal conductivity at 25^{o}C of highly filled graphene-polybenzoxazine composites as a function of graphene contents..... 73

Figure 5. 15 Relation between graphene contents and the flexural modulus of graphene-filled polybenzoxazine composites..... 74

Figure 5. 16 Relation between filler contents and the flexural strength of graphene-filled polybenzoxazine composites..... 75

Figure 5. 17 Water absorption of graphene-filled polybenzoxazine composites: (●) neat polybenzoxazine, (■) 10wt%, (◢) 20wt%, (◣) 30wt%, (♦) 40wt%, (▼) 50wt%, (▲) 60wt%..... 76

Figure 5. 18 Effect of the graphene contents on electrical conductivity (in-plane) of highly filled graphene-polybenzoxazine composites..... 77

Figure 5. 19 SEM micrograph of graphene-grade H from XG Sciences, USA used in this research..... 78

Figure 5. 20 SEM micrographs of fracture surface of graphene-filled polybenzoxazine composites: (a) neat polybenzoxazine (PBZ), (b) 1wt% graphene-filled PBZ, (c)

10wt% graphene-filled PBZ, (d) 20wt% graphene-filled PBZ, (e) 30wt% graphene-filled PBZ, (f) 40wt% graphene-filled PBZ, (g) 50wt% graphene-filled PBZ, (h) 60wt% graphene-filled PBZ..... 80

CHAPTER I

INTRODUCTION

1.1 General Introduction

The polymer electrolyte membrane fuel cell (PEMFC) have been known as the most promising alternative source of energy due to their high efficiency and zero emission [1]. The features of PEMFC are high power density, low temperature operation (50-80^{o}C) and no pollutant release [2].

The bipolar plate is an important part of PEMFC which account for 40-50% of the cost and 60-80% of total weight of fuel cell stacks. Therefore, the bipolar plate requires to be lightweight and inexpensive but should have good chemical compatibility with the oxidation/reduction environment of PEMFC. The main functions of bipolar plate include carrying current away from each fuel cell, distributing gas fuels within the cell and providing support for the Membrane Electrode Assembly (MEA) [3]. Department of energy, USA proposed a technical targets of bipolar plates for the year 2010, in which the main requirements are flexural modulus > 10 GPa, flexural strength > 25 MPa, electrical conductivity > 100 S/cm, thermal conductivity > 10 W/mK and weight < 0.4 kg/kW [4].

In the past, the most commonly used material for bipolar plate is graphite, because it possesses high electrical conductivity, excellent resistance to fuel cell environment. However, it has low mechanical strength and brittleness. Moreover, graphite bipolar plate limits to have several millimeters in thickness, which make the fuel cell stack to be heavy and voluminous [5]. In order to solve this problem, the graphite plates were replaced by the polymer composite bipolar plates. The main drawback to polymer composite is the lack of electrical conductivity. To enhance the electrical conductivity of bipolar plates, polymer composites were achieved by incorporating a conductive filler into a polymer matrix. Carbon black, carbon fibers, metallic fiber and metallic powder are principle conductive fillers but graphite is the most popular one due to its outstanding properties as aforementioned. Thus, several

researches have been referred to as graphite filled in polymer matrix for bipolar plate as can be seen in research of I. Dueramae et al. [6], H. Kimura et al. [7] and S. R. Dhakate et al. [8].

Recently, graphene was first achieved in 2004 by Prof. Andre Geim and Prof. Konstantin Novoselov at the University of Manchester, UK. Graphene, a two-dimensional (2-D) sheet composed of sp^2 carbon atoms arranged in a honeycomb structure, has been explored to be an excellent material due to its reported excellent mechanical strength (Young's modulus of 1 TPa, ultimate strength of 130 GPa), large specific area (theoretical limit: 2630 m^2/g) and low gas permeability. Especially, graphene exhibits a superior electrical conductivity (>6000 S/cm) and high thermal conductivity (5000 W/mK); thus, it gains much attention for bipolar plate utilization [2].

Two different main types of resins have been used to fabricate composite plates are thermoplastic and thermosetting. The thermosetting is more popular than thermoplastic because it has low viscosity and thereby it can contain a higher proportion of conductive filler. Polybenzoxazines are a novel class of thermosetting polymers which offer a number of attractive properties such as very low melt viscosity, high glass transition temperature, high thermal stability, good mechanical strength and modulus, low water absorption, low dielectric constant, good adhesive properties, high resistance to burning and chemicals and no by-product release during cure [9], [10]. The very low melt viscosity and good adhesion of benzoxazine resin results in its ease of filler mixing during the molding compound preparation thus giving its outstanding characteristics as matrix materials for composite fabrication.

In this research, had been prepared the highly filled system of graphene-polybenzoxazine composites and the influences of graphene contents on physical, mechanical, electrical, and thermal properties of graphene-polybenzoxazine composites had been investigated for an application as bipolar plates in PEMFC fuel cells.

1.2 Objectives

1.2.1 To examine the graphene-filled composites based on benzoxazine resin for an application as bipolar plates in fuel cell.

1.2.2 To investigate the maximum packing of the graphene-filled composites based on benzoxazine resin.

1.2.3 To evaluate the effects of graphene contents on electrical, thermal and mechanical properties of composites based on benzoxazine resin.

1.3 Scopes of the study

1.3.1 Synthesis of benzoxazine resin by solventless technology.

1.3.2 Determination of the optimum composition of graphene filled benzoxazine by varying composition of graphene at 0, 10, 20, 30wt%,..., maximum packing density.

1.3.3 Studying adhesion properties between graphene and benzoxazine resin.

1.3.4 Investigation of physical, electrical, thermal and mechanical properties of the graphene filled composites based on benzoxazine resin.

1.3.5 Evaluation of properties of the graphene based benzoxazine composites by

1.3.5.1 Dynamic Mechanical Analyzer (DMA)

1.3.5.2 Universal testing machine (Flexural mode)

1.3.5.3 Differential Scanning Calorimeter (DSC)

1.3.5.4 Thermogravimetric Analysis (TGA)

1.3.5.5 Thermal conductivity measuring apparatus

1.3.5.6 Electrical conductivity measurement

1.3.5.7 Density Accessory Kit

1.3.5.8 Scanning Electron Microscope (SEM)

1.4 Procedures of the study

1.4.1 Reviewing related literatures.

1.4.2 Preparation of chemicals and equipment for using in this research such as Graphene, Bisphenol-A, Formaldehyde, Aniline, etc.

1.4.3 Synthesis of benzoxazine resins (BA-a).

1.4.4 Preparation of the graphene-filled composites based on benzoxazine resin by varying composition of graphene at 0, 10, 20, 30wt%,..., maximum packing density.

1.4.5 Determine the physical properties of the graphene-filled composites based on benzoxazine resin (density, water absorption, and fracture surface).

1.4.6 Determine the mechanical properties (flexural properties).

1.4.7 Determine the thermal properties (glass transition temperature, thermal degradation temperature, thermal conductivity).

1.4.8 Determine the electrical property (electrical conductivity).

1.4.9 Analyze and conclude the experimental results.

1.4.10 Preparation of the final report.

CHAPTER II

THEORY

2.1 Fuel Cell

The fuel cell is an electrochemical energy device that converts chemical energy, from typically hydrogen, directly into electrical energy [5]. Fuel cells are expected to play a major role in the economy of this century and for the foreseeable future. It is anticipated that the development and deployment of economical and reliable fuel cells would usher in the sustainable hydrogen age [11].

Table 2. 1 lists the main features of the five main types of fuel cells summarized. Each of them has advantages and disadvantages relative to each other [12].

Table 2. 1 Types of fuel cells and their features.

Type of Fuel Cell	Operating Temp. (^{o}C)	Power Density (mW/cm^2)	Fuel Efficiency (Chem. to Elec.)	Lifetime (hr)	Capital Cost ($/kW)	Area of Applications
PEMFC	50 - 80	350	45 - 60	>10,000	>200	Portable, Mobile, Stationary
AFC	60 - 90	100 - 200	40 - 60	>10,000	>200	Space, Mobile
PAFC	160 - 220	200	55	>40,000	3000	Distributed Power
MCFC	600 - 700	100	60 - 65	>40,000	1000	Distributed Power Generation
SOFC	800 - 1000	240	55 - 65	>40,000	1500	Baseload Power Genertion

Note: PEMFC is Proton-exchange membrane fuel cell
AFC is Alkaline fuel cell
PAFC is Phosphoric acid fuel cell
MCFC is Molten carbonate fuel cell
SOFC is Solid oxide fuel cell

2.2 Proton-exchange membrane fuel cell (PEMFC)

The polymer electrolyte membrane fuel cells (PEMFCs) have been known as the most promising alternative source of energy due to their high efficiency and zero emission. Proton exchange membrane fuel cells deliver high-power density and offer the advantages of low weight and volume, compared with other fuel cells [12]. PEMFC use a solid polymer as an electrolyte and porous carbon electrodes containing a platinum catalyst. They need only hydrogen, oxygen from the air to operate and do not require corrosive fluids like some fuel cells. They are typically fueled with pure hydrogen supplied from storage tanks or on-board reformers [13].

PEMFCs operate at relatively low temperature, around 80°C (176°F). Low-temperature operation allows them to start quickly (less warm-up time) and results in less wear on system components, resulting in better durability. However, it requires that a noble-metal catalyst (typically platinum) be used to separate the hydrogen's electrons and protons, adding to system cost. The platinum catalyst is also extremely sensitive to CO poisoning, making it necessary to employ an additional reactor to reduce CO in the fuel gas if the hydrogen is derived from an alcohol or hydrocarbon fuels. This also adds cost. Developers are currently exploring platinum/ruthenium catalysts that are more resistant to CO.

PEMFCs are used primarily for transportation applications and some stationary applications. Due to their fast startup time, low sensitivity to orientation, and favorable power-to-weight ratio, PEM fuel cells are particularly suitable for use in passenger vehicles, such as cars and buses.

2.2.1 Operation of a PEMFC

At this time, hydrogen is the fuel of choice for high performance of fuel cell applications. Hydrogen powered fuel cells are also the “greenest” fuel cells since their only product is water. One advantage of hydrogen is that it easily undergoes catalyzed reactions under mild conditions [14].

The electrochemical reactions in fuel cells happen simultaneously on both sides of a membrane (the anode and the cathode). The basic PEM fuel cell reactions are shown as follows [11].

Figure 2. 1 shows a schematic of a PEMFC operation to gain a fundamental understanding of the polymer electrolyte membrane fuel cell technology.

At the anode, hydrogen is oxidized to liberate two electrons and two protons, producing the reaction (2.1).

$$H_2 \longrightarrow 2H^+ + 2e^- \tag{2.1}$$

The protons are conducted from the catalyst layer through the proton exchange membrane and the electrons travel through the external electronic circuit. At the cathode, oxygen permeates to the catalyst sites where it reacts with the protons and electrons when properly hydrated, producing the reaction (2.2).

$$\frac{1}{2}O_2 + 2H^+ + 2e^- \longrightarrow H_2O + 286\ kJ/mol \tag{2. 2}$$

The overall cell reaction is:

$$H_2 + \frac{1}{2}O_2 \longrightarrow H_2O + 286\ kJ/mol \tag{2. 3}$$

Consequently, the products of the PEMFC reactions are water, electricity and heat.

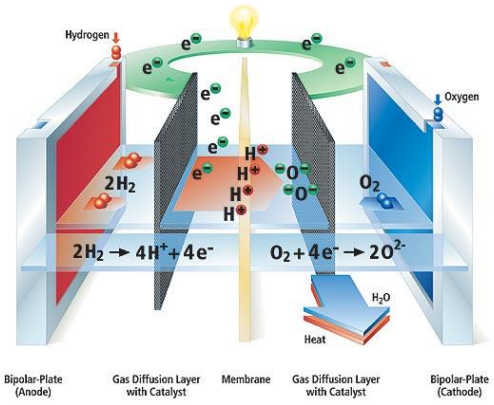

Figure 2. 1 Diagram of a PEM fuel cell [15].

2.2.2 PEMFC Components

A single fuel cell is only capable of producing about 1 volt, so typical fuel cell designs link together many individual cells to form a stack to produce a more useful voltage. A fuel cell stack can be configured with many groups of cells in series and parallel connections to further tailor the voltage, current, and power. The number of individual cells contained within one stack is typically greater than 50 and varies significantly with stack design [1].

The basic components of the fuel cell stack include the electrodes and electrolyte with additional components required for electrical connections and/or insulation and the flow of fuel and oxidant. These key components include current collectors and separator plates. The current collectors conduct electrons from the anode to the separator plate. The separator plates provide the electrical series connections between cells and physically separate the oxidant flow of one cell from the fuel flow of the adjacent cell. The channels in the current collectors serve as the distribution pathways for the fuel and oxidant. Often, the two current collectors and the separator plate are combined into a single unit called a bipolar plate.

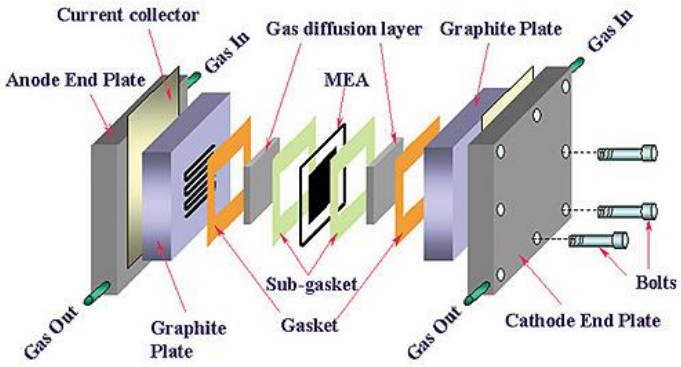

Figure 2. 2 Fuel cell stack [16].

The basic components of the fuel cell stack.

Membrane Electrode Assembly (MEA)

In the case of a PEMFC, the MEA is the heart of a PEM fuel cell. The membrane electrode assembly consists of two electrically and ionically conductive electrodes containing the platinum catalyst bonded to the proton exchange membrane (PEM). A schematic of the MEA with accompanying electrochemical reactions is shown in Figure 2. 3.

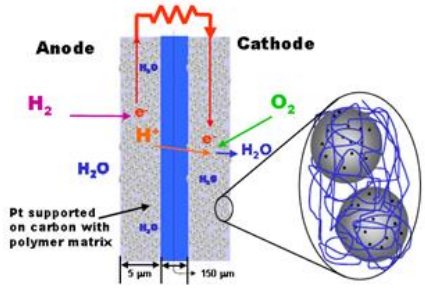

Figure 2. 3 MEA Schematic [14].

Polymer electrolyte membrane

The polymer electrolyte membrane (PEM) is a specially treated material that conducts only positively charged ions and blocks the electrons. The PEM is the key to the fuel cell technology; it must permit only the necessary ions to pass between the anode and cathode. Other substances passing through the electrolyte would disrupt the chemical reaction.

The thickness of the membrane in a membrane electrode assembly can vary with the type of membrane. The thickness of the catalyst layers depends upon how much platinum (Pt) is used in each electrode.

Electrode

An electric conductor through which an electric current enters or leaves a medium, whether it be an electrolytic solution, solid, molten mass, gas, or vacuum.

- **Anode**

The anode is the negative side of the fuel cell. It conducts the electrons that are freed from the hydrogen molecules so they can be used in an external circuit. Channels etched into the anode disperse the hydrogen gas equally over the surface of the catalyst.

- **Cathode**

The cathode, the positive side of the fuel cell, also contains channels that distribute the oxygen to the surface of the catalyst. It conducts the electrons back from the external circuit to the catalyst, where they can recombine with the hydrogen ions and oxygen to form water.

Catalyst

All electrochemical reactions in a fuel cell consist of two separate reactions: an oxidation half-reaction at the anode and a reduction half-reaction at the cathode. Normally, the two half-reactions would occur very slowly at the low operating temperature of the PEM fuel cell. Each of the electrodes is coated on one side with a catalyst layer that speeds up the reaction of oxygen and hydrogen. It is usually made of platinum powder very thinly coated onto carbon paper or cloth. The catalyst is rough and porous so the maximum surface area of the platinum can be exposed to the hydrogen or oxygen.

Bipolar Plates or Flow Field Plates

Flow field plates feature flow channels for reactant distribution over the active cell are and water removal, and provide an electrical interconnection between the porous transport layers and outer components. Furthermore, flow field plates conduct heat and provide mechanical support for more flexible cell components, such as Porous Transport. Layers (PTLs) and Membrane Electrode Assembly (MEA) [17].

Flow field plates in a fuel cell stack are often referred to as bipolar plates, because they act as an anode side plate for one unit cell and cathode side plate for another separating reactants and connecting adjacent cells electrically.

Bipolar plate or conductive plate in a fuel cell stack acts as an anode for one cell and a cathode for the adjacent cell. Bipolar plates represent one of the most important of the stack with about 80% of total weight and 45% of stack cost [18]. The bipolar plate is multifunctional component within the PEMFC as described below [1], [5], [18].

- Connecting individual fuel cells in series to form a fuel cell stack of the required voltage.
- Transporting collecting electrons from the anode and cathode.
- Providing a flow path for gas transport to distribute the gases over the entire electrode area uniformly.
- Separating oxidant and fuel gases and feeding H_2 to the anode and O_2 to the cathode, while removing product water and un-reacted gases.
- Providing thermal conduction to help regulate fuel cell temperature and removing heat from the electrode to the cooling channels.
- Providing mechanical strength and rigidity to support the thin membrane and electrodes and clamping forces for the stack assembly.
- Sealing fluids with port seals and MEA seals to avoid fluid leakage.

Figure 2. 4 A simple flow field plate with a serpentine flow channel [17].

The materials of the bipolar plate must have particular properties because of its responsibilities and the challenging environment in which the fuel cell operates. Properties of material must be considered for achievable design for a fuel cell application, specifically, electrical and thermal conductivity, gas permeability, mechanical strength, corrosion resistance and low weight. An ideal material should combine the following characteristics that are defined by Department of Energy (DOE) of the US as shown in Table 2. 2.

Table 2. 2 US DOE technical targets for composite bipolar plates [4], [5]

DOE 2010/2020 Performance Targets of Bipolar Plates for Transportation Fuel Cells			
Properties	Units	2010 Target	2020 Target
Electrical conductivity(bulk)	S/cm	>100	>100
Thermal conductivity	W/mK	>10	-
Flexural strength	MPa	>25	>25
Flexural flexibility	Percent (deflection at midspan)	3-5	3-5
Hydrogen permeation rate	Std. cm^3 /sec cm^2 Pa at 80^{O}C, 3 atm 100% RH	$<2\times10^{-6}$	$<2\times10^{-14}$
Water absorption	%	<0.3	<0.3
Weight	Kg/kW	<0.4	-
Cost	$/kW	5	3

2.4 Bipolar Plate Development

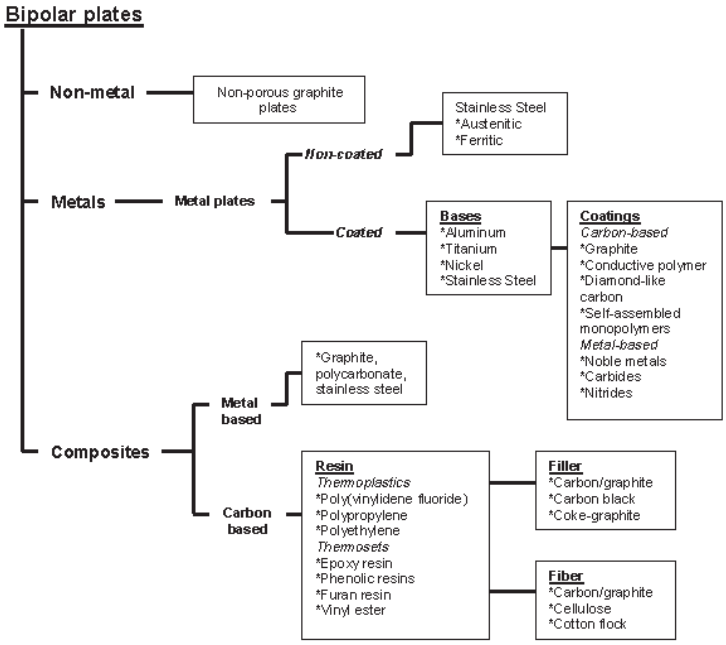

Figure 2. 5 Classification of materials for bipolar plates used in PEM fuel cells [10].

Currently, efforts to improve the PEMFC cost and reliability for the industry, including the automotive industry, comprise of reducing the cost and weight of the fuel cell stack. The bipolar plates in the stack require significant improvement, since bipolar plates account for approximately 80% of the PEMFC weight, and 45% of the stack. Accordingly, the development of bipolar plates may present opportunities for cost and weight reductions in PEMFCs. Moreover, bipolar plate characteristic requirements are a challenge for any class of materials, and none fits the profile characteristics exactly.

2.4.1. Non-Porous Graphite Bipolar Plates

Bipolar plates in the PEMFC have traditionally been made from graphite, since graphite has excellent chemical stability to survive the fuel cell environment. Other advantages of graphite are its excellent resistance to corrosion, low bulk resistivity, low specific density, and low electrical contact resistance with electrode backing materials. This low contact resistance results in high electrochemical power output. The disadvantages of graphite plates are their high cost, the difficulty of machining them,

their porosity, and their low mechanical strength (brittleness). Bipolar plates have traditionally been created from graphitic carbon impregnated with a resin or subjected to pyrolytic impregnation. A thermal treatment is used in the process to seal the pores. This seal renders the bipolar plates impermeable to fuel and oxygen gases. This type of bipolar plate is available in the fuel cell market from the likes of POCO Graphite and SGL Carbon. Due to the brittle nature of graphite, graphite plates used in fuel cell stacks must typically be several millimeters thick, which add to the volume and weight of the stack.

In order to solve this problem, flexible graphite was considered the material of choice for bipolar plates in PEMFC. Flexible graphite is made from a polymer/graphite composite, in which the polymer acts as a binder. The graphite principally used for the composite is expanded graphite (EG), produced from graphite flakes intercalated with highly concentrated acid. The flakes can be expanded up to a few hundred times their initial volume. The expansion leads to a separation of the graphite sheets into nano-platelets with a very high aspect ratio. This layered structure gives higher electrical and thermal conductivity. The expanded form is then compressed to the desired density and pressed to form the bipolar plate. In comparison to conventional graphite bipolar plates, the bipolar plates produced from EG are thinner [18], [19].

Figure 2. 6 Graphite bipolar plate [20].

2.4.2 Metallic Bipolar Plates

Metals, as sheets, are potential candidates for bipolar plate material since they have good mechanical stability, electrical and thermal conductivity and gas impermeability. Probably the most important benefit is that the resultant stack can be smaller and lighter than graphite bipolar plates. Two advantages the metallic plates that they can be stamped to accommodate flow channels and that the resultant plate can be varied thick, for example 100 μm. However, the main disadvantage of metal plates is their susceptibility to corrosion and dissolution in the fuel cell operating environment of 80°C and a pH of 2-3. This corrosion is harmful to fuel cell performance for the following reasons. First, surface oxide creation significantly enlarges the contact resistance between the plate and the GDL. Second, the corrosion process changes the morphology of the surface, potentially reducing the contact area with the GDLs. Lastly, when the metal plate is dissolved, and the dissolved metal ions diffuse into the PEM membrane and become trapped in the ion exchange sites. This trapping results in ionic conductivity diminution, leading to increased membrane degradation. To solve these issues, researchers have considered of non-coated metal alloys, precious non-coated metals, and coated metals with a protective layer. Metals investigated include aluminum, stainless steel, titanium and nickel [10], [18], [19], [21].

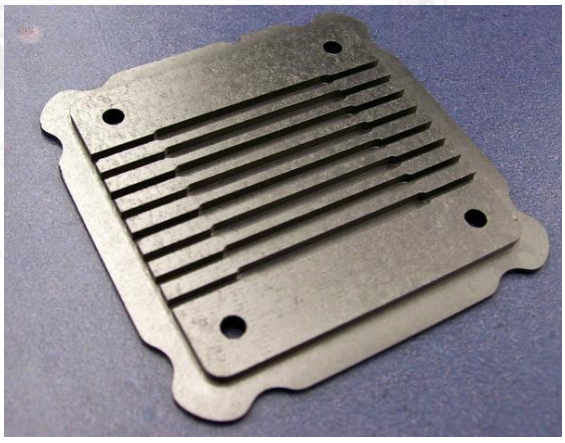

Figure 2. 7 Metallic bipolar plate [22].

2.4.2.1 Non-coated

Stainless steels (SSs) are the only material in this category to have received considerable attention due to their relatively high strength, high chemical stability, low gas permeability, wide range of alloy choice, and applicability to mass production and low cost. Major concerns have been extent of corrosion (and its products) and the contact resistance of the surface passivation film. Candidate SSs have been tested and used as BPs by different authors which showed that corrosion rate is low and PEM cell output is stable for thousands of hours.

2.4.2.2 Coated

Aluminum, stainless steel, titanium and nickel are considered as possible alternative materials for BP in PEM fuel cells. To avoid corrosion, metallic BPs are coated with protective coating layers. Coatings should be conductive and adhere to the base metal without exposing it. Further the coefficient of thermal expansion of the base metal and the coating should be as close as possible to eliminate the formation of micro-pores and micro-cracks in coatings due to unequal expansion. Two types of coatings, carbon-based and metal-based, have been investigated. Carbon-based coatings include graphite, conductive polymer, diamond-like carbon and organic self-assembled monopolymers. Noble metals, metal nitrides and metal carbides are some of the metal-based coatings.

2.4.3 Composite Bipolar Plate

The composite as a unique material normally refers to hybrid or mixed materials between dispersed filler or reinforcement in the form of fiber, powder, flake, etc. and the continuous matrix [1]. Thermoplastic or thermosetting composites are beneficial over metallic and traditional graphite materials with regard to corrosion resistance, flexible and low weight. In addition, polymer composites may be produced in economical processes, such as compression, transfer or injection molding processes, depending on the number of units to be manufactured. The main drawback to polymer composite is the lack of electrical conductivity. To enhance the electrical conductivity of the bipolar plates, electrically conductive polymeric materials have been used as

bipolar plate materials. Electrically conductive polymeric materials are organic based materials that permit electron transfer.

According to the electrically conductive structure, conductive polymeric materials can be divided into two categories: intrinsically conducting polymers (ICPs) and conductive polymeric composites (CPCs). ICPs are organic polymer semiconductors. Electrical conductivity is realized by the presence of chain unsaturation and electron delocalization effects. Much research effort and interest have therefore been devoted towards the development of polymers with intrinsic electrical conduction characteristics brought about by the presence of the conjugated group and by doping techniques. ICPs can be used for a few applications due to their poor production and the high manufacturing costs, although they own terrific conductive performance. In terms of CPCs, composite materials for bipolar plates can be categorized as metal or carbon-based. The combination of conventional polymers (ABS, PC, PP, and etc.) with conductive loads of fillers (e.g. carbon black or carbon fibers, metallic or metallic fibers, metallic powders) allows the creation of new polymeric composite materials with unique electrical properties. CPCs are advantageous over ICPs with regards to because of the large-scale variation in the conductivity, the favorable processability and low costs. However, CPCs would not be successful to improve conductive and mechanical performance simultaneously for the reason that high filler concentration improves on conductive performance but it deteriorates on mechanical performance [5].

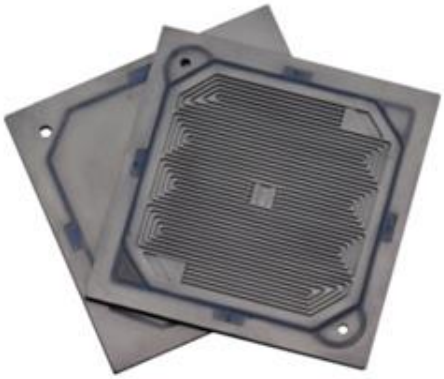

Figure 2. 8 Composites bipolar plates [23].

2.4.3.1 Metal-based Bipolar Plates

Metal-based bipolar plates are made of multiple materials, such as stainless steel, plastic, or porous graphite, so that the benefits of different materials can be harvested in a single bipolar plate. One of the main advantages of porous graphite bipolar plates is the production low cost. Los Alamos National Laboratory has developed a metal based composite bipolar plate based on porous graphite, polycarbonate plastic and stainless steel Stainless steel also provides rigidity to the structure while the graphite resists corrosion. The polycarbonate provides chemical resistance and can be molded to any shape to provide for gaskets and manifolding. The layered plate appears to be a very good alternative from stability and cost standpoints.

2.4.3.2 Carbon-based Bipolar Plates

Carbon-polymer composites are created by incorporating a carbonaceous material into a polymer binder. The preference for the polymer binder is governed by the chemical compatibility with the fuel-cell environment, mechanical and thermal stability, processability when loaded with conductive filler, and cost. Two different main types of resins are used to fabricate composite plates: thermoplastic and thermosetting. Among the thermosetting resins, such as phenolics, epoxies, polyester, and vinyl ester, etc., the epoxy resin is a popular choice for carbon-polymer bipolar plate production. The thermosetting resins have low viscosity, and thereby contain a higher proportion of conductive fillers. During the molding process, the thermosetting resin allows for molding of intricate details. Moreover, the resins can be highly cross-linked through a proper curing process, and the cross-linked structure gives good chemical resistance.

2.5 Graphene

Graphene is a fascinating material with many potential properties. In 2004, graphene is discovered by Prof. Andre Geim and Prof. Konstantin Novoselov at the University of Manchester. Graphene is single layer sheet of a two-dimensional sp^2-bonded carbon atoms arranged in a honeycomb crystal lattice. Graphene is basic structural unit for other carbon naonofiller such as wrapped to form 0-D fullerenes rolled to form 1-D carbon nanotubes, stacked to form 3-D graphite. The carbon-carbon bond length in graphene is about 0.142 nanometers. The graphene layer thickness ranges from 35 to 1 nanometers. Graphene has several advantages. Graphene is the strongest material with Young's Modulus of 1 TPa and ultimate strength of 130 GPa. It has very high electrical conductivity (>6000 S/cm), thermal conductivity (5000 W/mK), surface area (2630 m^2/g), elasticity and gas impermeability [2]. These properties indicate graphene has a potential for improving mechanical, thermal, electrical and gas barrier properties of polymer mean that graphene can be mixed with polymer to make composites which good physical properties.

Figure 2. 9 Graphene powder [24].

Properties of graphene [25]

2.5.1 Electronic Properties

Graphene is great conductor; electrons are able to flow through graphene more easily than through even copper. The electrons travel through the graphene sheet as if they carry no mass, as fast as just one hundredth that of the speed of light.

Graphene is a perfect thermal conductor. Its thermal conductivity was measured recently at room temperature and it is much higher than the value observed in all the other carbon structures as carbon nanotubes, graphite and diamond (> 5000 W/mK).

Table 2. 3 Properties of graphene [2].

Properties	**Values**
Physical properties	
Chemical formula	C
Color	Black
Crystal structure	Hexagonal
Density (ρ)	2.2 g/cm^3
Carbon-carbon bond length	0.142 nm
Thickness	35-1 nm
Extremely high surface area	2630 m^2/g
Low gas permeability	
High chemical and corrosion resistance	
Electrical property	
Electrical conductivity	> 6000 S/cm
Thermal properties	
Thermal conductivity	5000 W/mK in-plane
Low coefficient of thermal expansion	1×10^{-6} K^{-1}
Mechanical properties	
Mechanical properties	Young's modulus (1 TPa), Ultimate strength (130 GPa)

The ballistic thermal conductance of graphene is isotropic, i.e. same in all directions. Similarly to all the other physical properties of this material, its 2-D structure make it particularly special. Graphite, the 3-D version of graphene, shows a thermal conductivity about 5 times smaller (1000 W/mK). The phenomenon is governed by the presence of elastic waves propagating in the graphene lattice, called phonons.

The study of thermal conductivity in graphene may have important implications in graphene-based electronic devices. As devices continue to shrink and circuit density increases, high thermal conductivity, which is essential for dissipating heat efficiently to keep electronics cool, plays an increasingly larger role in device reliability.

2.5.2 Thermal and thermoelectric properties

Graphene is a perfect thermal conductor. Its thermal conductivity was measured recently at room temperature and it is much higher than the value observed in all the other carbon structures as carbon nanotubes, graphite and diamond (> 5000 W/mK). The ballistic thermal conductance of graphene is isotropic, i.e. same in all directions. Similarly to all the other physical properties of this material, its 2-D structure make it particularly special. Graphite, the 3-D version of graphene, shows a thermal conductivity about 5 times smaller (1000 W/mK). The phenomenon is governed by the presence of elastic waves propagating in the graphene lattice, called phonons.

The study of thermal conductivity in graphene may have important implications in graphene-based electronic devices. As devices continue to shrink and circuit density increases, high thermal conductivity, which is essential for dissipating heat efficiently to keep electronics cool, plays an increasingly larger role in device reliability.

2.5.3 Mechanical properties

To calculate the strength of graphene, scientists used a technique called Atomic Force Microscopy. By pressing graphene that was lying on top of circular wells, they measured just how far you can push graphene with a small tip without breaking it.

It was found that graphene is harder than diamond and about 300 times harder than steel. The tensile strength of graphene exceeds 1 TPa.

Even though graphene is so robust, it is also very stretchable. You can stretch graphene up to 20% of its initial length. It is expected that graphene's mechanical properties will find applications into making a new generation of super strong

composite materials and along combined with its optical properties, making flexible displays.

2.5.4 Optical properties

Graphene, despite being the thinnest material ever made, is still visible to the naked eye. Due to its unique electronic properties, it absorbs a high 2.3% of light that passes through it, which is enough that you can see it in air.

To help enhance the visibility of graphene flakes we deposit them on to silicon wafers which have a thin surface layer of silicon dioxide. Light shining on to these three-layer structures will be partially transmitted and partially reflected at each interface.

This leads to complex optical interference effects such that, depending on the thickness of the silicon-dioxide layer (which we can control to a high degree of accuracy), some colors are enhanced and some are suppressed. This technique takes advantage of the same physics which causes the "rainbow effect" that you see when you have a thin layer of oil floating on water. In this case, the different colors correspond to longer/shorter optical path lengths that the light has had to travel through the oil film.

The excellent thermal stability of graphene-based nanocomposites can be used for producing flame-retardant materials. Networks of CNT, 185 CNF, 209 and EG210 are known to retard flammability of PMMA and also PU foams. Its aromatic and 2-D nature makes graphene an ideal alternative for the flame-retarding additives. Also, high electrical or thermal conductivity of graphene/polymer nanocomposites may satisfy conditions for heat- or electricity-activated shape memory, static charge dissipation, and electromagnetic wave reflective materials. Especially near the percolation threshold, resistivity of composites can vary dramatically upon temperature change, solvent attack and strain. This on-off phenomena in electrical conductivity by external stimuli can be used for electrical switching and strain/solvent sensing. Graphene nanocomposites have potential as photo- or electromechanical actuators since mechanical response has been induced by infrared radiation or electric

potential in CNT composites. The transmittance of visible light is attenuated by 2.3% as it penetrates through a single layer of graphene. If thin layers of electrically conductive graphene can be deposited on glass or polymer surfaces, flexible displays, thin film transistors, and photovoltaic and liquid crystal devices will be made possible. TRG conductive inks are already being offered commercially. Recently, homogeneous coating of a few-layer-thick graphene has been demonstrated via direct transfer of graphene films from CVD metal substrates or from vacuum filtration membranes as well as by conventional spin-coating.

2.6 Benzoxazine Resin

Polybenzoxazine is a newly developed class of thermosetting resins. Polybenzoxazines are heterocyclic macromolecules processed nitrogen and oxygen in their cyclic molecular structure and fuse to another benzene ring. Polybenzoxazine can be prepared through the ring-opening polymerization at oxazine-ring by thermal activation with no further addition of initiator or catalyst [9]. The benzoxazine resin is synthesized from the reaction of bisphenol-A, paraformaldehyde and aniline at 1:4:2 mole ratio at 110^{o}C without the use of any solvent as disclosed by Ishida in 1996 [26]. This solvent-less synthesis method is a convenient, cost competitive, and environmentally friendly method for preparation various types of benzoxazine monomers. The synthesis path of this monomer is shown in Figure 2. 10. The obtained benzoxazine resin can, then, be polymerized by the ring-opening polymerization of cyclic monomers via thermal cure without an addition of any catalyst or curing agent. The structural change in benzoxazine monomer to polybenzoxazine via thermal polymerization is shown in Figure 2. 11.

Upon polymerization, polybenzoxazines provide various outstanding characteristic of no catalytic needed for curing, near zero volumetric change (near zero shrinkage) upon thermal curing rendering dimensional stability, no by-product released during polymerization leading to no additional removal of volatile by-product. Moreover, polybenzoxazines offer a number of attractive properties such as low melt viscosity, high glass transition temperature, high thermal stability, good mechanical

strength and modulus, low water absorption, low dielectric constant, good adhesive properties and high resistance to burning and chemical.

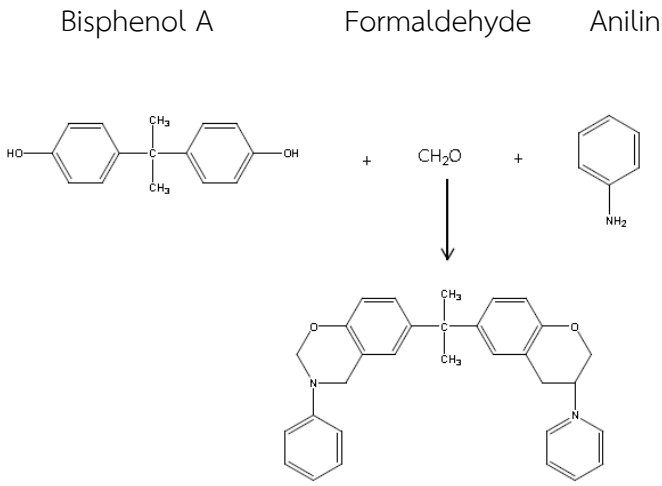

Figure 2. 10 Synthesis route of BA-a-type benzoxazine resin [9].

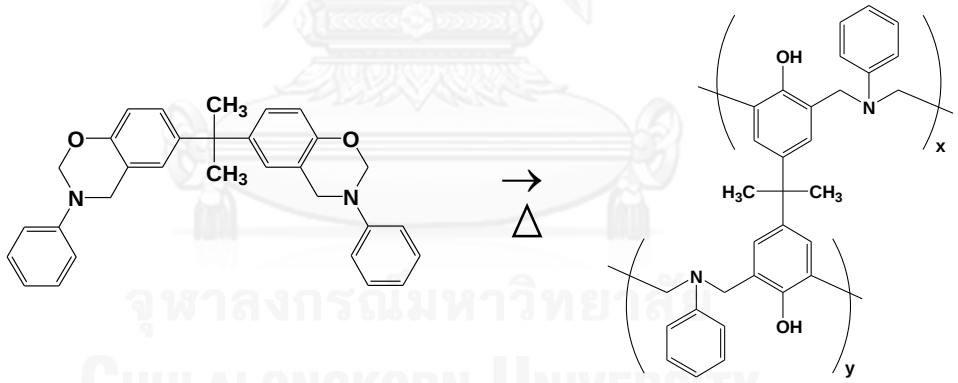

Figure 2. 11 Formation of polybenzoxazine resin network by thermal curing process [9].

Among various outstanding properties of BA-a resin, its low melt viscosity before curing is one of those useful properties, rendering the ability of BA-a to easily wet the filler or reinforcement in a compounding process in highly-filled systems composites. This property is desirable and crucial in various composite applications.

The other advantages of polybenzoxazine include easy processing ability, lack of volatile formation, all attractive for composite material manufacturing. Furthermore, benzoxazine resin is able to be alloyed with several other polymer or resins. In the literature reported that the mixture of the benzoxazine resin with bisphenol-A typed epoxy which the addition of epoxy to the polybenzoxazine network greatly increases the crosslink density of the thermosetting matrix and strongly influences its mechanical properties. Consequently, polybenzoxazines have gained much attention from scientists in the field of polymer research as well as from the industrial researchers.

In this research, we use benzoxazine resins which will be synthesized from bisphenol-A, formaldehyde and aromatic amine-based (aniline). Properties of these aromatic amines (arylamines) are shown in Table 2. 4 and properties of arylamine-based benzoxazine resin are shown in Table 2. 5.

Table 2. 4 Properties of aromatic amines [27].

Properties	Aniline
Molecular weight (g/mol)	93.127
Melting point (°C)	-6.02
Boiling point (°C)	184.17
Density (g/cm^3)	1.0217

Table 2. 5 Properties of arylamine-based benzoxazine resin [28].

Properties	BA-a
T_g (DSC, °C)	168
Char yield (% at 800°C)	30
Td at 5% wt. loss (°C)	315
Storage modulus at 28°C (GPa)	1.39
Loss modulus at 28°C (MPa)	15.7
Crosslink density (mol/cm^3)	1.1x10^{-3}

CHAPTER III

LITERATURE REVIEWS

H. B. Zhang et al. (2010) [29] developed the electrical conductivity of polyethylene terephthalate (PET) composites filled with graphene and pristine graphite fillers. From Figure 3. 1, PET/graphene nanocomposites exhibited a sharp transition from insulator to semiconductor. The electrical conductivity of PET/graphene nanocomposites quickly rose to 7.4×10^{-2} S/m from 2.0×10^{-13} S/m with a slight increase in content from 0.47 to 1.2vol%. At 3.0vol% of graphite, the electrical conductivity approached 2.11 S/m. On the contrary, PET/graphite composites showed a higher percolation threshold of 2.4vol% and a broad percolation transition within a range of graphite content from 2.4 to 5.8vol%, the conductivity of PET/ pristine graphite composite with 7.1vol% of graphite is 2.45 $\times10^{-4}$ S/m. A low percolation of graphene was due to the advantage of graphene nanosheets such as high aspect ratio, large specific surface area of graphene than pristine graphite.

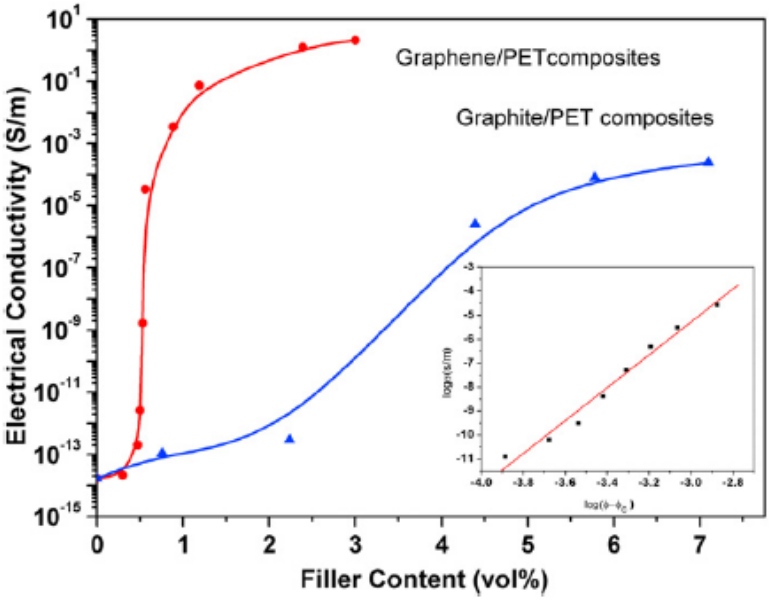

Figure 3. 1 The electrical conductivity versus filler content for PET/graphene nanocomposites and PET/graphite composites [29].

I. Zaman et al. (2011) [30] studied the thermal stability of epoxy/graphene platelets nanocomposites with graphene platelets and pristine graphite fillers. The tan δ curve as a function of temperature for neat epoxy and epoxy/graphene platelets nanocomposites were shown in Figure 3. 2. The result showed that, all nanocomposites revealed an increase in T_g by the addition graphene. The neat epoxy T_g increases 8.1% to 102.4 ^{o}C at 2.5wt% graphene. The increment was caused by the interaction between the matrix and the filler, which hindered the matrix chains mobility near graphene surface.

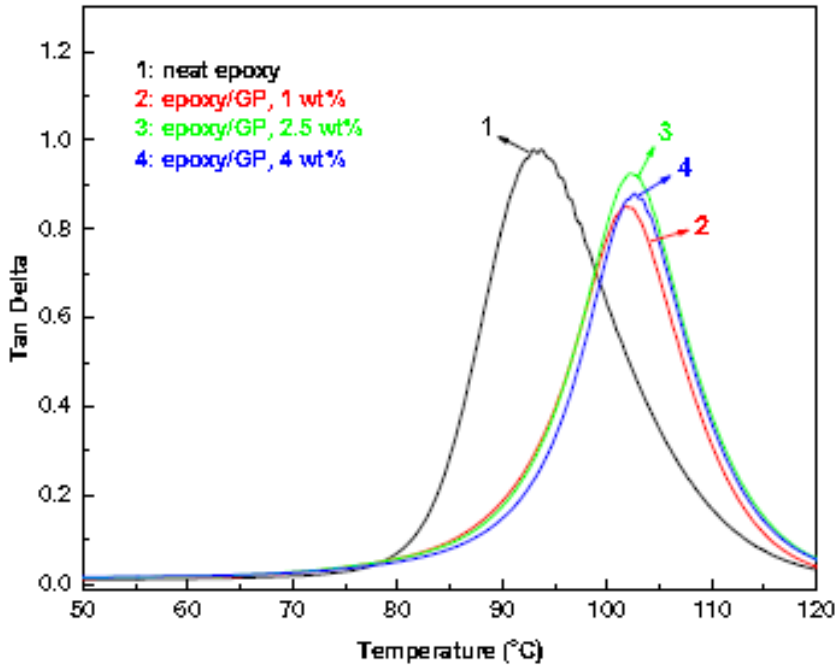

Figure 3. 2 Damping behavior of neat epoxy and epoxy/graphene nanocomposites [30].

G. Gedler et al. (2012) [31] developed the graphene-reinforced polycarbonate as can be seen in Figure 3. 3. The results showed that, the degradation of graphene-reinforced polycarbonate composites (PCg) followed a one-step decomposition, with important decomposition delays during degradation when compared to unfilled PC. At 5% weight loss of the composite with 0.5wt% of graphene Nanoplatelets (GNPs), T_d of composite increases from 407 to 462^{o}C. Because its particular flat-like morphology of GNPs results promote a gas barrier effect. The gas tortuous path effect is creased by the well dispersed in polycarbonate, delaying the escape of volatile degradation product during decomposition.

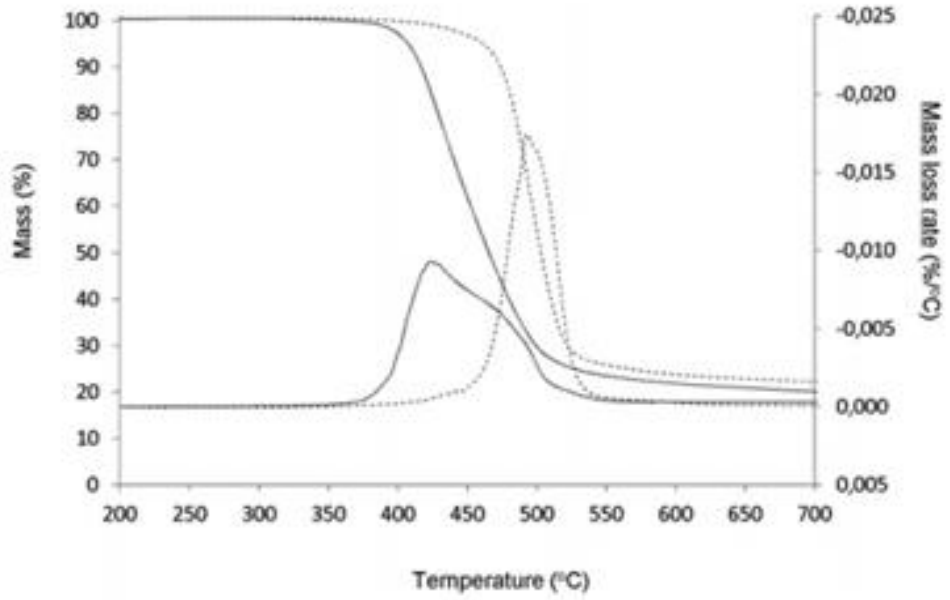

Figure 3. 3 TGA and DTG thermograms for the unfilled solid (PC) and graphene reinforced solid polycarbonate (PCg) [31].

X. Jiang and L. T. Drzal (2012) [32] studied the flexural properties of Polyphenylene Sulfide (PPS)/Graphene Nanoplatelets (GNP) nanocomposites made by compression molding was shown in Figure 3. 4. From this figure, the flexural modulus of these nanocomposites exhibits a monotonic increase with the increasing GNP content. At 60wt% GNP loading, the modulus is enhanced by almost 200% compared to that of neat PPS. Meanwhile, the flexural strength of these PPS/GNP nanocomposites is found to be much lower than the neat PPS but it is not affected much by the increase of GNP content. This behavior is due to the presence of interface between the filler and the matrix of these heterogeneous systems. However at 60wt% of GNP loading, the flexural strength of the nanocomposite is still as high as 66 MPa, which is more than twice as much as the DOE requirement for bipolar plates application in fuel cells (>25 MPa).

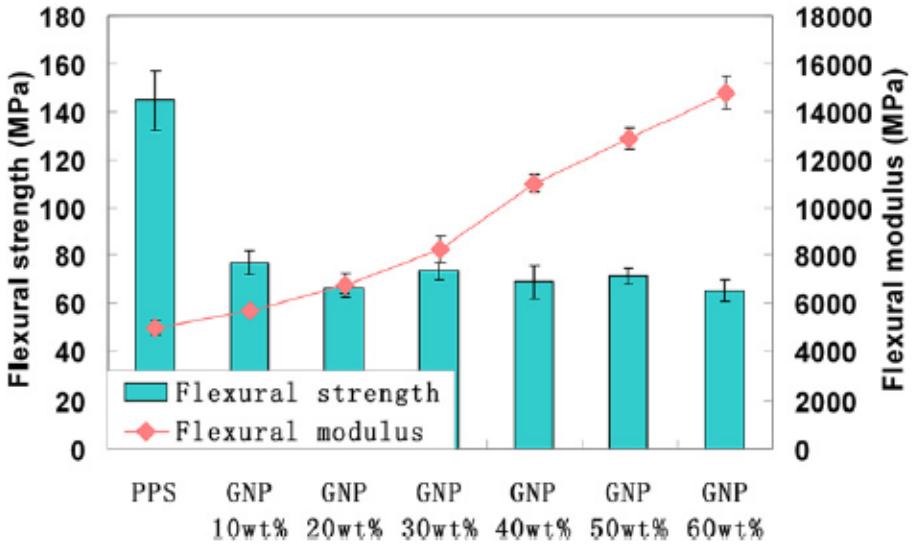

Figure 3. 4 Flexural properties of PPS/GNP nanocomposites made by Solid state ball mill [32].

S. Chatterjee et al. (2012) [33] developed thermal conductivity of Graphene Nanoplatelets (EGNP)/epoxy composites. The EGNPs form a conducting pathways in the epoxy matrix allowing for increased thermal conductivity of the composites. Figure 3. 5 the thermal conductivity increases steadily with the incorporation of the EGNPs. At 2wt% of EGNP loading an increment by 36% was observed as compared to neat epoxy. The increasing trend promises higher thermal conductivity at larger EGNP contents. Since efficient heat propagation in EGNPs is mainly due to acoustic phonons, a uniform dispersion and network of EGNPs in the polymer matrix may contribute to the steady increase in thermal conductivity in the composites. A network of well-dispersed EGNPs may provide a conductive path and a proportional improvement in thermal conductivity was recorded with incorporation of EGNPs.

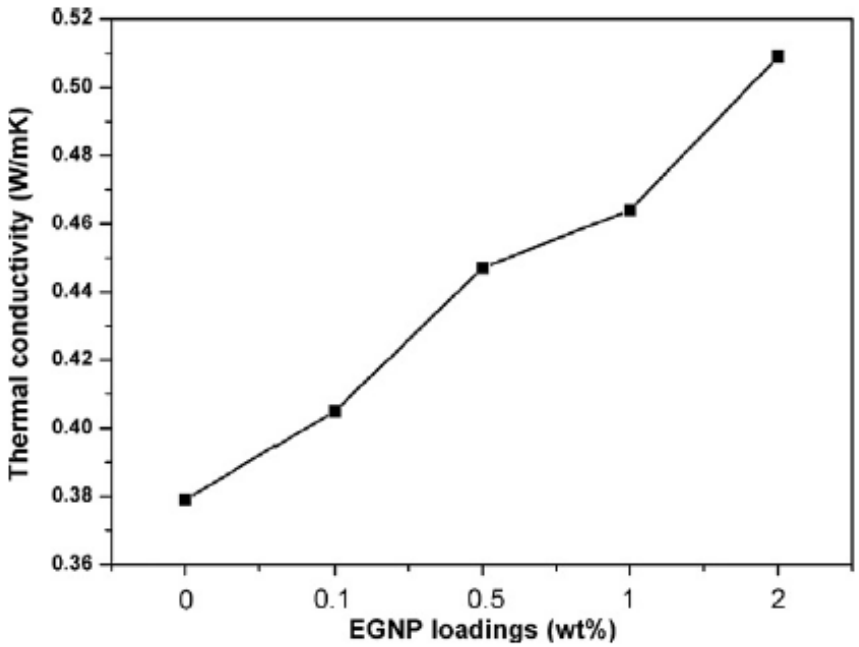

Figure 3. 5 Thermal conductivity of EGNP/epoxy composites [33].

A. Yu et al. [34], X. Huang et al. [35] and M. O. Khan et al. [36] had been developed systems of highly filled composites with thermal conductivity as shown in Table 3. 1. From the table, all of the highly-filled systems exhibit substantially enhancement the thermal conductivity in the composites. This phenomenon is due to the high graphene contents in polymer matrix attributed to the significant conducting pathways for thermal transport formed in the composites.

Table 3. 1 Polymer composites systems with thermal conductivity value.

Polymers	Fillers	Filler size (d)Diameter (t)Thickness	Content (vol%)	K (W/mK)	Improvement (%)	References
Epoxy	GNP	N/A	25	6.87	>3000	[34]
Epoxy	GNP	d = 5 μm t ~ 20 nm	50	6.60	2689	[35]
PPS	GNP	d = 25 μm t = 10 nm	22.44	1.91	768	[36]

H. Ishida and S. Rimdusit (1998) [37] developed highly-filled system of thermally conductive boron nitride-polybenzoxazine composites. From figure 3. 6, we can see that, they have produced a composite with a remarkably high value of thermal conductivity of 32.5 W/mK at 78.5vol% of boron nitride filler. The conductive networks of the large particle size are formed, the thermal conductivity of the composites will exceed that of the smaller particles as the formation of the conductive paths of the large particles renders less thermal resistance along the paths. The phenomenon is more pronounced at the filler content exceeding the maximum packing of smaller particles since the maximum packing of smaller particle size is less than the maximum packing of the larger particles. Moreover, the very low melt viscosity and good adhesion of benzoxazine resin results in its ease of filler mixing during the molding compound preparation thus giving its outstanding thermal conductivity.

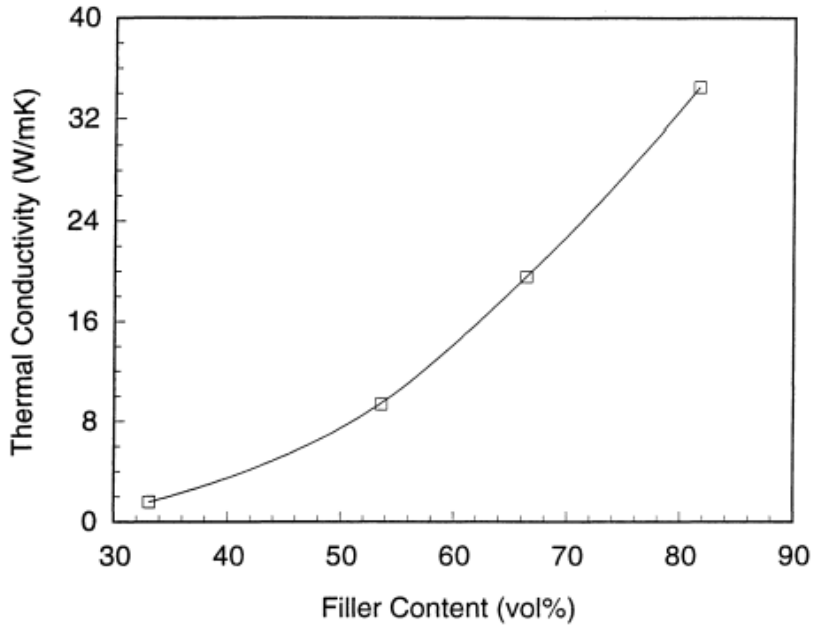

Figure 3. 6 Thermal conductivity of boron nitride-filled polybenzoxazine as a function of filler contents [37].

I. Dueramae. A. Pengdam and S. Rimdusit (2012) [6] developed highly-filled graphite-polybenzoxazine composites. Figure 3. 7 illustrations the experimentally measured thermal conductivity of the composites with different graphite content at 25°C. The thermal conductivity increases with increasing graphite content. When filler concentration reaches 80wt%, thermal conductivity increases to 10.2 W/mK, more than 44 times that of pure polybenzoxazine (0.23 W/mK). This rapid growth may be attributed to the significant conductive pathways formed in the composite. As per the recent benchmark given by Department of Energy, USA the recommended value of thermal conductivity for bipolar plate is to be graphite than 10 W/mK. The highly filled graphite based polybenzoxazine composite at 80wt% of graphite content is a promising bipolar plate for the PEM fuel cell application as it shows relatively high thermal conductivity. The value is substantially greater than the DOE requirement.

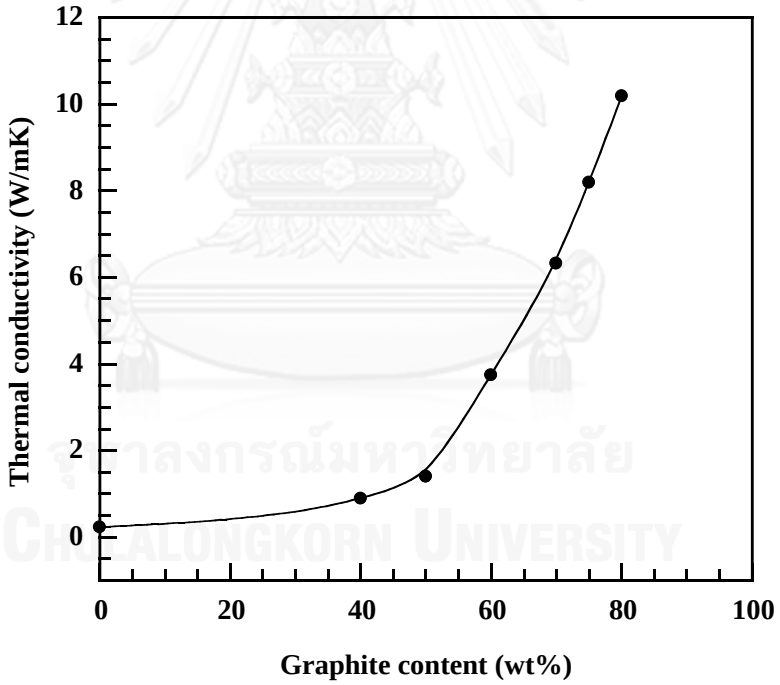

Figure 3. 7 Thermal conductivity at 25°C of graphite-filled polybenzoxazine as a function of filler contents [6].

I. Dueramae. A. Pengdam and S. Rimdusit (2012) [6] developed highly-filled graphite based polybenzoxazine composites. Figure 3. 8 shows electrical conductivity of the highly filled systems of graphite and polybenzoxazine composites at different weight fraction of graphite. From the result the conductivity of the composite increased non-linearly with an increase in graphite content up to 80wt%. At 40-60wt% of the graphite, the electrical conduction values increased only slightly with the filler loading. Beyond 60wt% of the graphite filler, the conductivity values tended to increase sharply up to about 245 S/cm. The phenomenon is due to the gradual formation of the percolating network of the graphite particles within the plate with an increase in the graphite content. As per the recent benchmark given by Department of Energy, USA the recommended value of electrical conductivity for bipolar plate is to be graphite than 100 S/cm. The highly filled graphite-polybenzoxazine composites at 70 and 80wt% of graphite content are a promising bipolar plate for the fuel cell application as it shows relatively high electrical conductivity of 104 and 245 S/cm, respectively. The value is substantially greater than the DOE requirement.

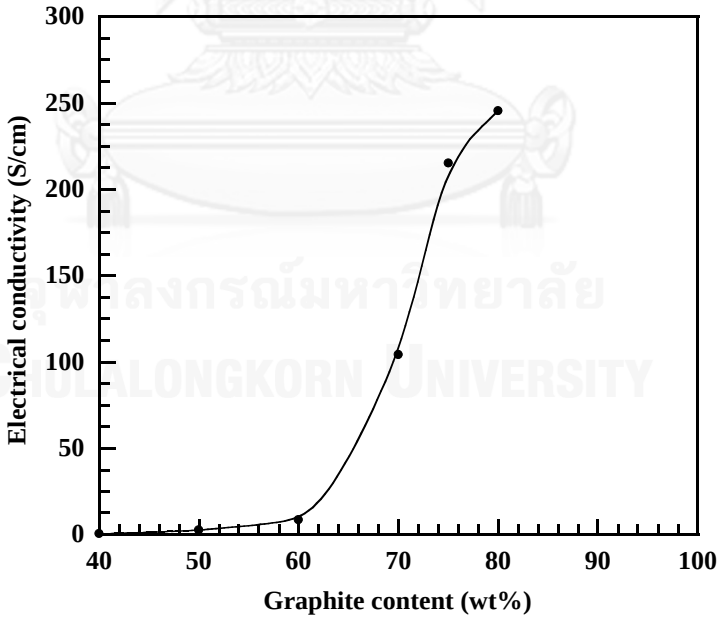

Figure 3. 8 Effect of the graphite content on electrical conductivity (in-plane) of graphite-filled polybenzoxazine composites [6].

CHAPTER IV

EXPERIMENTAL

4.1 Materials and Monomer Preparation

The materials in this research are benzoxazine resin and graphene. Benzoxazine resin (BA-a) is based on bisphenol-A, aniline, and formaldehyde. Thai Polycarbonate Co., Ltd. (TPCC) supplied the bisphenol-A (polycarbonate grade). Paraformaldehyde (AR grade) was purchased from Merck Company and aniline (AR grade) was obtained from Panreac Quimica SA Company. XGnP Graphene Nanoplatelets (Grade H) was purchased from XG Sciences, USA.

4.1.1 Benzoxazine Monomer Preparation

The benzoxazine resin used is based on bisphenol-A, aniline and formaldehyde in the molar ratio of 1:4:2. This resin was synthesized by using a patented solventless method in the U.S. Patent 5,543,516. The obtained benzoxazine monomer is clear-yellowish powder at room temperature and can be molten to yield a low viscosity resin at about 70-80^{o}C. The product is then ground to fine powder and can be kept in a refrigerator for future-use. The density is 1.2 g/cm^{3} and it has a reported dielectric constant of about 3-3.5.

4.1.2 Graphene Characteristics

XGnP Graphene Nanoplatelets grade H was purchased from XG Sciences USA. (purity 99.5%). The diameter and thickness of grade H Graphene Nanoplatelets is 5 to 25 μm and 15 nm thick with surface area of 50-80 m^{2}/g. The density is 2.2 g/cm^{3}. Grade H Graphene Nanoplatelets provide moderate properties of the obtained materials with suitable price [38].

Table 4. 1 Typical Properties of xGNP Graphene Nanoplatelets

Properties	Typical Value-Parallel to Surface	Typical Value-Perpendicular to Surface	Unit of Measure
Density	2.2	2.2	g/cm^3
Carbon Content	>99.5	>99.5	%
Thermal Conductivity	3,000	6	W/mK
Thermal Expansion (CTE)	4×10^{-6} to 6×10^{-6}	0.5×10^{-6} to 1.0×10^{-6}	m/mK
Tensile Modulus	1,000	na	GPa
Tensile Strength	5	na	GPa
Electrical Conductivity	1.0×10^{7}	1.0×10^{2}	S/m

4.2 Specimen Preparation

The graphene-filled samples were prepared with graphene loadings of 0, 10, 20, 30, 40, 50 and 60wt% to yield molding compounds. The graphene was firstly dried at 110°C for 24 hours in an air-circulated oven until a constant weight was achieved and was then kept in a desiccator at room temperature. The filler was mechanically stirred to achieve uniform dispersion in benzoxazine resin using an internal mixer at about 110°C. For thermal-cured specimen, the compound was compression-molded by hot pressing. The thickness was controlled by using a metal spacer. The hot-press temperature of 160°C was applied for 1 hour and 200°C for 3 hours using a hydraulic pressure of 15 MPa. All samples were air-cooled to room temperature in the open mold and were cut into desired shapes before testing.

4.3 Characterization Methods

4.3.1 Differential Scanning Calorimetry (DSC)

The curing characteristic of the graphene-polybenzoxazine composites were examined by using a differential scanning calorimeter (DSC) model 2910 from TA Instrument. For each experimental, a small amount of the sample ranging from 5-10 mg was placed on the aluminum pan and sealed hermetically with aluminum lids. The experiment was done using a heating rate of 10°C/min to heat the sealed sample from 30°C up 300°C under N_2 purging. The purge nitrogen gas flow rate was maintained to be constant at 50 ml/min. The processing temperature and time were obtained from the thermograms while the percentage of benzoxazine resin conversion was calculated from the area under the DSC thermograms.

4.3.2 Density Measurement

Actual Density Measurement

The density of each specimen was determined by water displacement method according to ASTM D 792 (Method A). The dimension of all specimens were 50 mm × 25 mm × 2 mm. Each specimen was weighed in air and in water. The average density value of each sample obtained from at least five specimens was calculated as following equation:

$$\rho = \frac{A}{A - B} \times \rho_0 \qquad (4.1)$$

where ρ = density of the specimen, g/cm^3)

A = weight of the specimen in air, g

B = weight of the specimen in liquid (water) at 23±2°C, g

ρ_0 = density of the liquid (water) at the given temperature, g/cm^3

Theoretical Density Measurement

The theoretical density by mass of polybenzoxazine filled with graphene can be calculated as follow:

$$\rho_c = \frac{1}{\frac{W_f}{\rho_f} + \frac{(1-W_f)}{\rho_m}} \quad (4.2)$$

Where ρ_c = composite density, g/cm^3

ρ_f = filler density, g/cm^3

ρ_m = matrix density, g/cm^3

W_f = filler weight fraction

$(1\text{-}W_f)$ = matrix weight fraction

4.3.3 Dynamic Mechanical Analysis (DMA)

The dynamic mechanical analyzer (DMA) model DMA242 from NETZSCH Instrument was used to investigate dynamic mechanical properties of the composites. The dimension of specimen was 50 mm × 10 mm × 2.5 mm. The test was performed under the three-point bending mode. A strain in the range of 0 to 30 μm was applied sinusoidally at a frequency of 1 Hz. The temperature was scanned from 30 to 300°C with a heating rate of 5°C/min under nitrogen atmosphere. The glass transition temperature was taken as the maximum point on the loss modulus curve in the temperature sweep tests. The storage modulus (G'), loss modulus (G''), and loss tangent ($\tan\delta$) were then obtained.

4.3.4 Thermogravimetric Analysis (TGA)

The thermal stability of graphene-polybenzoxazine composites were evaluated using a thermogravimetric analyzer (model TGA1 Module) from Mettler-Toledo (Thailand). The initial weight of the sample to be tested was about 10 mg. It was heated from room temperature to 1000°C and a heating rate of 20°C/min under nitrogen atmosphere. The degradation temperature at 5% weight loss and solid residue determined at 800°C were recorded for each specimen.

4.3.5 Specific Heat Capacity Measurement

Specific heat capacities of all samples were measured using a differential scanning calorimeter (DSC) model 2920 from Perkin-Elmer (Norwalk, CT) Instruments. All samples were crimped in non-hermetic aluminum pans with lids. The mass of the reference and sample pans with lids were measured to within 15-20 mg. The sample was purged with dry nitrogen gas at a flow rate of 50 ml/min. The test was performed from room temperature up to 100°C at a heating rate of 10°C/min.

4.3.6 Thermal Diffusion Measurement

Thermal diffusivity of the graphene-filled polybenzoxazine composites were measured by laser flash diffusivity instrument (Nano-Flash-Apparatus, LFA 447, NETZSCH). The composite samples were prepared in a rectangular shape (10 mm×10 mm×1 mm). All measurements were conducted at atmosphere from room temperature to 180°C. In these tests, the front side of a plane-parallel sample is heated by a short light pulse. The resulting temperature rise on the rear surface is measured using an infrared detector. Thermal diffusivity was calculated from Equation (4.3):

$$\alpha = \frac{kL^2}{t_{0.5}} \tag{4.3}$$

Where: α = the thermal diffusivity

k = the haft-rise constant (0.1388 under ideal conditions at half-rise)

L = the sample thickness

$T_{0.5}$ = the time for the rear face temperature to reach half of its maximum value

For each specimen, its thermal diffusivity was averaged from three measurements at each temperature.

4.3.7 Thermal Conductivity Measurement

The thermal conductivity (k) was calculated using the measured thermal diffusivity (α), specific heat capacity at constant pressure (C_p), and the measured density (ρ) of the sample obtained through Equation (4.4):

$$k = \alpha \times \rho \times C_p \quad (4.4)$$

4.3.8 Flexural Properties Measurement

Flexural properties of graphene-polybenzoxazine composites were determined using a Universal Testing Machine (model 5567) from Instron Instrument. The flexural properties of each specimens were determined according to ASTM D 790M. The specimen size is 50 mm × 25 mm × 2 mm. The method of the test used is a three-point bending mode with a support span of 32 mm. Bending test was succeeded at the crosshead speed of 0.85 mm/min. The flexural modulus and the flexural strength of the composites were calculated by Equations (4.5) and Equations (4.6), respectively.

$$E_B = \frac{L^3 m}{4bd^3} \quad (4.5)$$

$$S = \frac{3PL}{4bd^2} \quad (4.6)$$

Where E_B = flexural modulus, MPa

S = flexural strength, MPa

P = load at a given point on the load-deflection curve, N

L = support span, mm

b = width of the beam tested, mm

d = depth of the beam tested, mm

m = slope of the tangent to the initial straight-line portion of the load deflection curve, N/mm.

4.3.9 Water Absorption

Water absorption of the composites were determined according to ASTM D570 using disk-shaped specimens having a 50 mm diameter and a 3 mm thick. All specimens were dried in oven, weighed, and submerged in distilled water at 25°C for 24 hours. The specimens were occasionally removed, wiped dry, weighed, and immediately returned to the water bath. The values of the water absorption as percentages were calculated with the following equation:

$$\% \text{ Water absorption} = \left(\frac{W - W_d}{W_d}\right) \times 100 \quad (4.7)$$

Where W is the weight of the specimen at time t

W_d is the weight of the dry specimen

4.3.10 Electrical Conductivity Measurement

The electrical conductivity of all samples was measured at room temperature with KEITHEY Model 580 Micro ohmmeter based on a four-point probe method. For this technique, a high impedance current source is used to supply current through the outer two probes, a voltmeter measures the voltage across the inner two probes to determine the sample resistivity. An average electrical conductivity value from of about 3 readings on each plate (in plane) was reported.

4.3.11 Scanning Electron Microscope (SEM)

Interfacial bonding between the filler and the matrix were investigated using a JSM-5410LV scanning electron microscope (SEM) at an acceleration voltage of 15 kV. All samples were coated with thin film of gold using a JEOL ion sputtering device (model JFC-1200) for 4 min to obtain a thickness of approximately 30 Å and the micrographs of the sample fracture surface were taken. The obtained micrographs were used to qualitatively evaluate the interfacial interaction between the graphene filler and the polybenzoxazine matrix.

CHAPTER V

RESULTS AND DISCUSSION

5.1 Curing Behavior of Benzoxazine Resin Filled with Graphene Curing Condition

The curing reaction of benzoxazine resin filled with 0-60wt% of graphene contents observed by differential scanning calorimeter in a temperature range of 30 to 300°C and at a heating rate of 10°C/min is depicted in Figure 5. 1. From the thermograms, a single dominant exothermic peak of all these molding compounds was observed. The exothermic peak of the neat benzoxazine resin centered at 233°C was attributed to the ring-opening polymerization of its oxazine-ring. Interestingly, the curing peak maximum of the molding compounds evidently shifted to lower temperature with higher amount of graphene loading. The characteristic exothermic peak of 10, 20, 30, 40, 50 and 60wt% of graphene content in benzoxazine molding compound were 218, 212, 211, 209, 202 and 196°C, respectively. The results indicated that graphene might act as a catalyst for oxazine-ring opening reaction thus minimal the curing condition in terms of energy consumption to undergo polymerization. The result of the catalytic reaction was also confirmed by FTIR spectra of pure graphene as can be seen in Figure 5. 3.

The characteristic peak of C=O stretch of the carboxylic (COOH) group was noticed at 1733. These noticeable peaks were also observed by K. J. Huang [39]. The effect of carboxylic group on the catalyst of ring-opening polymerization of polybenzoxazine was also noticed by P. Kasemsiri in the study of cashew nut shell liquid and benzoxazine resin [40].

In addition, area under exothermic peak indicated the heat of reaction of the polymerization process. As seen in Figure 5. 1, the area under the exothermic peaks was found to decrease with increasing the graphene content in the molding compounds. Those values reduced from 336 J/g of the neat polybenzoxazine to 330 J/g of molding compound containing 10wt% of graphene and to the value as low as 133 J/g of the molding compound containing 60wt% of graphene. This expected

phenomenon is related to the decreasing amount of benzoxazine resin in the molding compounds with increasing of the graphene contents [6].

Figure 5. 2 exhibits the DSC thermograms of graphene-filled benzoxazine molding compound at 10wt% of graphene loading cured at 200°C at various curing time. In theory, the fully cured stage has been reported to provide a polymer with desirable properties including sufficiently high thermal and mechanical integrity. From the results, the heat of reaction of the uncured benzoxazine molding compound determined from the area under the exothermic peak was measured to be 245 J/g and the value decreased to 19, 11 and 4 J/g, which corresponded to the degree of conversions estimated by Equation 5.1 of 89, 95 and 98% after curing at 200°C for 1 hour, 2 hours and 3 hours, respectively. The curing condition at 200°C for 3 hours was therefore used to cure all benzoxazine molding compounds to prepare the specimens for further characterization.

$$\% \text{ conversion} = \left(1 - \frac{H_{rxn}}{H_0}\right) \times 100 \qquad (5.1)$$

Where: H_{rxn} is the heat of reaction of the partially cured specimens.

H_0 is the heat of reaction of the uncured resin.

5.2 Actual Density and Theoretical Density Measurement of Highly Filled Graphene-Polybenzoxazine Composites

Density of composites is a major characteristic used to efficiently evaluate the quality of composites due to the void formation or air gap in the samples. The theoretical densities of graphene filled polybenzoxazine composites with different graphene contents were calculated from Equation 4.2 and their actual densities were calculated according to Equation 4.1. The reported densities of polybenzoxazine and graphene are 1.19 and 2.20 g/cm^3, respectively [2], [6]. Figure 5. 4 shows the calculated or theoretical densities of the graphene filled polybenzoxazine composites at 0-65wt% of graphene contents based on the two known density values of the matrix and the filler compared with their actual or measured densities. From the results, the

theoretical and actual densities of the graphene-filled polybenzoxazine composites were linearly increased with increasing graphene content following the rule of mixture thus suggesting negligible void or air gap in the composites samples. The actual densities of the composites were determined to be 1.247, 1.310, 1.377, 1.449, 1.540, 1.637 and 1.642 at 10, 20, 30, 40, 50, 60 and 65wt% of graphene content, respectively. Due to the advantages of very low melt viscosity and good interfacial adhesion of benzoxazine resin, the highly filled graphene composite with negligible void formation was thus provided. However, the experimental density of the composite with 65wt% (i.e. 50.1vol%) of graphene content in our polybenzoxazine was found to be slightly lower than that of its theoretical density value. It might be due to the presence of small content of void or air gap in the composite specimen from the incomplete wetting of the resin at such too high amount of the graphene. As a consequence, the highly filled graphene-polybenzoxazine composites could be prepared with graphene content up to 60wt% or about 44.8vol%. This graphene content is therefore defined as the maximum packing density for the polybenzoxazine.

5.3 Dynamic Mechanical Properties of Highly Filled Graphene-Polybenzoxazine Composites

The dynamic mechanical analysis plots of the storage modulus (E′) and loss modulus (E″) of the graphene filled polybenzoxazine composites with the graphene content ranging from 0 to 60wt% are shown in Figures 5. 5 and 5. 6, respectively. As seen from the results of storage modulus at room temperature in Figure 5. 5, the graphene filled polybenzoxazine composites possessed the higher modulus values compared to that of the neat polybenzoxazine. The storage moduli at room temperature of the composites were ranging from 5.9 GPa to 25.1 GPa of the composites with 10-60wt% of graphene contents whereas that of the neat polybenzoxazine was found to be about 5.9 GPa. About 322% enhancement of storage modulus of the composite with 60wt% of graphene was thus achieved compared to the neat polybenzoxazine indicating the outstanding enhancement in stiffness of the resulting graphene-filled composites. The storage modulus at 60wt% of graphene contents in polybenzoxazine composite is also greater than that of graphite-filled

polybenzoxazine composite at its maximum graphite contents as high as 80wt% as reported by I. Dueramae et al. [6]. This phenomenon is likely due to the reinforcing effect of the graphene filler in polybenzoxazine composites. The results also suggested the substantial interfacial adhesion between the graphene filler and the polybenzoxazine matrix. Furthermore, the moduli of the graphene filled polybenzoxazine in the rubbery plateau region were also investigated and were found to increase significantly with increasing amount of the graphene, again, implying substantial interaction between the filler and the polymer matrix.

Loss modulus curves of graphene filled polybenzoxazine at 0-60wt% of graphene contents as a function of temperature were investigated as depicted in Figure 5. 6 and the glass-transition temperatures (T_g) obtained from the maximum peak of loss modulus of the graphene filled polybenzoxazine composites were also reported. The T_g values of the composites were observed to be in the range of 176 to 188^{o}C with 10-60wt% of graphene contents which were higher than the T_g of the neat polybenzoxazine as reported to be 174°C. Moreover, it could be seen that the T_g values systematically increased with increasing graphene contents in the polybenzoxazine composites. This phenomenon also implies good adhesion between the graphene filler and the polybenzoxazine matrix which substantially impedes the polymeric chain movement reflecting in the observed higher T_g values [6], [37].

In addition, Figure 5. 7 exhibits α-relaxation peaks of the loss tangent (tanδ) of the graphene filled polybenzoxazine composites. Tanδ curves were obtained from the ratio of energy loss (E'') to storage energy (E') in a sinusoidal deformation. From the figure, it was found that the maximum peaks of the composites were shifted to higher temperature with increasing graphene contents and was in good agreement with the results from loss modulus curves. Moreover, the magnitude of tanδ peak of the neat polybenzoxazine was higher than those of the graphene-filled polybenzoxazine, reflecting the large scale mobility of the neat polybenzoxazine than the composites and associated with the more pronounced α-relaxation process of the unfilled polybenzoxazine. In addition, the width at half height of tanδ curves of graphene-filled polybenzoxazine composites were observed to be greater than that of the neat

polybenzoxazine suggesting the greater network heterogeneity in the composites with the presence of the graphene filler. The benzoxazine monomers with the closer proximity to the graphene surface should be catalyzed by the graphene better than the father monomers thus resulting in the different in the network forming characteristic of the observed network heterogeneity above.

5.4 Effect of Graphene Loading on Thermal Stability of Highly Filled Graphene-Polybenzoxazine Composites

Thermal stability of the graphene filled polybenzoxazine composites was evaluated by TGA under a nitrogen atmosphere. The TGA curves of polybenzoxazine, graphene and graphene-filled polybenzoxazine composites with different graphene loadings are illustrated in Figure 5. 8. As can be seen in Figure 5. 8, the degradation temperature of 461^{o}C was obtained at a 5% weight loss of pure graphene. The increase in weight loss of our pure graphene around 200 to 700^{o}C might be associated with the removal of oxygen-containing functional groups such as carboxyls, or hydroxyls [31], which were reported to be naturally presented during typical graphene synthesis such as that suggested in the technical data sheet of graphene nanoplatelets-grade H from XG Sciences, USA [38]. Moreover, the presence of these functional groups was also confirmed by FTIR spectra of the pure graphene used in this study as can be seen in Figure 5. 3. The presence of oxygen-containing functional groups in graphene has been reported to help improve the modulus of the composites from better interfacial bonding with the matrix [41]. In addition, the enhancement in the modulus of graphene-filled polybenzoxazine composites was observed particularly when compared to that of graphite-filled polybenzoxazine composites [6]. However, TGA curves of graphene showed a relatively high thermal stability behavior, presenting a total char residue of about 91.40% at 800^{o}C. This char value of graphene was found to be consistent with that reported by G. Gedler et al. (93%) [31]. In addition, the polybenzoxazine matrix possessed a degradation temperature at its 5% weight loss of 327^{o}C and the char residue at 800^{o}C of 25%. These values were consistent with the results reported by S. Rimdusit et al. [6], [42] etc. Additionally, the degradation temperature at 5% weight loss of our highly filled polybenzoxazine composites with 0

to 60wt% of graphene loading were found to systematically increase with increasing graphene contents. The T_d values of the composites were reported to be in the range of 327 to 353°C. That is the T_d value of the composite at 60wt% of graphene content was enhanced by 26°C compared to that of the neat polybenzoxazine, which represented about 8% improvement. This enhancement is attributed to the graphene flakes which acted as a gas barrier and could delay the decomposition of volatile products [43], [44].

Char residue of the highly filled graphene polybenzoxazine composites were illustrated in Figure 5. 9. Char content of the composites were expectedly found to increase with increasing graphene contents. The char residue of the polybenzoxazine composites with 0, 10, 20, 30, 40, 50 and 60wt% of graphene content were 25.2, 35.7, 44.1, 51.7, 59.8, 68.1 and 75.6%, respectively. The increase in char content with the increasing graphene loading in the composites was found to correspond relatively well with the rule of mixture and the results were tabulated and compared in Table 5. 1. In principle, the higher char residue can provide a sample with enhanced flammability [45].

5.5 Specific Heat Capacity of Highly Filled Graphene-Polybenzoxazine Composites at Various Graphene Contents

Energy storage is critical in enhancing the applicability performance, and reliability of a wide range of energy systems [46]. The specific heat of a material is defined as the amount of energy required to rise a unit mass of material by one unit of temperature at constant pressure. Figure 5. 10 illustrates the effect of temperature on graphene-filled polybenzoxazine composites' specific heat capacity at different graphene loadings. From this figure, the specific heat capacity of the composites was found to increase with increasing temperature. The increase in specific heat of the composites with temperature is attributed to the greater degree of molecular vibrations at elevated temperature as other contributions are normally negligible [47].

Figure 5.11 exhibits the plot of the specific heat capacities extrapolated at 25^{o}C of graphene-filled polybenzoxazine composites as function of graphene loading ranging from 0 to 60wt%. As seen in the figure, the specific heat of the composites was found to systematically decrease with increasing graphene loading. This phenomenon was expected from the lower specific heat capacity of the graphene compared to the polymer matrix. Furthermore, the specific heat capacity of the composites is the structure-insensitive property characteristic, which, in general, having a linear relationship with filler loadings [47]. Therefore, specific heat capacity values at different filler loading are normally predicted by the rule of mixture according to Equation (5.2).

$$C_{pc} = C_{pf}W_f + C_{pp}(1\text{-}W_f) \quad (5.2)$$

From our measurement, the specific heat capacity of the pure graphene (C_{pf}) and the neat polybenzoxazine (C_{pp}) are 1.076 and 1.753 J/gK, respectively and the corresponding equation then became:

$$C_{pc} = 1.076W_f + 1.753(1 - W_f) \quad (5.3)$$

The specific heat capacity values of the polybenzoxazine composites with different graphene contents obtained from the experimental results were compared with the values calculated from Equation (5.3). The measured values were thus in good agreement with those predicted by the rule of mixture with an error within ±2.0% as seen in Table 5. 2. The specific heat capacity of composites is an essential parameter for the determination of thermal conductivity since in this work, we determined the thermal conductivity values of our graphene-filled composites via the measurement of the composites' thermal diffusivity. In theory, thermal conductivity can be determined from the known thermal diffusivity, density and heat capacity values using Equation 4.4.

5.6 Effects of Graphene Contents on Thermal Diffusivity of Highly Filled Graphene-Polybenzoxazine Composites

Thermal diffusivity is a material specific property for characterizing unsteady heat conduction. The value describes how quickly a material reacts to a change in temperature. Thermal diffusivity measurements are generally conducted with the

“laser flash” technique, which being a relatively fast and accurate method and using a small sample. In the laser flash method, for a given geometry of the samples, heat propagates from the top to the bottom surface of the material under testing. The thermal diffusivity of our graphene-filled polybenzoxazine as a function of graphene loadings was measured at room temperature as illustrated in Figure 5. 12. With the presence of highly thermally conductive graphene, the significant enhancement in thermal diffusivity of the composites was obviously obtained. In comparison with the neat polybenzoxazine, those values of the composites were found to increase with increasing graphene content. The increase in thermal diffusivity of the composites could be divided into two stages in accordance with graphene filler content. The first stage was at filler content up to 20wt%, a slightly increased in thermal diffusivity of the composites was noticed. At the greater graphene loadings up to its maximum content of 60wt%, or in the second stage, the thermal diffusivity of the composites sharply increased with the amount of the graphene which could be explained by the formation of tremendous amount of conductive paths in the filled systems with the graphene loading approaching their maximum packing i.e. the highly filled composites. This behavior was also observed by H. Ishida et al. [37] in the highly filled systems of boron nitride and polybenzoxazine and by I. Dueramae et al. [6] in highly filled systems of graphite and polybenzoxazine.

Furthermore, the thermal diffusivities of graphene-filled polybenzoxazine as a function of temperature are shown in Figure 5. 13. From the figure, it was observed that thermal diffusivity values of the samples tended to decrease with increasing temperature as a result of more pronounced phonon-phonon scattering or heat resistant phenomena in the samples [48]. Additionally, the composites with a higher graphene loading showed a greater slope in its thermal diffusivity value with temperature than those with a lower filler content suggesting a more temperature sensitivity of the composites with increasing the graphene contents.

5.7 Thermal Conductivity of Highly Filled Graphene-Polybenzoxazine Composites

Thermal conductivities of the graphene-filled polybenzoxazine composites as a function of graphene loading at 25°C were determined according to Equation (4.4) with the known parameters of thermal diffusivities, heat capacities and densities of the composites. The values were also summarized in Table 5. 6.

Figure 5. 14 shows a plot of the thermal conductivity of graphene-filled polybenzoxazine composites as a function of graphene weight fractions. As seen in this figure, thermal conductivity of the neat polybenzoxazine was calculated to be 0.23 W/mK which is in good agreement with the previous reported value [6]. In addition, the thermal conductivity values of the composites were found to systematically increase with increasing graphene content. The maximum thermal conductivity of our highly filled graphene-polybenzoxazine composites was determined to be 8.03 W/mK at 60wt% of the graphene which represented about 35 times greater than that of the neat polybenzoxazine. The relatively high thermal conductivity value obtained in our polybenzoxazine composite is attributed to the maximizing formation of conductive networks of graphene particles with small heat resistance in this highly filled system. Since efficient heat propagation in graphene is mainly due to diffusion of phonons, a uniform dispersion and network of a highly thermally conductive graphene in the polybenzoxazine matrix significantly contribute to the steady increase in thermal conductivity in the composites [33]. Moreover, platelet structure of graphene with a relatively high aspect ratio can more readily form continuous thermally conductive pathways in the polymer matrix than a low aspect ratio filler and thus is more effective in enhancing the thermal conductivity of the composite sample [34], [49]. However, thermal conductivity values observed in our highly-filled composites are through-plane thermal conductivity, which is lower than that of the in-plane values. The in-plane thermal conductivity of graphene based composites was found and reported by X. Tian et al. [50].

Comparing at the same filler content, the thermal conductivity of our highly filled graphene-polybenzoxazine composites was found to be greater than the values obtained from graphite-filled polybenzoxazine reported by I. Dueramae et al. [6]. This

is possibly due to the much smaller particle size as well as higher aspect ratio of the graphene platelets used compared to the graphite particles i.e. nanometer range vs micrometer range. These characteristics of the graphene particles should render a much greater ability to form conductive network of the filler particles than the graphite particles comparing at the same filler loading. Furthermore, our highly filled graphene-polybenzoxazine composites also showed higher thermal conductivity value than some reported high filler loading composites. For example, the thermal conductivity value was reported to be 5.5 W/mK or about 27.5 times enhancement in epoxy/graphene at the maximum graphene content of 50vol% [35] and 6.6 W/mK in epoxy/graphite nanoplatelets at the maximum filler content of 40vol% [51].

5.8 Effect of the Graphene Loading on Flexural Properties of Highly-Filled Graphene-Polybenzoxazine Composites

One common function of bipolar plate is to provide structural support for the fuel cell stack and withstand the vibration occurred from the moving vehicle. Moreover, the bipolar plate material must withstand the pressure during cell assembly which must be done under certain compression condition to achieve good electrical contact with gas diffusion layer, thus the materials with excellent mechanical properties must be required [52]. The flexural properties of graphene filled polybenzoxazine composites with different graphene loading were systematically investigated. As displayed in Figure 5. 15, the flexural modulus the composites were found to systematically increase with increasing graphene contents, following an additive rule. The flexural modulus values were determined to be in a range of 5.2 to 17.5 GPa and the highest value of 17.5 GPa was obtained at 60wt% of graphene loading, which was enhanced by almost 246% compared to that of the neat polybenzoxazine, having the value of 5.2 GPa. Additionally, the value is also higher than that of a highly filled system of polyphenylene sulfide and graphene nanoplatelets as reported by X. Jiang et al. [32] for PEM fuel cell i.e. 15 GPa at graphene content of 60wt%. The enhancement in flexural modulus was believed to be due to a uniform dispersion and strong interfacial bonding between the filler and the polybenzoxazine matrix [53]. It is, therefore, evident that an addition of much greater rigidity of particulate graphene into

the polybenzoxazine matrix attributed to significant enhancement in the stiffness of the obtained polybenzoxazine composites [6]. Interestingly, the flexural modulus of the graphene filled polybenzoxazine at 30-60wt% of graphene contents exceeded the DOE requirement of 10 GPa for a bipolar plate application [8].

The flexural strength of the highly filled graphene-polybenzoxazine composites was also investigated as depicted in Figure 5. 16. The flexural strength values of the composites were found to be lower than that of the neat polybenzoxazine. For the composite at 10wt% of graphene loading, the strength of the composite rapidly decreased and was observed to be 69.1 MPa comparing with the value of 119.7 MPa of the neat polybenzoxazine. This behavior is due to the presence of interface between the filler and the matrix of these heterogeneous systems. Moreover, the lower flexural strength values might be related to the effect of discontinuous longer interparticle distance on stress transferring in the composite [54]. However, the flexural strength of our highly filled graphene-polybenzoxazine composites tended to be lowered by an increase of graphene contents from 10-50wt%. The slight decrease in the strength values implied that the highly filled graphene particles can form continuous network in the composites thus leading to better continuous stress transferring. The further lowering of the flexural strength of the composite was observed at 60wt% graphene loading which might be owing to the more aggregate formation of the graphene in the polybenzoxazine matrix. The observed strength reduction with an increase in rigid particle loading is also observed in those reported by X. Jiang et al. [32] in highly filled systems of graphene nanoplatelets/polyphenylene sulfide and by I. Dueramae et al. [6] in highly filled graphite/polybenzoxazine composites. The other graphene-filled composite system with low range of graphene content (2wt%), the strength of the composites was found to show a sharp decrease with increasing graphene content such as that reported by J. Li et al. in graphite nanoplatelets/epoxy nanocomposites [55]. This suggested the benefit of making a highly filled system on the enhancement of the obtained composite strength compared to that obtained in the low range of filler content. In addition, at 60wt% graphene loading, the flexural strength of our highly filled composite remains as high

as 41.7 MPa, which was significantly greater than the flexural strength value of the DOE targets for bipolar plate material (>25MPa) [4].

5.9 Water Absorption of Polybenzoxazine and Graphene-Filled Polybenzoxazine Composites at Various Graphene Contents

The influence of moisture on polymeric materials via the measurement of can be effectively reduced by incorporating nano-size hydrophobic additive into polymers [56]. The percentage of water absorption of composite was determined as weight gain per unit weight of the dried specimen using Equation 4.7. Water absorption behavior by the neat polybenzoxazine and its composites filled with graphene (0-60wt% of graphene) is shown in Figure 5. 17. From the figure, the percentage of water absorbed plotted against time for all composites showed a similar behavior. The absorption curves are rapidly increased at the early stage of water uptake (i.e. 0-24 hours). The water uptake of typical composites for bipolar plate in fuel cell applications at 24 hours has to be less than 0.3%, which is the value required by DOE [57]. Our polybenzoxazine showed water uptake value at 24 hours to be 0.152% which is decreased with increasing the graphene contents. The water uptake value of the graphene-filled polybenzoxazine was calculated to be only 0.06% at a graphene content of 60wt% (maximum packing density). The water uptakes of the composites were found to steadily increase with time but at a lower rate comparing with the first 24 hours. From the curves, the water uptake of the composites up to 60 days of immersion remained less than 0.8% at the filler content of 0-60wt%. In addition, the water absorption of all composites was decreased with increasing graphene content. This phenomenon implied that the addition of plate-like filler with high aspect ratio provided tortuous pathways for water molecules to enter the composites and could acted as efficient barriers against transport of water through the composites [44], [56]. Another reason for less water absorption could be the hydrophobic and water repelling nature of graphene surface that tended to immobilize some of moisture, which inhibited the water permeation in the polymer matrix [44], [58]. Moreover, the reduction of water absorption resulted from the relatively good filler dispersion and interfacial bonding between the filler and the matrix that minimized the formation of

air gaps between the filler and the matrix. This low water uptake is highly desirable characteristic in bipolar plate application.

5.10 Electrical Conductivity of Highly Filled Graphene-Polybenzoxazine Composites

According to PEMFC operation, electrons must transfer through bipolar plates to complete a circuit, so one critical fuel cell performance factor is the electrical conductivity of the bipolar plate to minimize voltage loss. [52]. Figure 5. 18 shows a plot of the electrical conductivity of graphene filled polybenzoxazine composites as a function of graphene weight fractions. As can be seen in this figure, the electrical conductivity of the composites at 10-40wt% of graphene contents increased slightly with increasing graphene loading. Those conductivity values of the composites were measured to be 1.52, 2.50, 7.42 and 9.26 S/cm.at 10, 20, 30 and 40wt% of graphene. Furthermore, a sharp increase in electrical conductivity of graphene filled polybenzoxazine was evidently observed at the composites containing 50 and 60wt% of graphene. The conductivity values at these relatively high loading of graphene were measured to be 125 and 357 S/cm, respectively. Generally, electrical conductivity of polymer composite is immensely influenced by the amount and type of filler. The observed substantial enhancement in the electrical conductivity values was attributed to the good interfacial bonding between the graphene filler and polybenzoxazine matrix and the formation of the continuous graphene particle network having tremendous amount of the conductivity paths particularly at very high graphene loading that was achieved in our polybenzoxazine composites. In comparison with graphite filled polybenzoxazine recently reported by I. Dueramae et al. [6], the electrical conductivity of graphene-filled polybenzoxazine was found to be significantly higher than those obtained using graphite-filler comparing at the same percentage of the filler loading. Furthermore, electrical conductivity values of the graphene filled polybenzoxazine composites at 50wt% (125 S/cm) and 60wt% (357 S/cm) meet the value recommended by the US Department of Energy (DOE) of 100 S/cm for bipolar plate application, whereas at least 70wt% of graphite contents in graphite filled polybenzoxazine having the value of 104 S/cm was required to achieve the DOE

requirement. Consequently, the graphene filled polybenzoxazine at 50 and 60wt% of the graphene contents are a potential candidate to be used in a bipolar plate for PEM fuel cell applications.

5.11 SEM Characterization of Highly Filled Graphene-Polybenzoxazine Composites

The significant improvement in mechanical properties of the composites with incorporation of graphene fillers were further supported by SEM micrographs. Due to strong Van der Waals attraction, large surface areas and $\pi-\pi$ interaction [33], nanofiller dispersion is an important issue since graphene nanoplatelets (GNPs) have a nature inherency to form agglomerates as evidently seen in the micrograph in Figure 5. 19. The morphological characteristic of graphene-filled polybenzoxazine composites at various graphene loading was observed. Figure 5. 20 (a) illustrated the fracture surface of the neat polybenzoxazine revealing a relatively smooth surface. Figure 5.20 (b) shows a SEM micrograph of fracture surface of polybenzoxazine composites with 1wt% of graphene filler. As seen in the figure, the graphene particles were well dispersed in the polybenzoxazine matrix, attributed to the very low melt viscosity of the benzoxazine resin used, thus resulting in good flow-ability and wetting of the graphene filler. The Figure also shows flake liked shaped of graphene particle encapsulated with the polybenzoxazine matrix, indicating substantial interfacial adhesion between the filler and the matrix. The result was confirmed by no separation of graphene fillers from the polybenzoxazine matrix on fracture surface.

Figures 5. 20 (c)-(h) show the SEM micrographs of the graphene filled polybenzoxazine composites with filler contents of 10, 20, 30, 40, 50 and 60wt%, respectively. The fracture surface of the composites was clearly observed to be rougher compared to the neat polybenzoxazine which was due to the cover of graphene filler on the polybenzoxazine matrix. Moreover, only some area of polybenzoxazine matrix was noticed at low graphene content whereas no smooth area of the polybenzoxazine matrix was observed at a high graphene content. The graphene-filled polybenzoxazine composites show relatively good graphene distribution and substantial interfacial adhesion between the matrix and the graphene.

These results might be attributed to the very low viscosity and good wettability of the benzoxazine resin at the molding temperature [6], [7]. Furthermore, the graphene fillers in the composites with such a high loading were in good contact with each other to give a well-developed electrical pathways and relatively high electrical conductivity useful for bipolar plate utilization. There were some chance of void formation between the graphene particles and the polybenzoxazine due to a presence of the agglomerates that were detected in the samples at 60wt% of graphene loading which exhibited slightly lower value of its measured density compared to the theoretical density. This causes the flexural strength of the composites at 60wt% of graphene content to be more abruptly reduced, as compared with the composites filled with the lower contents of graphene.

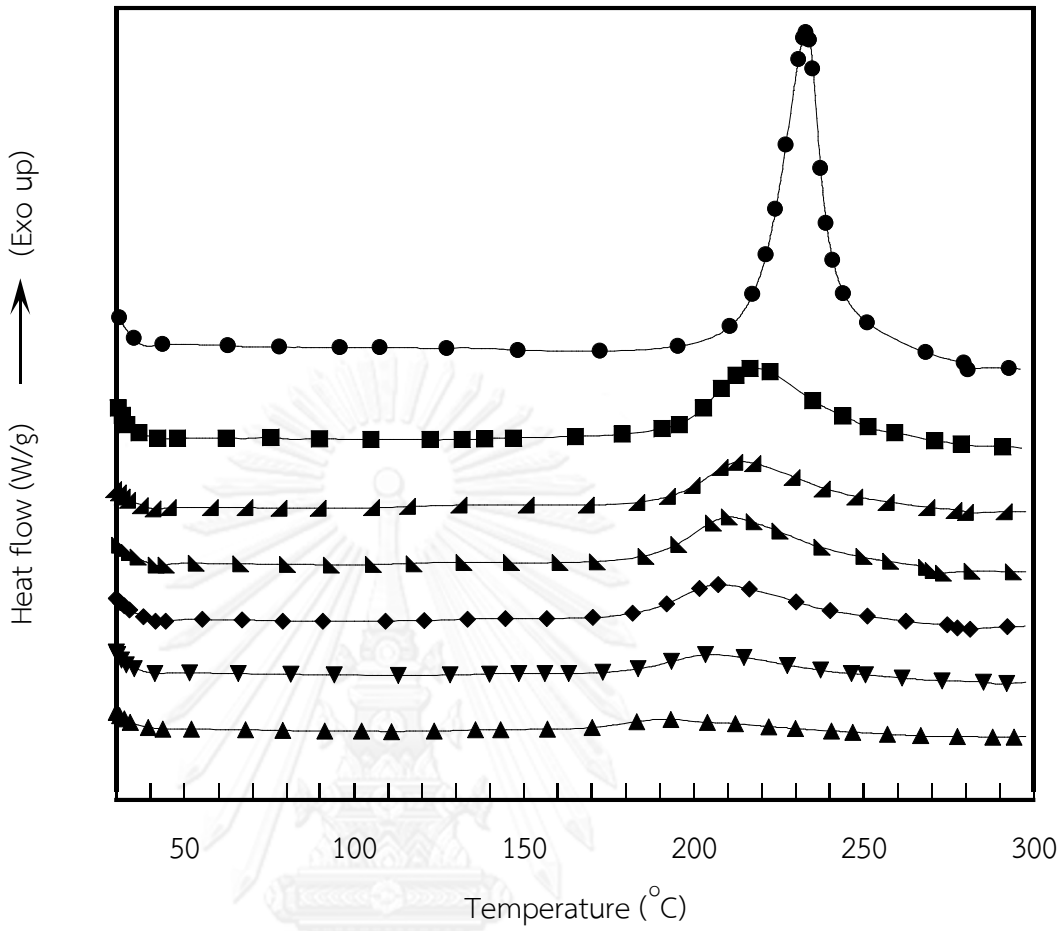

Figure 5. 1 DSC thermograms of benzoxazine molding compound at different graphene contents: (●) neat polybenzoxazine, (■) 10wt%, (◢) 20wt%, (◣) 30wt%, (♦) 40wt%, (▼) 50wt%, (▲) 60wt%.

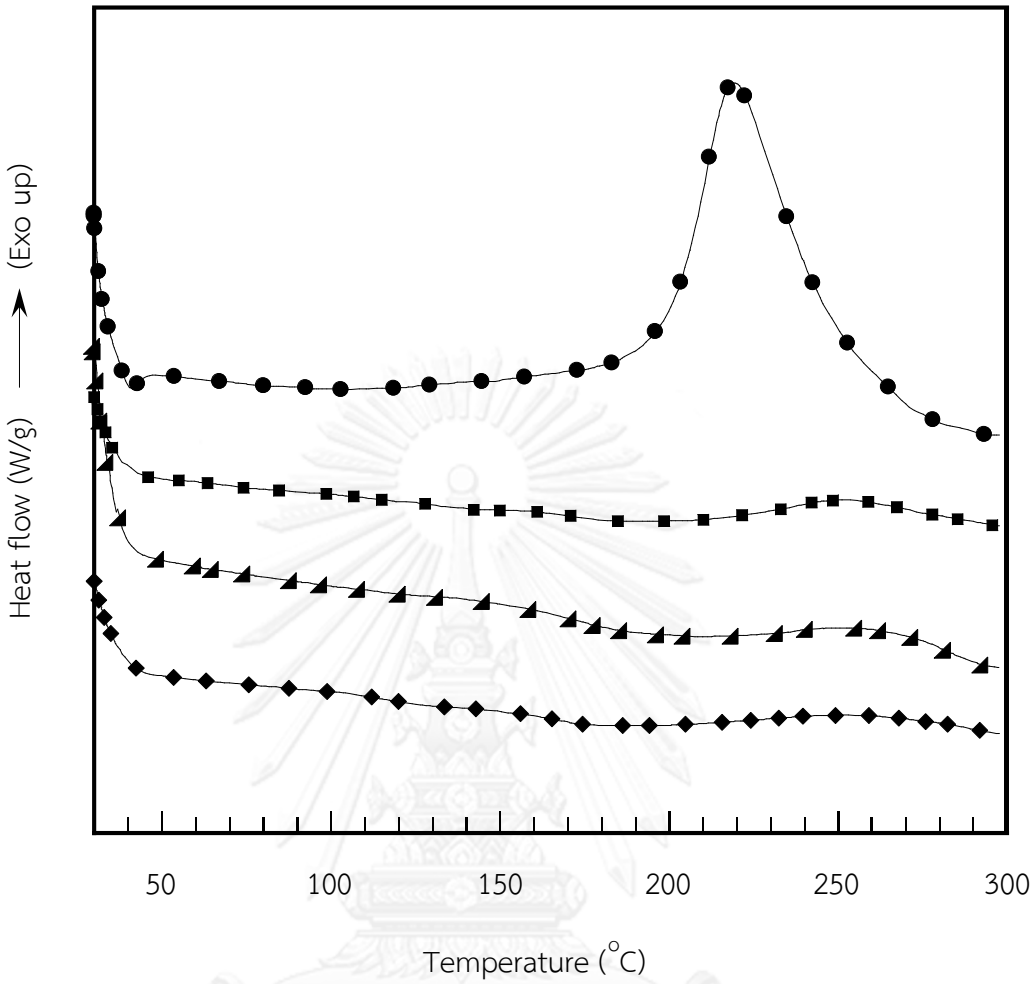

Figure 5. 2 DSC thermograms of the composite at 10wt% of graphene content with various curing times at 200°C: (●) uncured molding compound, (■) 1 hour, (◢) 2 hours, (♦) 3 hours.

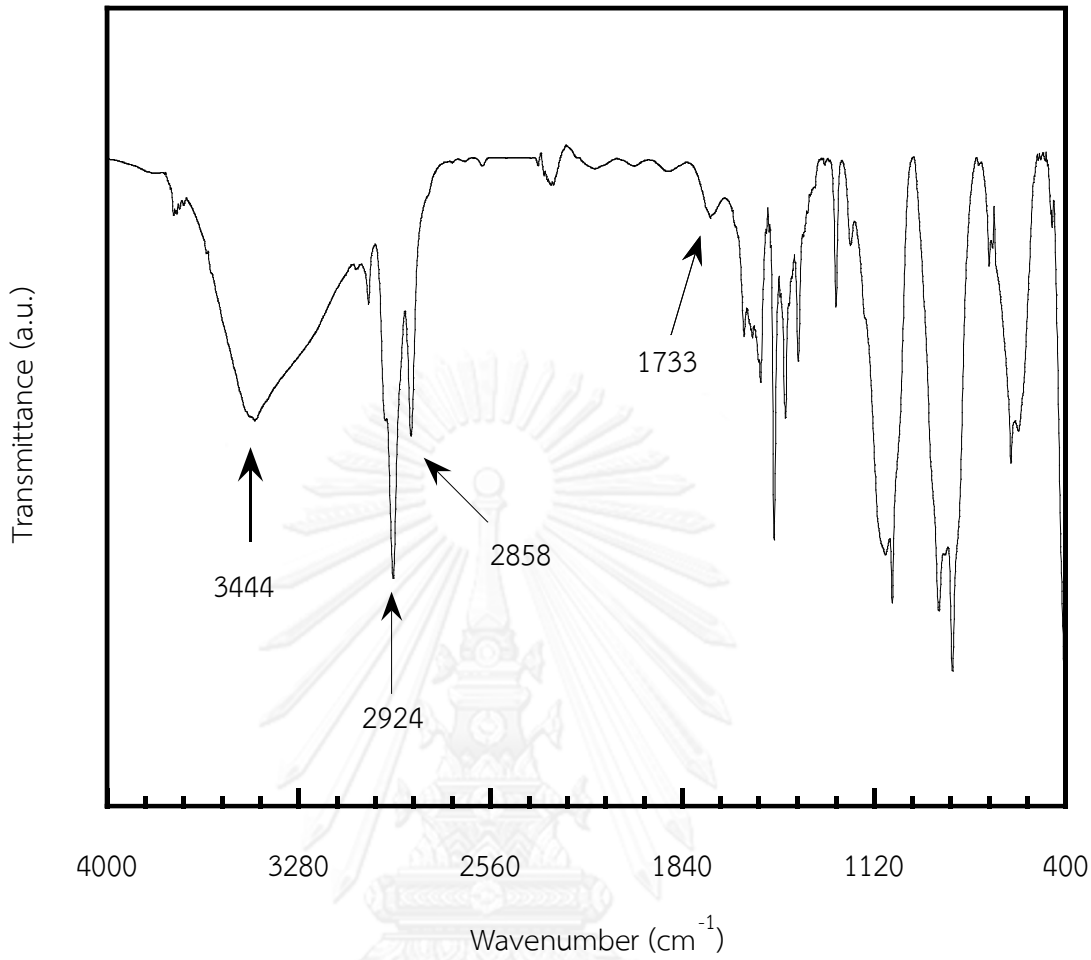

Figure 5. 3 FTIR spectra of as-received graphene-grade H from XG Sciences, USA use in this research.

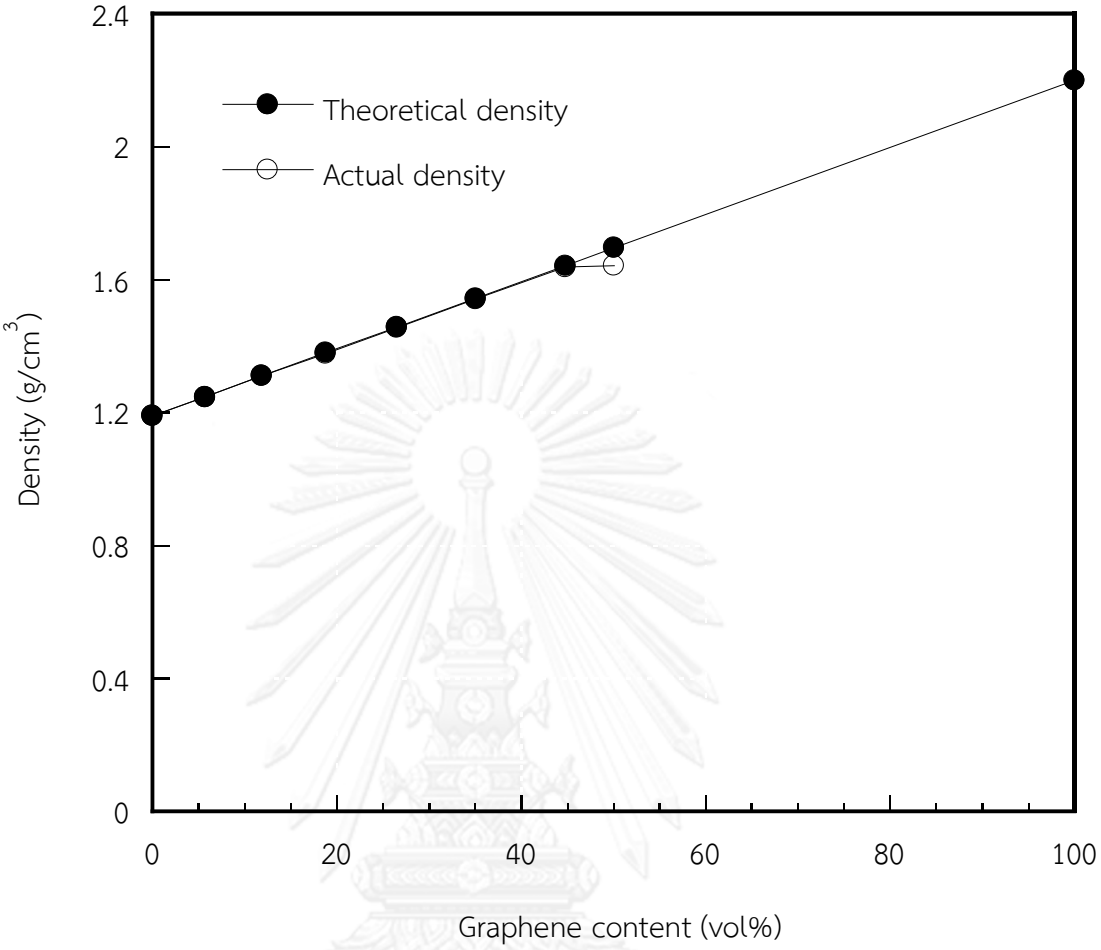

Figure 5. 4 Theoretical and actual densities of graphene-filled polybenzoxazine composites at different contents of graphene: (●) theoretical density, (**O**) actual density.

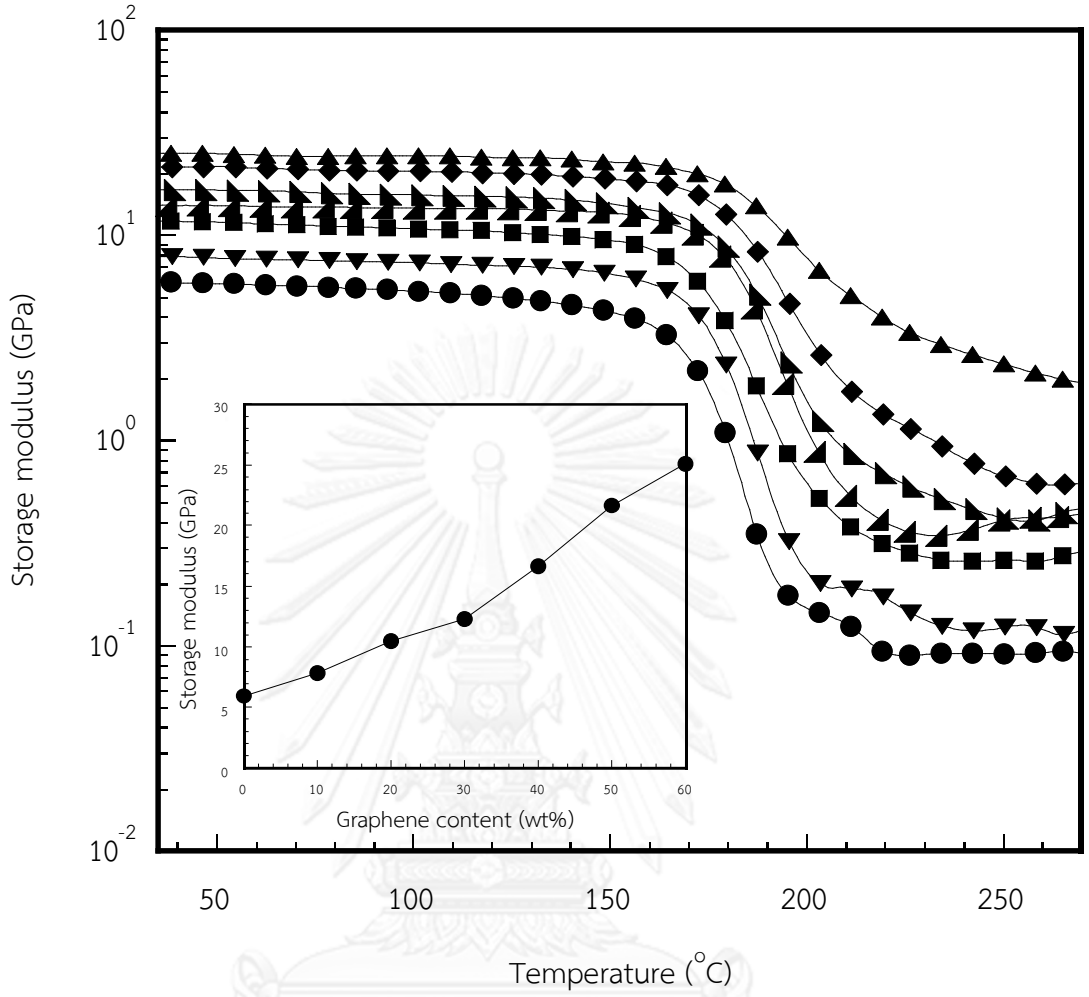

Figure 5. 5 DMA thermograms of storage modulus of graphene-filled polybenzoxazine composites: (●) neat polybenzoxazine, (■) 10wt%, (◢) 20wt%, (◣) 30wt%, (♦) 40wt%, (▼) 50wt%, (▲) 60wt%.

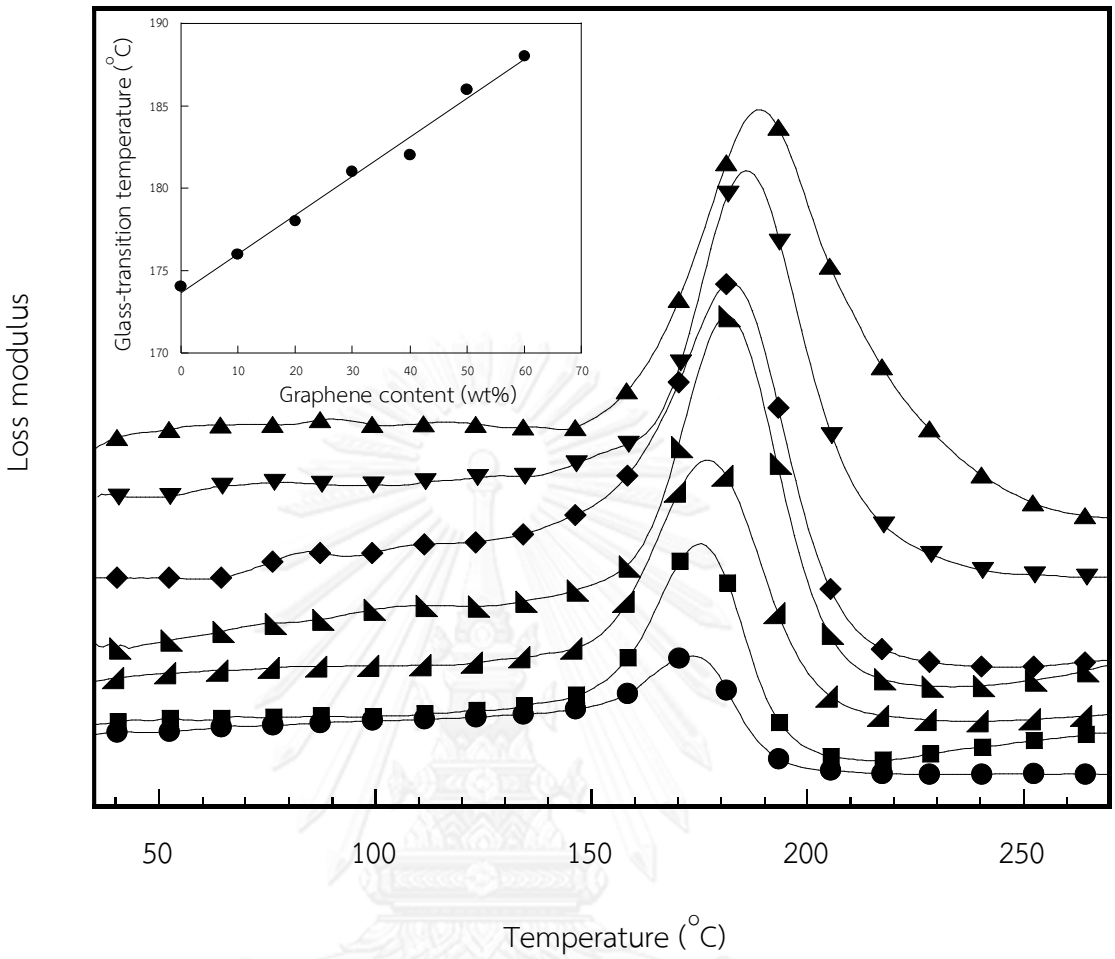

Figure 5. 6 DMA thermograms of loss modulus of graphene-filled polybenzoxazine composites: (●) neat polybenzoxazine, (■) 10wt%, (◢) 20wt%, (◣) 30wt%, (♦) 40wt%, (▼) 50wt%, (▲) 60wt%.

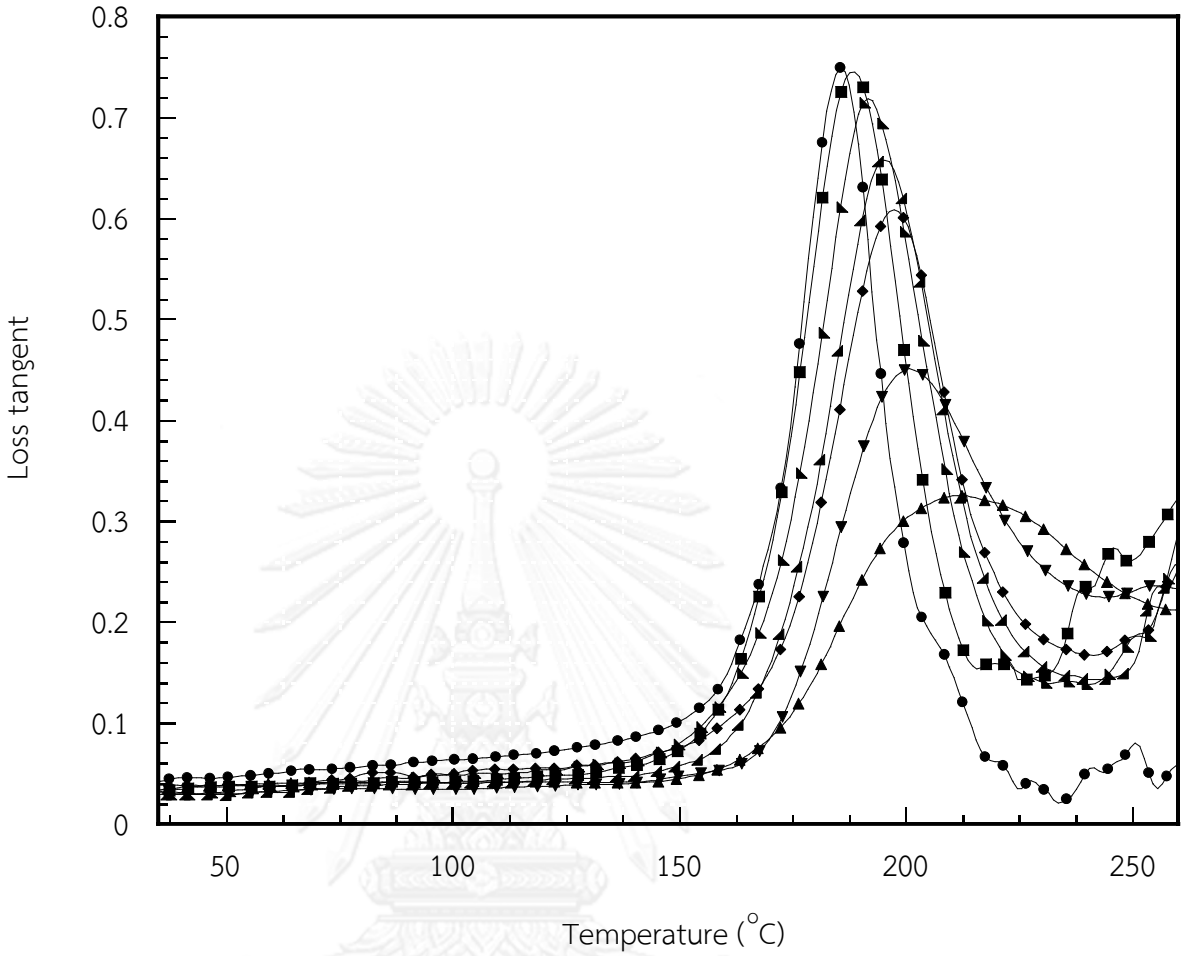

Figure 5. 7 DMA thermograms of loss tangent of graphene-filled polybenzoxazine composites: (●) neat polybenzoxazine, (■) 10wt%, (◢) 20wt%, (◣) 30wt%, (♦) 40wt%, (▼) 50wt%, (▲) 60wt%.

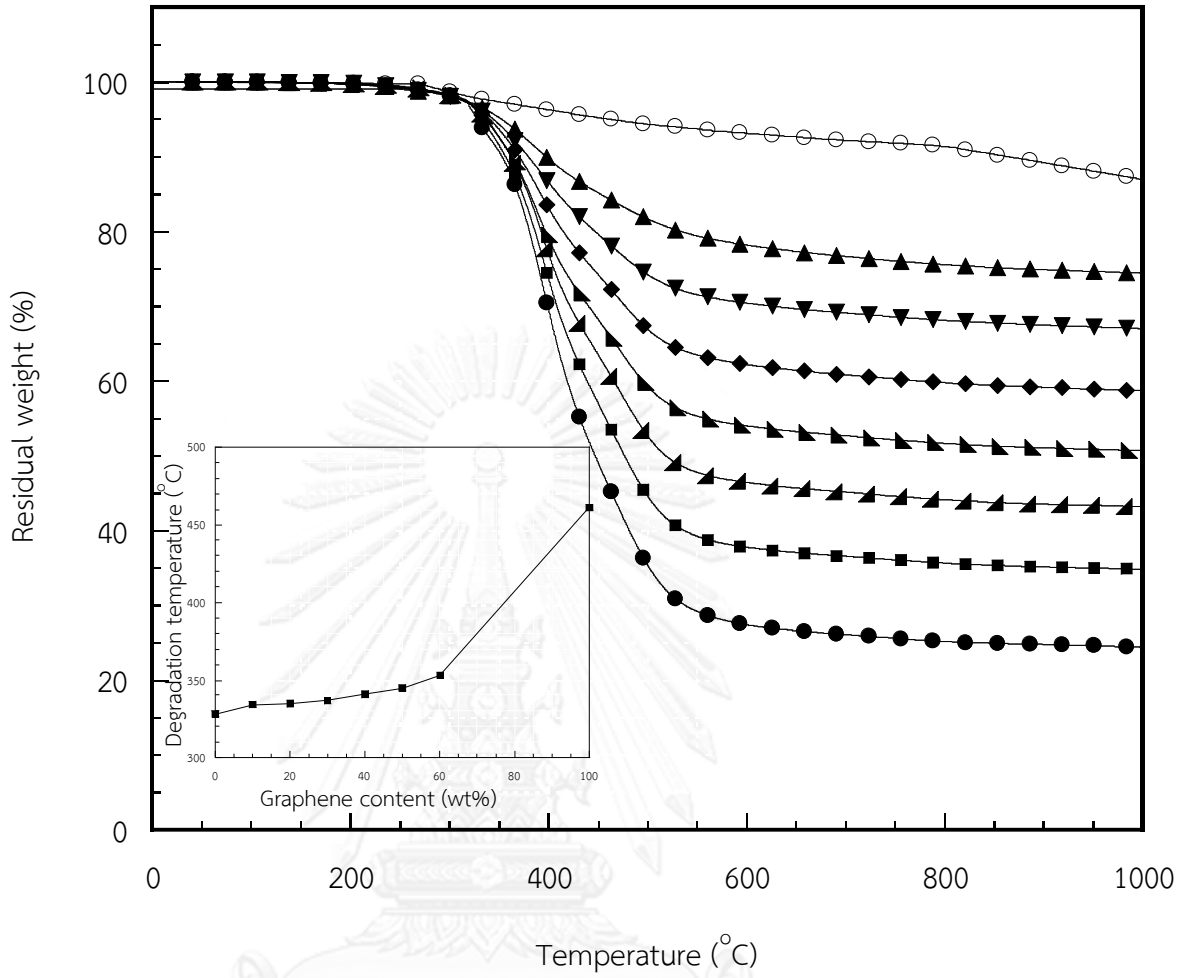

Figure 5. 8 TGA thermograms of graphene-filled polybenzoxazine composites: (●) neat polybenzoxazine (■) 10wt%, (◢) 20wt%, (◣) 30wt%, (♦) 40wt%, (▼) 50wt%, (▲) 60wt%, (O) neat graphene.

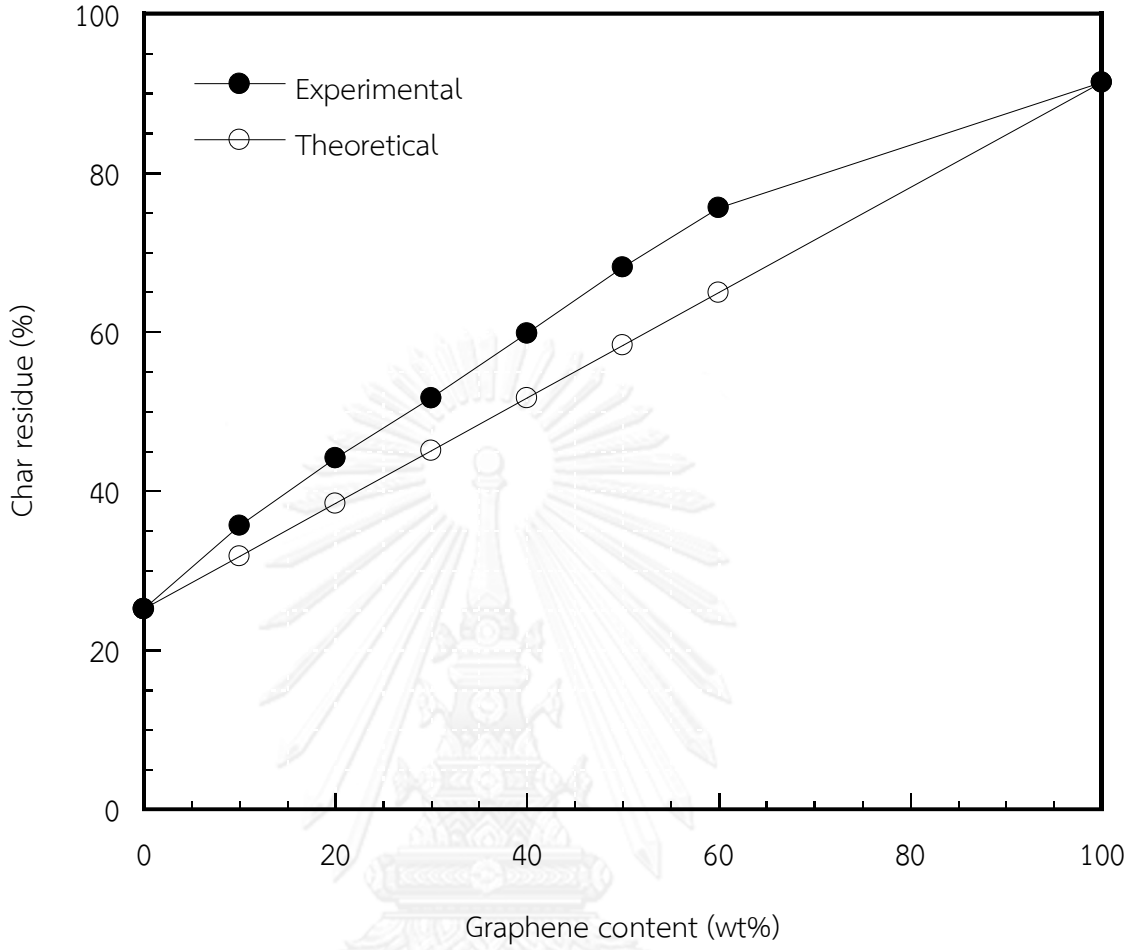

Figure 5. 9 Calculation and experimental char yield at 800^{o}C of graphene-filled polybenzoxazine composites at difference graphene contents: (**O**) theoretical char yield, (●) experimental char yield.

Table 5. 1 Thermal characteristics of polybenzoxazine and graphene-filled polybenzoxazine composites.

Graphene content (wt%)	T_d (^oC) at 5% weight loss	Char yield (%) at 800^oC (Experimental)	Char yield (%) (Calculation)
0	327	25.20	-
10	333	35.67	31.82
20	335	44.13	38.44
30	337	51.67	45.06
40	341	59.80	51.68
50	345	68.13	58.30
60	353	75.57	64.92
100	461	91.40	-

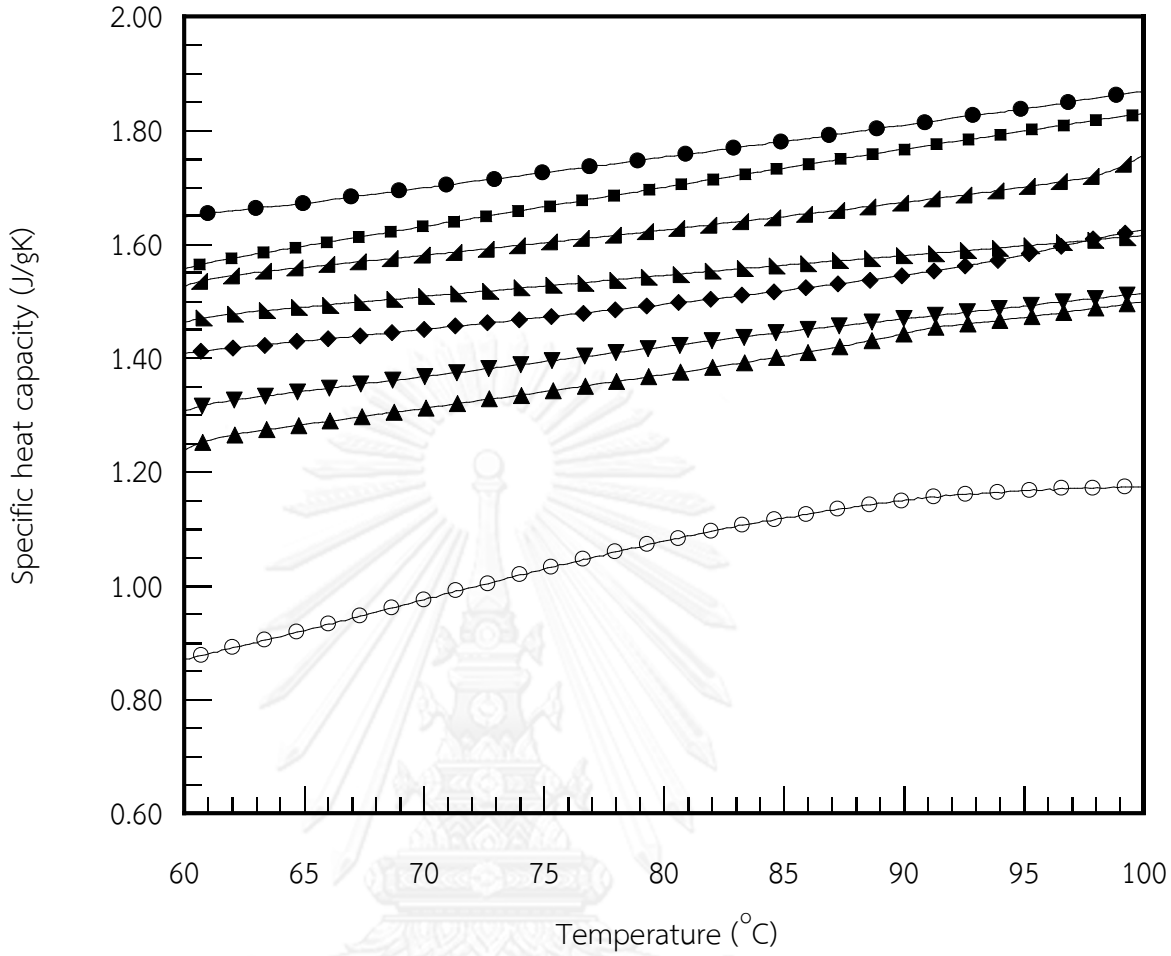

Figure 5. 10 Specific heat capacity of graphene-filled polybenzoxazine composites: (●) neat polybenzoxazine (■) 10wt%, (◢) 20wt%, (◣) 30wt%, (♦) 40wt%, (▼) 50wt%, (▲) 60wt%, (O) neat graphene.

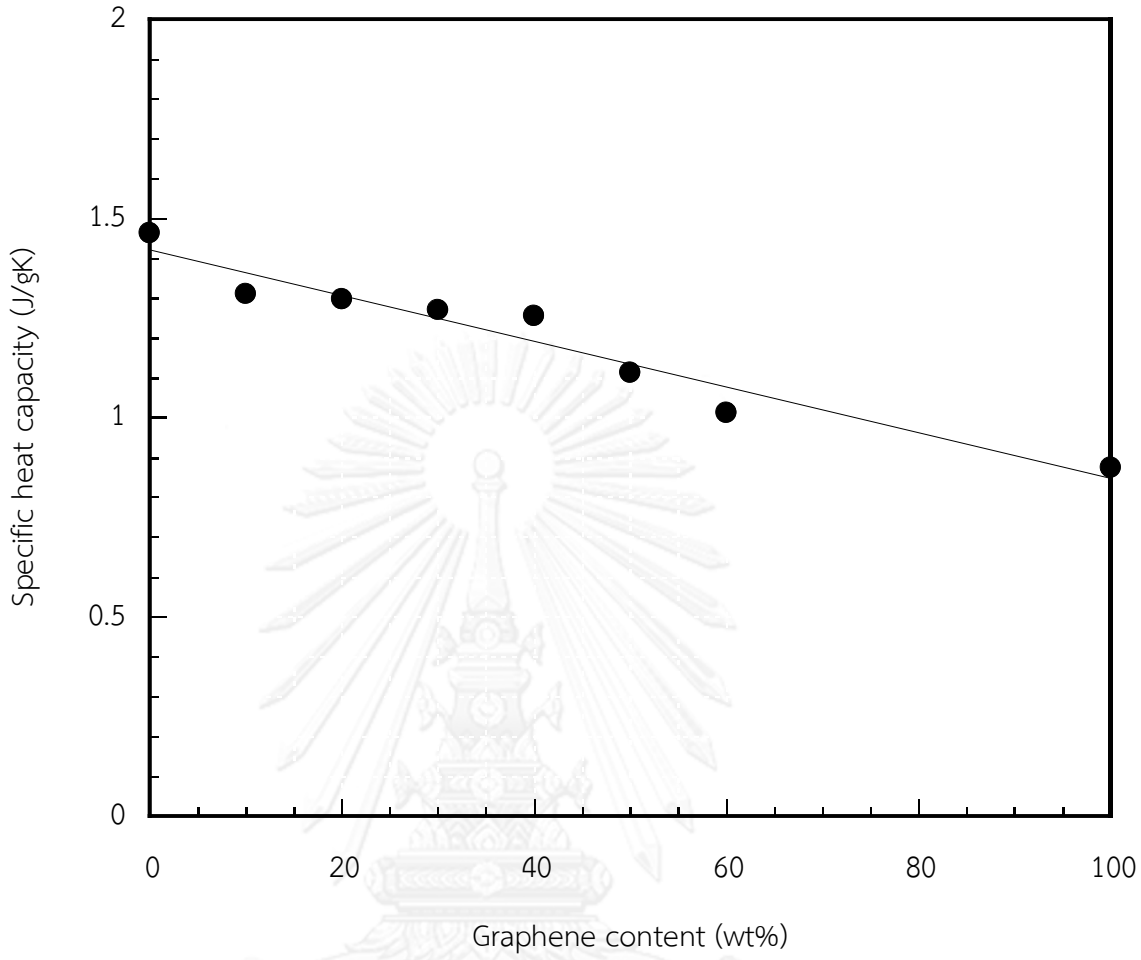

Figure 5. 11 Specific heat capacity extrapolated at 25^{o}C of graphene-filled polybenzoxazine as a function of graphene contents.

Table 5. 2 Specific heat capacity values of graphene-filled polybenzoxazine at different graphene contents.

Graphene content (wt%)	Specific heat capacity (J/gK)		Error (%)
	Experimental	Calculated	
0	1.753	-	-
10	1.700	1.685	+0.88
20	1.625	1.618	+0.43
30	1.546	1.550	-0.26
40	1.495	1.483	+0.81
50	1.420	1.415	+0.35
60	1.371	1.347	+1.78
100	1.076	-	-

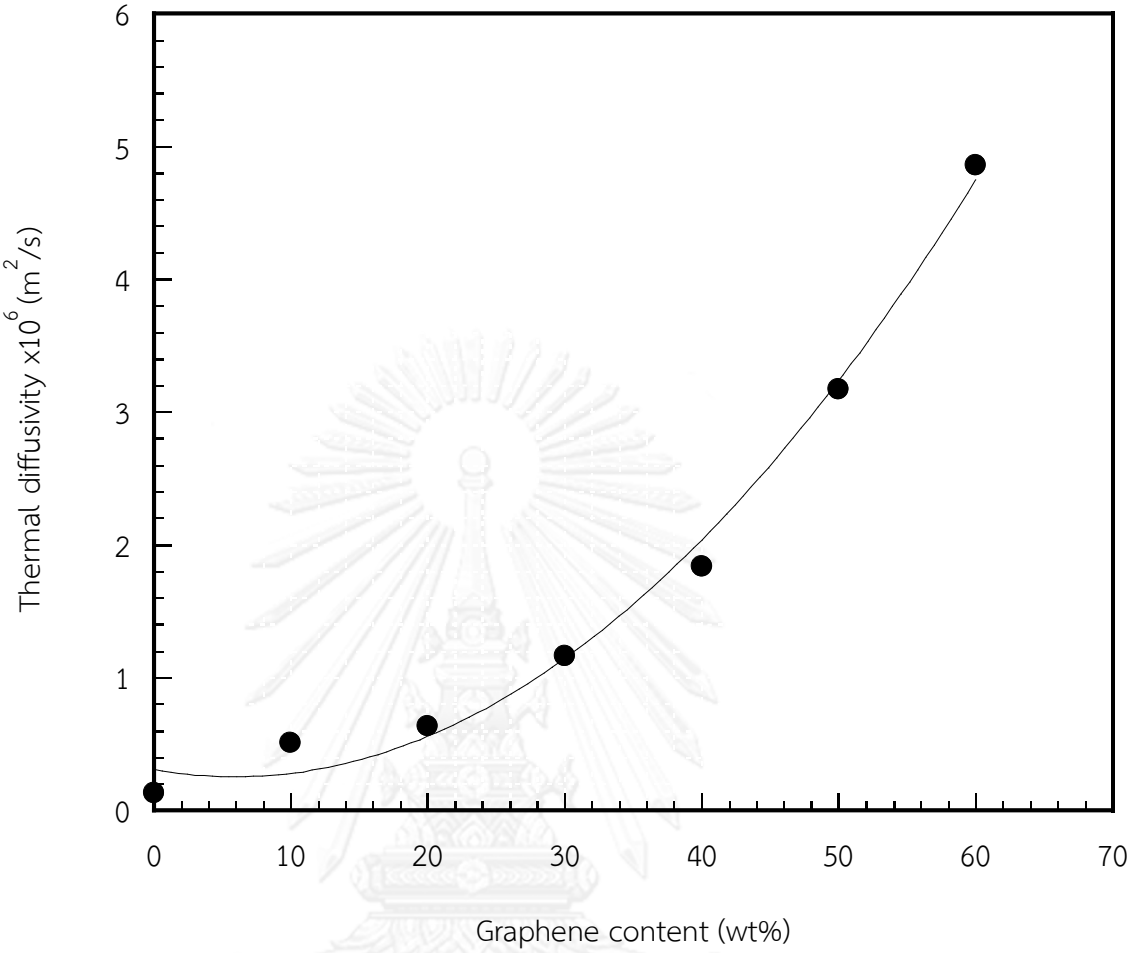

Figure 5. 12 Thermal diffusivity at 25^{o}C of graphene-filled polybenzoxazine as a function of graphene contents.

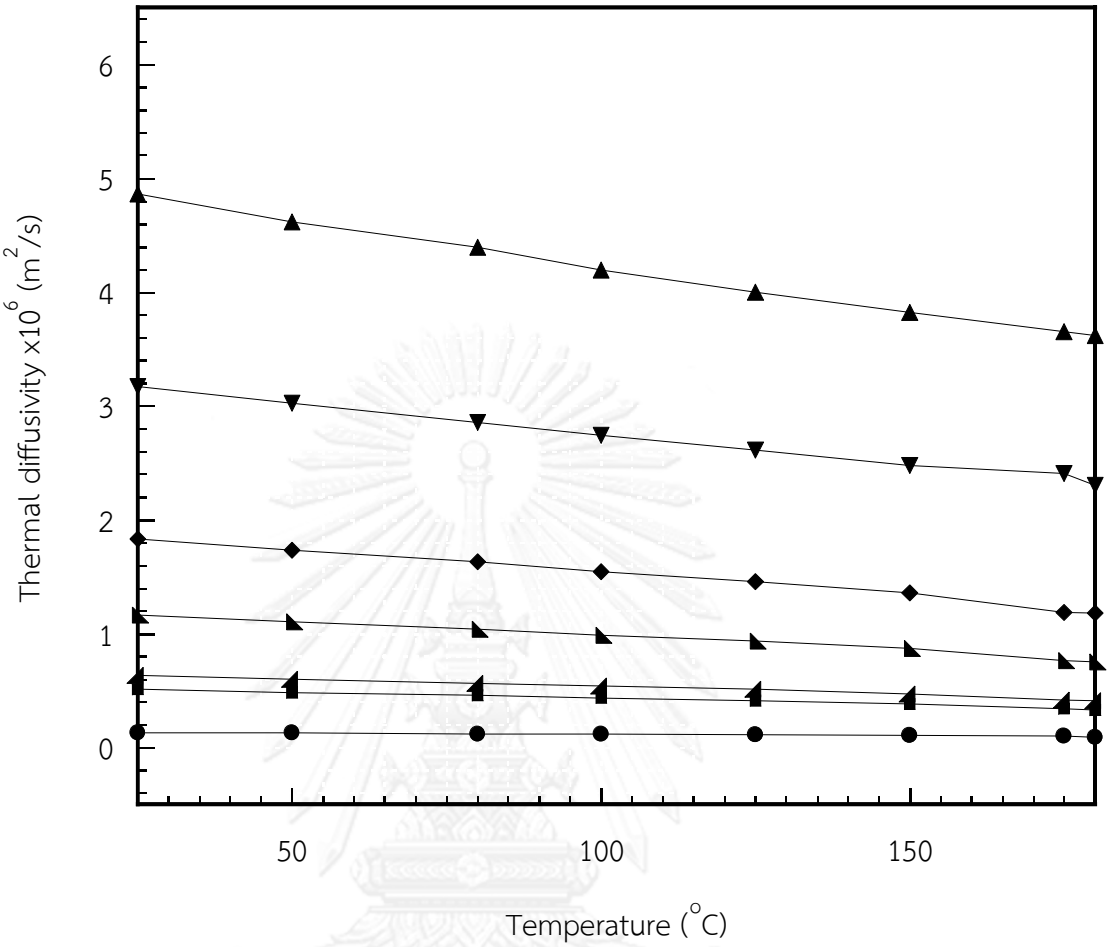

Figure 5. 13 Thermal diffusivity of graphene-filled polybenzoxazine composites: (●) neat polybenzoxazine (■) 10wt%, (◢) 20wt%, (◣) 30wt%, (♦) 40wt%, (▼) 50wt%, (▲) 60wt%.

Table 5. 3 Thermal conductivity of highly filled-graphene polybenzoxazine composites at 25^{o}C.

Filler content (wt%)	$\alpha \times 10^6$ (m^2/s)	C_p (J/gK)	ρ (g/cm^3)	K (W/mK)
0	0.131	1.464	1.185	0.227
10	0.509	1.311	1.247	0.832
20	0.635	1.298	1.310	1.079
30	1.162	1.271	1.377	2.032
40	1.836	1.256	1.455	3.355
50	3.171	1.112	1.540	5.430
60	4.861	1.011	1.637	8.037

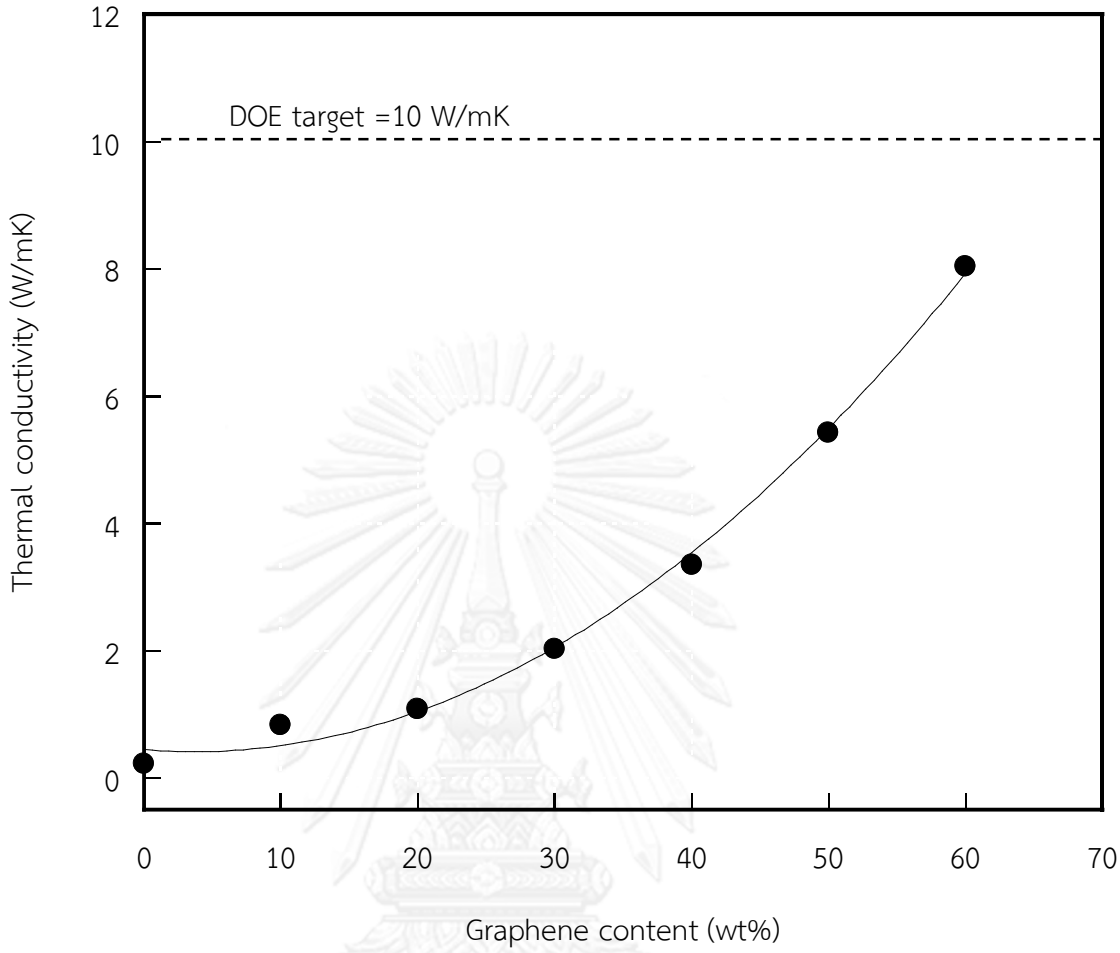

Figure 5. 14 Thermal conductivity at 25^{o}C of highly filled graphene-polybenzoxazine composites as a function of graphene contents.

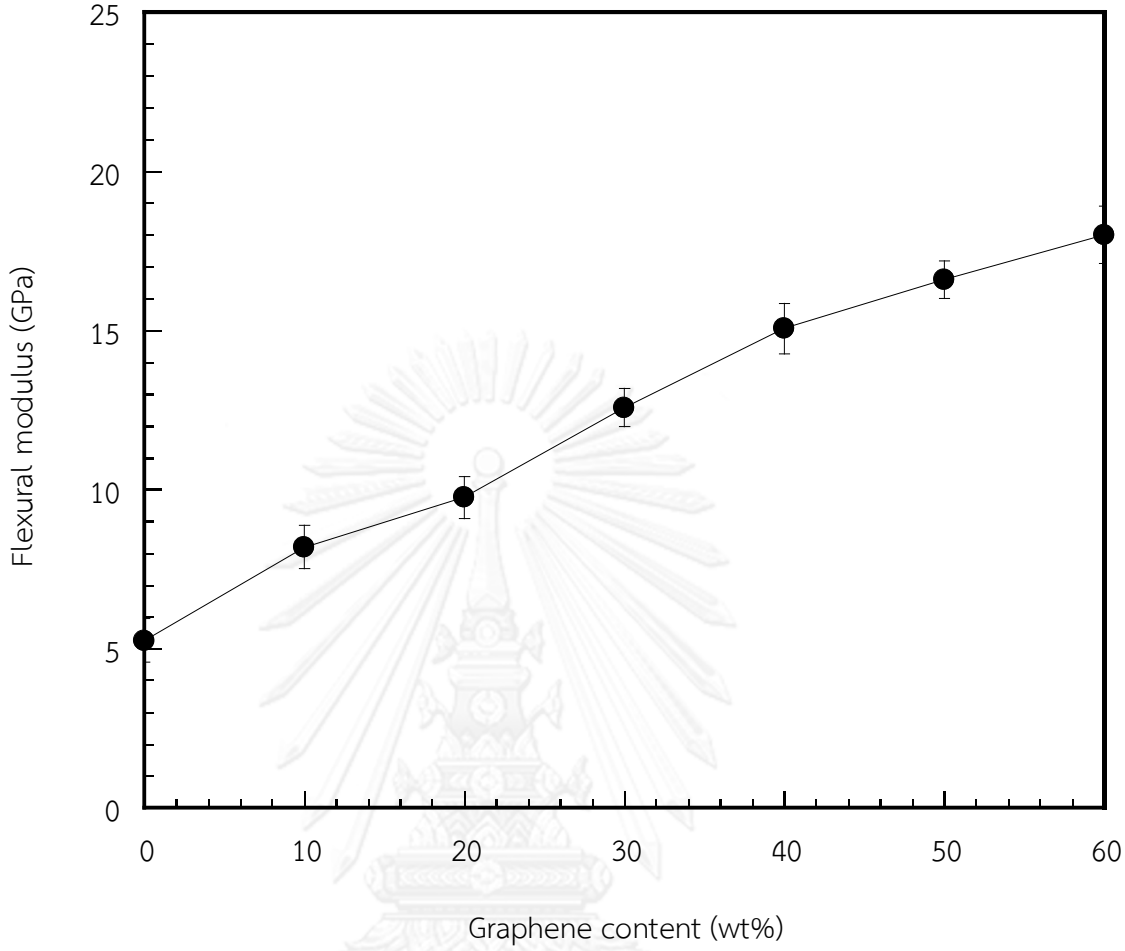

Figure 5. 15 Relation between graphene contents and the flexural modulus of graphene-filled polybenzoxazine composites.

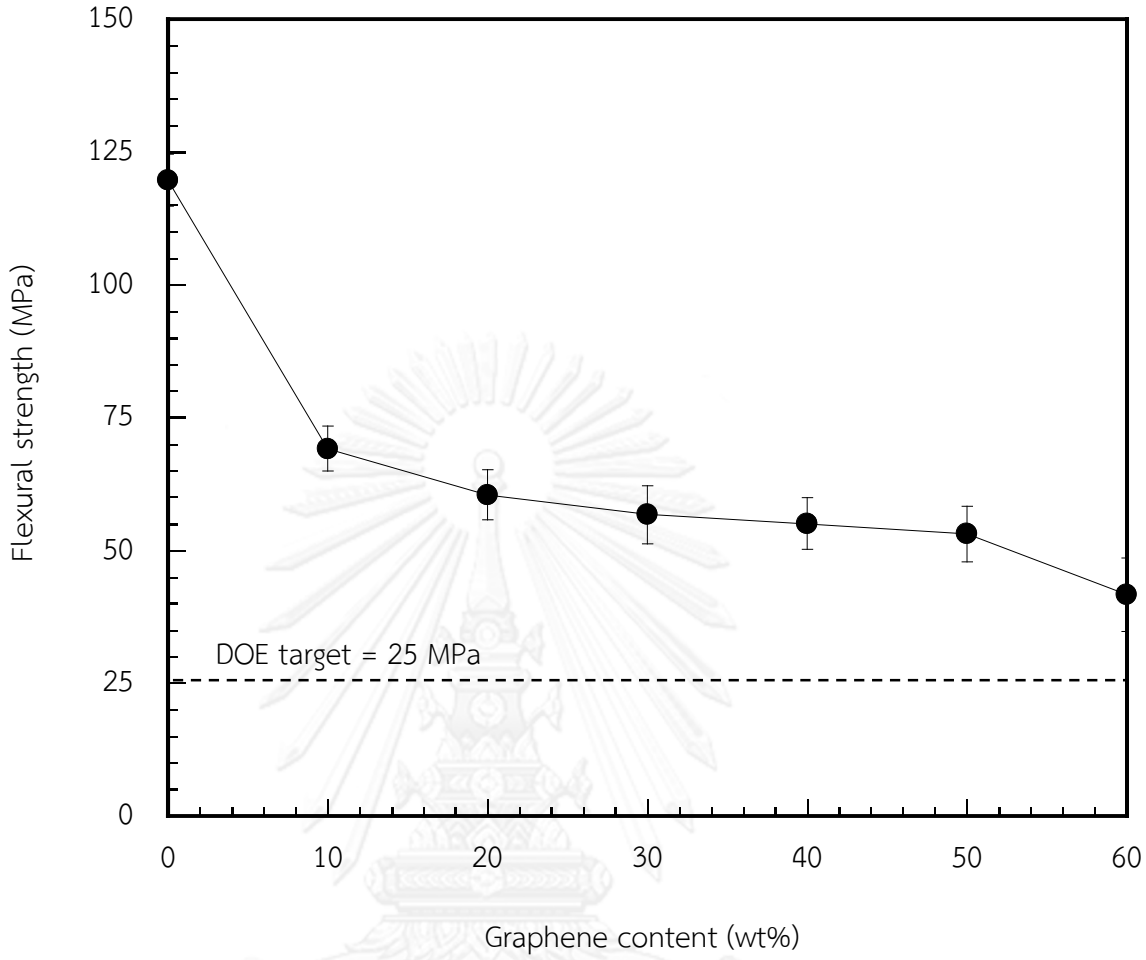

Figure 5. 16 Relation between filler contents and the flexural strength of graphene-filled polybenzoxazine composites.

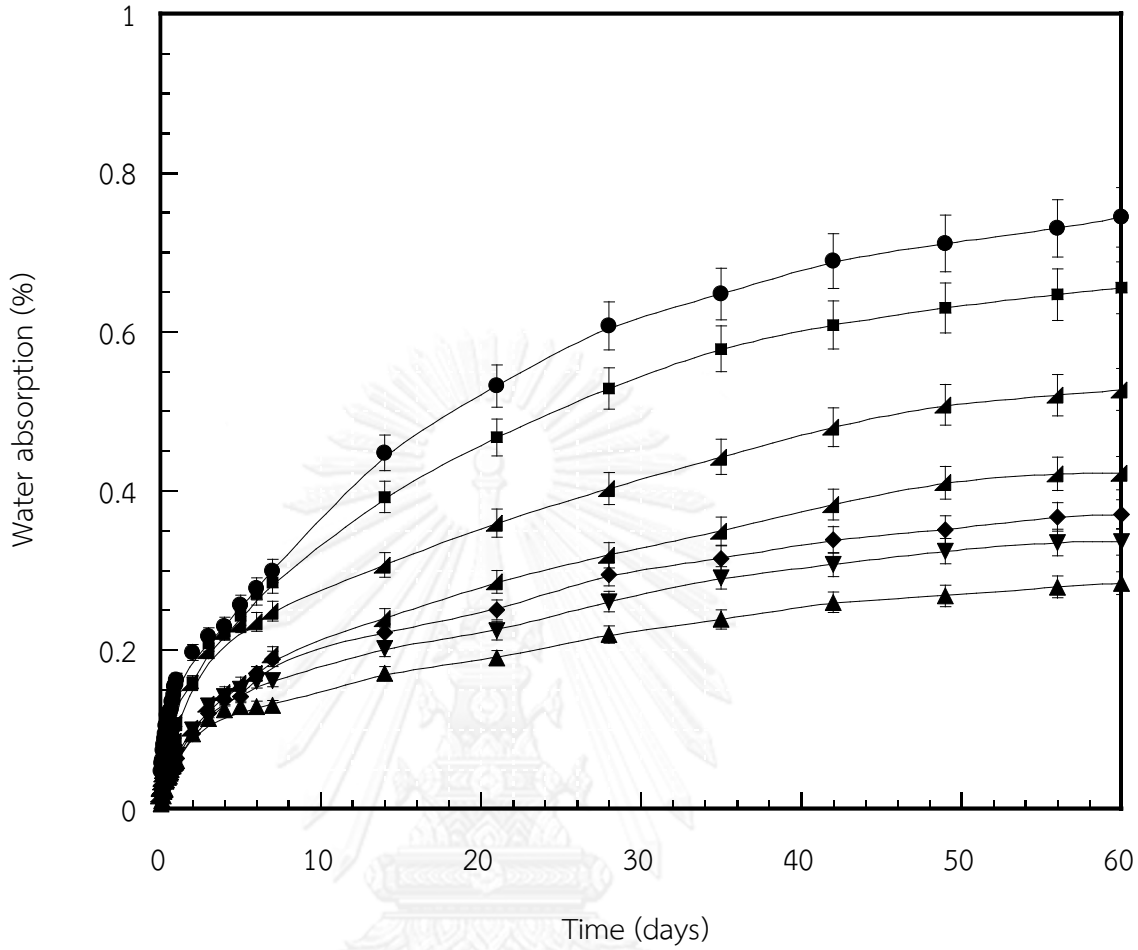

Figure 5. 17 Water absorption of graphene-filled polybenzoxazine composites: (●) neat polybenzoxazine, (■) 10wt%, (◢) 20wt%, (◣) 30wt%, (♦) 40wt%, (▼) 50wt%, (▲) 60wt%.

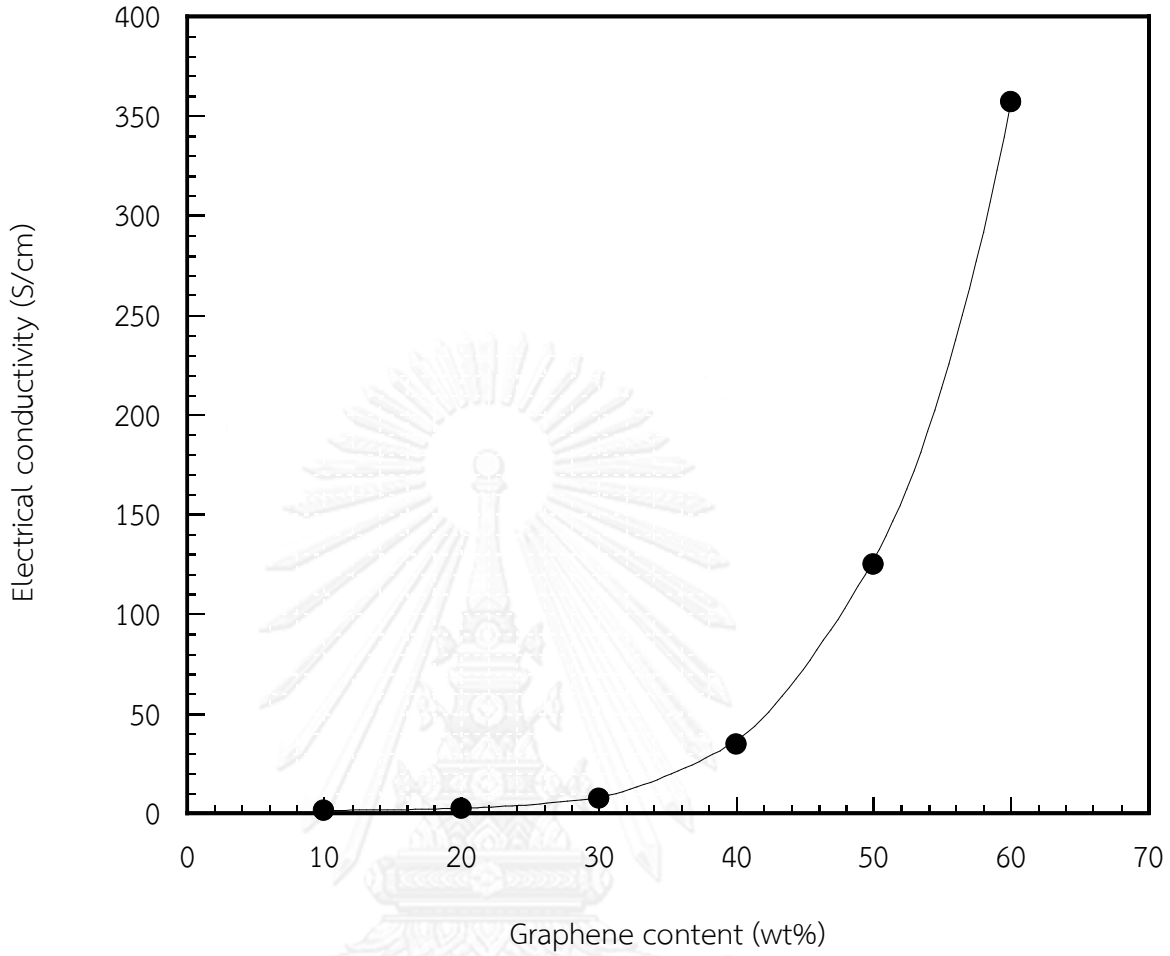

Figure 5. 18 Effect of the graphene contents on electrical conductivity (in-plane) of highly filled graphene-polybenzoxazine composites.

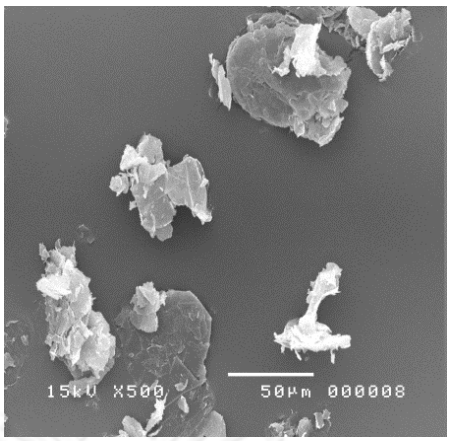

Figure 5. 19 SEM micrograph of graphene-grade H from XG Sciences, USA used in this research.

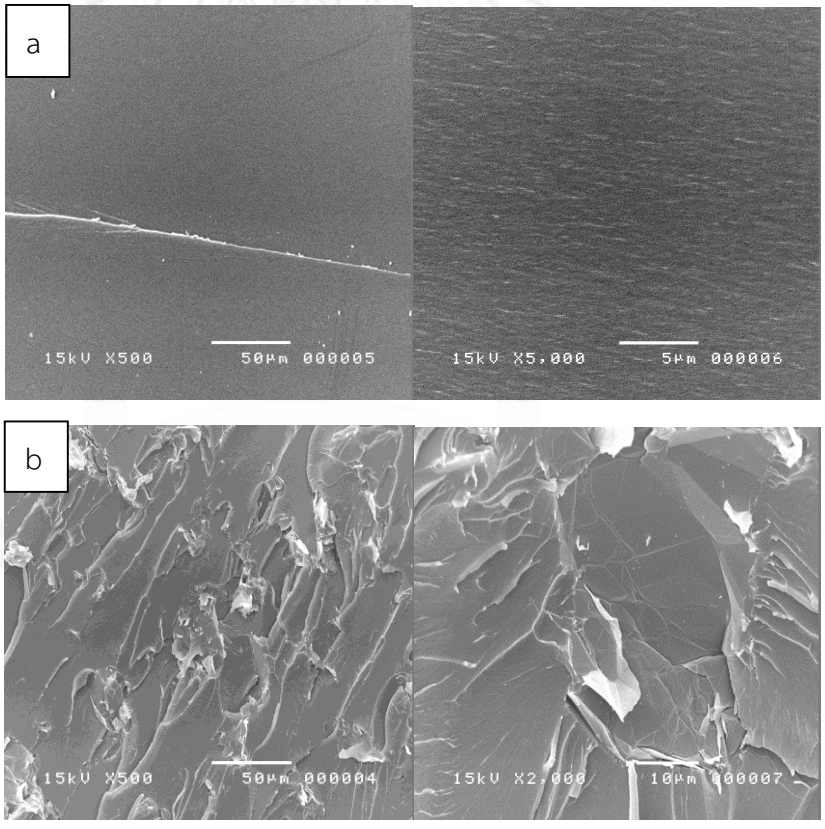

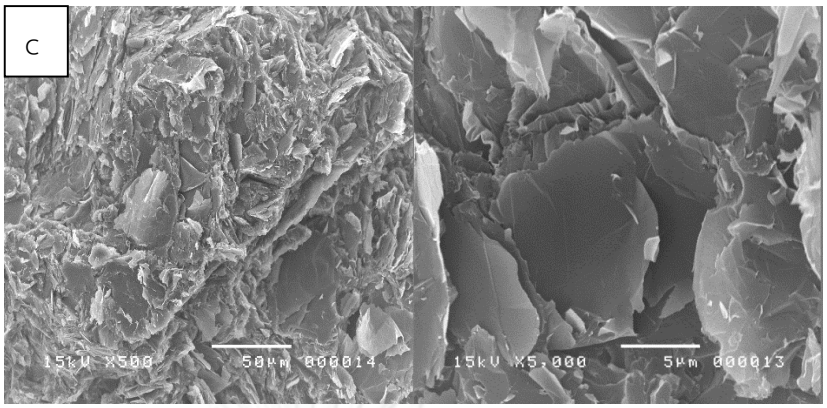

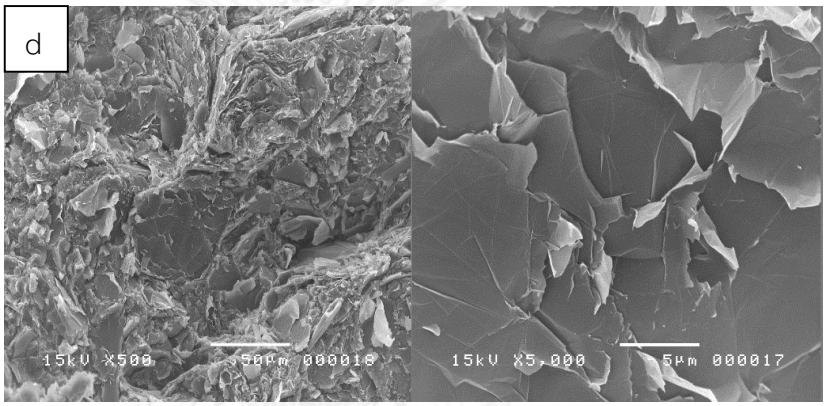

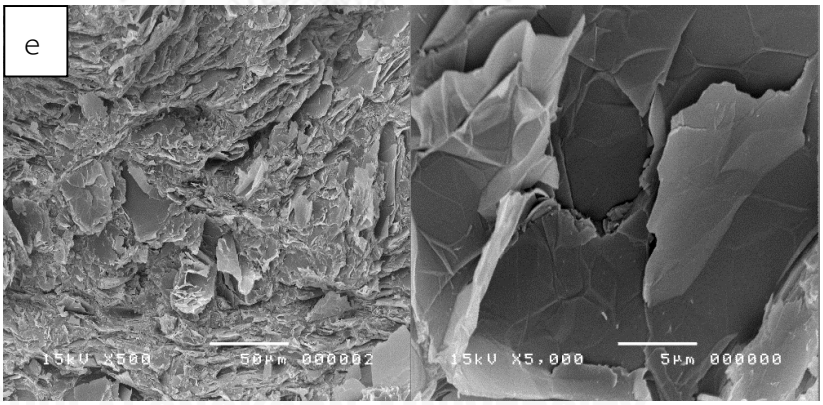

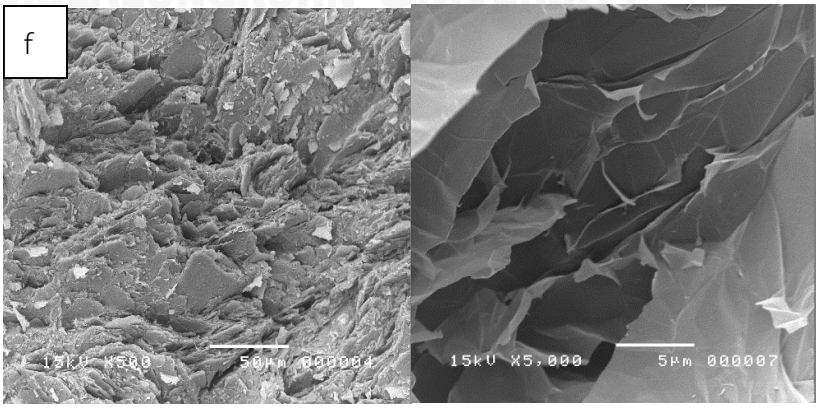

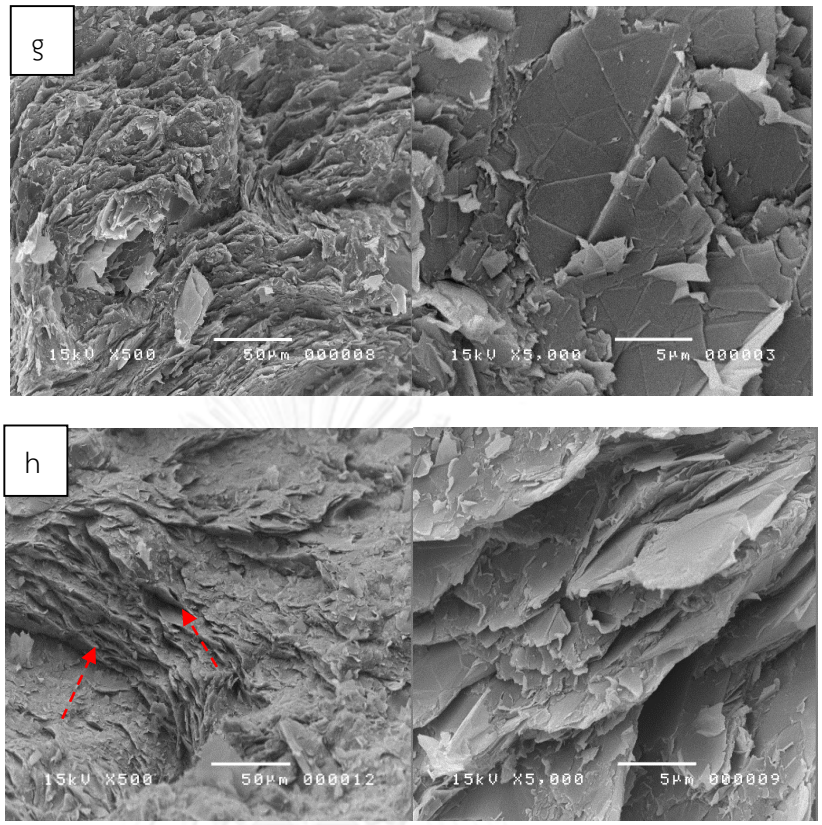

Figure 5. 20 SEM micrographs of fracture surface of graphene-filled polybenzoxazine composites: (a) neat polybenzoxazine (PBZ), (b) 1wt% graphene-filled PBZ, (c) 10wt% graphene-filled PBZ, (d) 20wt% graphene-filled PBZ, (e) 30wt% graphene-filled PBZ, (f) 40wt% graphene-filled PBZ, (g) 50wt% graphene-filled PBZ, (h) 60wt% graphene-filled PBZ.

CHAPTER VI

CONCLUSIONS

The system of highly filled graphene-polybenzoxazine with the maximum graphene loading of 60wt% was achieved in this work. The composites exhibit various properties highly suitable for a bipolar plate in fuel cell applications comparing with most existing system and pass those requirements by the Department of Energy of United States (DOE).

The DSC thermograms revealed that the graphene might act as a catalyst for oxazine-ring opening reaction of polybenzoxazine. The optimal curing condition to obtain the fully-cured specimens of the graphene-polybenzoxazine composites was by heating at 200°C for 3 hours in a compression molder with a hydraulic pressure of 15 MPa. The actual densities of the composites were measured to be close to the theoretical densities which follow the rule of mixture suggesting negligible amount of void was presented in the composites. The glass transition temperature of graphene-polybenzoxazine composites were found to increase with increasing graphene contents, due to the substantially bonding between the polymer and the filler. The degradation temperatures (at 5% weight loss under nitrogen atmosphere) and solid residue (at 800°C) of the composites were also found to increase with increasing the graphene contents.

In addition, modulus of the graphene-polybenzoxazine composites was significantly enhanced by the presence of the graphene at only few percent weight of loading. The storage modulus at room temperature of the composites also exhibited the similar trend with the flexural modulus. Meanwhile, the flexural strength of the composites was slightly decreased with an increasing graphene content. Furthermore, water absorption of graphene-polybenzoxazine composites were significantly suppressed by the addition of the graphene filler.

Finally, thermal conductivity and electrical conductivity of the obtained composites were found to increase as a polynomial function with the graphene

loading. Scanning electron micrographs show good distribution of graphene in the polybenzoxazine matrix and substantial interfacial adhesion with tight interfaces between and the graphene. The obtained mechanical properties and electrical conductivity of the highly filled graphene-polybenzoxazine composites is found to be a promising candidate for bipolar plates in polymer electrolyte fuel cells application. Those properties were found to exceed the DOE requirements for bipolar plate applications in fuel cell.

However, thermal conductivity, of our highly filled composites with the maximum graphene loading of 60wt% have not been successfully satisfy DOE requirement for bipolar plates application. A research in the combination of graphite and graphene filled polybenzoxazine composites are suggested to enhance thermal conductivity of the system in order to meet the DOE requirement.

REFERENCES

[1] Cheng, T., Bipolar plates and plate materials in proton exchange membrane fuel cells (materials properties and performance), D.P. Wilkinson, et al., Editors. 2010, CRC Press Taylor&Francis Group: USA. p. 305-313.

[2] Kim, H., Abdala, A.A., and Macosko, C.W., Graphene/polymer nanocomposites. Macromolecules, 2010. 43(16): p. 6515-6530.

[3] Guo, N. and Leu, M.C., Effect of different graphite materials on the electrical conductivity and flexural strength of bipolar plates fabricated using selective laser sintering. International Journal of Hydrogen Energy, 2012. 37(4): p. 3558-3566.

[4] DOE, U.S. *Technical targets: bipolar plates. Multiyear research, development and demonstration plan*. 2013 [cited 2013 Oct 20]; Available from: http://www1.eere.energy.gov/hydrogenandfuelcells/mypp/pdfs/fuel_cells.pdf.

[5] Yeetsorn, T., Fowler, M.W., and Tzoganakis, C., A Review of thermoplastic composites for bipolar plate materials in PEM fuel cells, in nanocomposites with unique properties and applications in medicine and industry, J. Cuppoletti, Editor. 2011, InTech Janeza Trdine 9, 51000 Rijeka, Croatia p. 317.

[6] Dueramae, I., Pengdam, A., and Rimdusit, S., Highly filled graphite polybenzoxazine composites for an application as bipolar plates in fuel cells. Journal of Applied Polymer Science, 2013. 130(6): p. 3909-3918.

[7] Kimura, H., Ohtsuka, K., and Matsumoto, A., Performance of graphite filled composite based on benzoxazine resin. Journal of Applied Polymer Science, 2010. 117(3): p. 1711-1717.

[8] Dhakate, S.R., Mathur, R.B., Kakati, B.K., and Dhami, T.L., Properties of graphite-composite bipolar plate prepared by compression molding technique for PEM fuel cell. International Journal of Hydrogen Energy, 2007. 32(17): p. 4537-4543.

[9] Rimdusit, S., Jubsilp, C., and Tiptipakorn, S., Alloys and composites of polybenzoxazines 2013, Singapore: Springer.

[10] Hermann, A., Chaudhuri, T., and Spagnol, P., Bipolar plates for PEM fuel cells: A review. International Journal of Hydrogen Energy, 2005. 30(12): p. 1297-1302.

[11] Peighambardoust, S.J., Rowshanzamir, S., and Amjadi, M., Review of the proton exchange membranes for fuel cell applications. International Journal of Hydrogen Energy, 2010. 35(17): p. 9349-9384.

[12] Weaver, G., World fuel cells-an industry profile with market prospects to 2010.

2002, Oxford, United Kingdom: Elsevier Science & Technology.

[13] DOE, U.S. *Fuel Cells*. 2014 [cited 2014 Apr 2]; Available from:http://www1.eere.energy.gov/hydrogenandfuelcells/fuelcells/fc_types.html.

[14] Hickner, M.A. Transport and structure in fuel cell proton exchange membranes Doctoral dissertation Chemical Engineering, Virginia Polytechnic Institute and State University, 2003.

[15] *PEMFC Single Cell*. 2014 [cited 2014 Apr 2]; Available from: http://www.bloggang.com/viewdiary.php?id=wing41&month=07-2007&date=12&group=1&gblog=2.

[16] *Fuel cell design (Fuel for through on cars of the future)*. 2014 [cited 2014 Apr 2]; Available from: http://www.scientific-computing.com/features/feature.php?feature_id=126.

[17] *PEMFC components (Flow field plates)*. 2014 [cited 2014 Apr 2]; Available from: http://tfy.tkk.fi/aes/AES/projects/renew/fuelcell/pem_4.html.

[18] Dihrab, S.S., Sopian, K., Alghoul, M.A., and Sulaiman, M.Y., Review of the membrane and bipolar plates materials for conventional and unitized regenerative fuel cells. Renewable & Sustainable Energy Reviews, 2009. 13(6-7): p. 1663-1668.

[19] Mehta, V. and Cooper, J.S., Review and analysis of PEM fuel cell design and manufacturing. Journal of Power Sources, 2003. 114(1): p. 32-53.

[20] *Carbon and graphite electrode*. 2014 [cited 2014 Apr 2]; Available from:http://www.electrographite.co.za/products-materials/carbon-graphite-electrodes/.

[21] Tawfik, H., Hung, Y., and Mahajan, D., Metal bipolar plates for PEM fuel cell - A review. Journal of Power Sources, 2007. 163(2): p. 755-767.

[22] Ryan, C. *Green machine competition-fuel cell pressurized air bipolar plate (cathode Side)*. 2014 [cited 2014 Apr 2]; Available from: http://www.chiefdelphi.com/media/photos/26116 .

[23] *Fuel cells*. 2014 [cited 2014 Apr 2]; Available from: http://www.ingenieurparadies.de/en/ipar/18281.

[24] Integraphene. *Nanoplatelets bulk powder*. 2013 [cited 2014 Apr 2]; Available from: http://integraphene.com/applications/nanoplatelets-bulk-powd.

[25] *The graphene story*. 2013 [cited 2013 Oct 20]; Available from: http://www.graphene.manchester.ac.uk/story/.

[26] Ishida, H., *Process for preparation of benzoxazine compounds in solventless systems* 1996: U.S. .

[27] Lide, D.R., CRC Handbook of Chemistry and Physics 85th edition. 2004, New York: CRC Press Taylor&Francis Group.

[28] Ishida, H. and Sanders, D.P., Improved thermal and mechanical properties of

polybenzoxazines based on alkyl-substituted aromatic amines. Journal of Polymer Science Part B-Polymer Physics, 2000. 38(24): p. 3289-3301.

[29] Zhang, H.B., Zheng, W.G., Yan, Q., Yang, Y., Wang, J.W., Lu, Z.H., Ji, G.Y., and Yu, Z.Z., Electrically conductive polyethylene terephthalate/graphene nanocomposites prepared by melt compounding. Polymer, 2010. 51(5): p. 1191-1196.

[30] Zaman, I., Phan, T.T., Kuan, H.C., Meng, Q.S., La, L.T.B., Luong, L., Youssf, O., and Ma, J., Epoxy/graphene platelets nanocomposites with two levels of interface strength. Polymer, 2011. 52(7): p. 1603-1611.

[31] Gedler, G., Antunes, M., Realinho, V., and Velasco, J.I., Thermal stability of polycarbonate-graphene nanocomposite foams. Polymer Degradation and Stability, 2012. 97(8): p. 1297-1304.

[32] Jiang, X. and Drzal, L.T., Exploring the potential of exfoliated graphene nanoplatelets as the conductive filler in polymeric nanocomposites for bipolar plates. Journal of Power Sources, 2012. 218: p. 297-306.

[33] Chatterjee, S., Nafezarefi, F., Tai, N.H., Schlagenhauf, L., Nuesch, F.A., and Chu, B.T.T., Size and synergy effects of nanofiller hybrids including graphene nanoplatelets and carbon nanotubes in mechanical properties of epoxy composites. Carbon, 2012. 50(15): p. 5380-5386.

[34] Yu, A.P., Ramesh, P., Itkis, M.E., Bekyarova, E., and Haddon, R.C., Graphite nanoplatelet-epoxy composite thermal interface materials. Journal of Physical Chemistry C, 2007. 111(21): p. 7565-7569.

[35] Huang, X.Y., Zhi, C.Y., and Jiang, P.K., Toward Effective Synergetic Effects from graphene nanoplatelets and carbon nanotubes on thermal conductivity of ultrahigh volume fraction nanocarbon epoxy composites. Journal of Physical Chemistry C, 2012. 116(44): p. 23812-23820.

[36] Khan, M.O., Leung, S.N., Chan, E., Naguib, H.E., Dawson, F., and Adinkrah, V., Effects of microsized and nanosized carbon fillers on the thermal and electrical properties of polyphenylene sulfide based composites. Polymer Engineering and Science, 2013. 53(11): p. 2398-2406.

[37] Ishida, H. and Rimdusit, S., Very high thermal conductivity obtained by boron nitride-filled polybenzoxazine. Thermochimica Acta, 1998. 320(1-2): p. 177-186.

[38] XGSciences. *Technical data sheet of XGnP® Grade H product characteristics*. 2014 [cited 2014 Mar 12]; Available from: http://xgsciences.com/.

[39] Huang, K.J., Niu, D.J., Sun, J.Y., Han, C.H., Wu, Z.W., Li, Y.L., and Xiong, X.Q., Novel electrochemical sensor based on functionalized graphene for simultaneous

determination of adenine and guanine in DNA. Colloids and Surfaces B-Biointerfaces, 2011. 82(2): p. 543-549.

[40] Kasemsiri, P., Hiziroglu, S., and Rimdusit, S., Effect of cashew nut shell liquid on gelation, cure kinetics, and thermomechanical properties of benzoxazine resin. Thermochimica Acta, 2011. 520(1-2): p. 84-92.

[41] Yadav, S.K. and Cho, J.W., Functionalized graphene nanoplatelets for enhanced mechanical and thermal properties of polyurethane nanocomposites. Applied Surface Science, 2013. 266: p. 360-367.

[42] Rimdusit, S., Kampangsaeree, N., Tanthapanichakoon, W., Takeichi, T., and Suppakarn, N., Development of wood-substituted composites from highly filled polybenzoxazine-phenolic novolac alloys. Polymer Engineering and Science, 2007. 47(2): p. 140-149.

[43] Wang, X., Yang, H.Y., Song, L., Hu, Y., Xing, W.Y., and Lu, H.D., Morphology, mechanical and thermal properties of graphene-reinforced poly(butylene succinate) nanocomposites. Composites Science and Technology, 2011. 72(1): p. 1-6.

[44] Sheshmani, S., Ashori, A., and Fashapoyeh, M.A., Wood plastic composite using graphene nanoplatelets. International Journal of Biological Macromolecules, 2013. 58: p. 1-6.

[45] Jubsilp, C., Panyawanitchakun, C., and Rimdusit, S., Flammability and thermomechanical properties of dianhydride-modified polybenzoxazine composites reinforced with carbon fiber. Polymer Composites, 2013. 34(12): p. 2067-2075.

[46] Sari, A. and Karaipekli, A., Thermal conductivity and latent heat thermal energy storage characteristics of paraffin/expanded graphite composite as phase change material. Applied Thermal Engineering, 2007. 27(8-9): p. 1271-1277.

[47] Ishida, H. and Rimdusit, S., Heat capacity measurement of boron nitride-filled polybenzoxazine - The composite structure-insensitive property. Journal of Thermal Analysis and Calorimetry, 1999. 58(3): p. 497-507.

[48] Xu, Y.S., Ray, G., and Abdel-Magid, B., Thermal behavior of single-walled carbon nanotube polymer-matrix composites. Composites Part a-Applied Science and Manufacturing, 2006. 37(1): p. 114-121.

[49] Min, C., Yu, D.M., Cao, J.Y., Wang, G.L., and Feng, L.H., A graphite nanoplatelet/epoxy composite with high dielectric constant and high thermal conductivity. Carbon, 2013. 55: p. 116-125.

[50] Tian, X.J., Itkis, M.E., Bekyarova, E.B., and Haddon, R.C., Anisotropic thermal and

electrical properties of thin thermal interface layers of graphite nanoplatelet-based composites. Scientific Reports, 2013. 3: p. 6.

[51] Yu, A.P., Ramesh, P., Sun, X.B., Bekyarova, E., Itkis, M.E., and Haddon, R.C., Enhanced thermal conductivity in a hybrid graphite nanoplatelet - carbon nanotube filler for epoxy composites. Advanced Materials, 2008. 20(24): p. 4740.

[52] Yeetsorn, R. Development of electrically conductive thermoplastic composites for bipolar plate application in polymer electrolyte membrane fuel cell. Doctoral dissertation Chemical Engineering, Waterloo, 2010.

[53] Li, B. and Zhong, W.H., Review on polymer/graphite nanoplatelet nanocomposites. Journal of Materials Science, 2011. 46(17): p. 5595-5614.

[54] Kajohnchaiyagual, J., Jubslip, C., Dueramae, I., and Rimdusit, S., Thermal and mechanical properties enhancement obtained in highly filled alumina-polybenzoxazine composite, in Polymer Composites2014.

[55] Li, J., Sham, M.L., Kim, J.K., and Marom, G., Morphology and properties of UV/ozone treated graphite nanoplatelet/epoxy nanocomposites. Composites Science and Technology, 2007. 67(2): p. 296-305.

[56] Starkova, O., Chandrasekaran, S., Prado, L., Tolle, F., Mulhaupt, R., and Schulte, K., Hydrothermally resistant thermally reduced graphene oxide and multi-wall carbon nanotube based epoxy nanocomposites. Polymer Degradation and Stability, 2013. 98(2): p. 519-526.

[57] Cho, E.A., Jeon, U.S., Ha, H.Y., Hong, S.A., and Oh, I.H., Characteristics of composite bipolar plates for polymer electrolyte membrane fuel cells. Journal of Power Sources, 2004. 125(2): p. 178-182.

[58] Wang, J.C., Wang, X.B., Xu, C.H., Zhang, M., and Shang, X.P., Preparation of graphene /poly(vinyl alcohol) nanocomposites with enhanced mechanical properties and water resistance. Polymer International, 2011. 60(5): p. 816-822.

APPENDIX

APPENDIX

Characterization of Graphene filled Polybenzoxazine Composites

Appendix 1 Maximum packing density evaluation of graphene-filled polybenzoxazine composites.

Graphene content (wt%)	Graphene content (vol%)	Theoretical density (g/cm^3)	Actual density (g/cm^3)
0	0	1.190	1.185
10	5.7	1.247	1.247
20	11.9	1.310	1.310
30	18.8	1.380	1.377
40	26.5	1.457	1.455
50	35.1	1.544	1.540
60	44.8	1.642	1.637
65	50.1	1.696	1.642

Appendix 2 Storage modulus (E') at 35°C and glass transition temperature (Tg, loss modulus), of graphene filled polybenzoxazine composites at various graphene contents.

Graphene content (wt%)	Storage modulus (E′) at 35 °C (GPa)	Glass transition temperature (°C)
0	5.9	174
10	7.9	176
20	10.5	178
30	12.3	181
40	16.6	182
50	21.6	186
60	25.1	188

Appendix 3 Mechanical properties of graphene-filled polybenzoxazine composites at room temperature.

Graphene content (%wt)	Flexural strength (MPa)	Flexural modulus (GPa)
0	119.7 ± 4.930	5.2 ± 0.680
10	69.1 ± 4.205	8.2 ± 0.682
20	60.5 ± 4.732	9.6 ± 0.661
30	56.7 ± 5.445	12.6 ± 0.596
40	55.1 ± 4.897	15.1 ± 0.786
50	53.1 ± 5.234	16.6 ± 0.595
60	41.7 ± 6.910	17.5 ± 0.902

Appendix 4 Water absorption of graphene-filled polybenzoxazine composites at various graphene contents.

Graphene content (wt%)	24 hrs (%)	7 days (%)	60 days (%)
0	0.152±0.014	0.299±0.014	0.740±0.012
10	0.132±0.019	0.284±0.010	0.655±0.010
20	0.108±0.019	0.248±0.016	0.527±0.010
30	0.071±0.015	0.193±0.019	0.422±0.010
40	0.068±0.015	0.188±0.017	0.370±0.014
50	0.067±0.013	0.161±0.012	0.336±0.014
60	0.060±0.014	0.129±0.010	0.248±0.015

VITA

Ms. Ratcha Plengudomkit was born in Nakhon Pathom, Thailand on October 1, 1989. She graduated at high school from Phrapathom Witthayalai School, Thailand in 2007. She received the Bachelor's Degree in Chemical Engineering from Engineering Faculty of King Mongkut's University of Technology Thonburi, Bangkok, Thailand in 2011. She continued her study for Master's Degree of Chemical Engineering at the Department of Chemical Engineering, Faculty of Engineering, Chulalongkorn University, Bangkok, Thailand.

Some part of this work was selected for oral presentation in The Fifth Pure and Applied Chemistry International Conference which was held during January 8-10, 2014 at Khon Kaen, Thailand and The eighth APA International Conference on Polymer: Vision & Innovations was held during February 19-21, 2014 at New Delhi, India.